

# **Performance Evaluation of Very Early Strength Latex-Modified Concrete (LMC-VE) Overlay**

**Final Report  
October 2024**

---

**IOWA STATE UNIVERSITY**  
**Institute for Transportation**

**Sponsored by**  
Iowa Highway Research Board  
(IHRB Project TR-771)  
Iowa Department of Transportation  
(InTrans Project 19-688)

## **About the Institute for Transportation**

The mission of the Institute for Transportation (InTrans) at Iowa State University is to save lives and improve economic vitality through discovery, research innovation, outreach, and the implementation of bold ideas.

## **Iowa State University Nondiscrimination Statement**

Iowa State University does not discriminate on the basis of race, color, age, ethnicity, religion, national origin, pregnancy, sexual orientation, gender identity, genetic information, sex, marital status, disability, or status as a US veteran. Inquiries regarding nondiscrimination policies may be directed to the Office of Equal Opportunity, 3410 Beardshear Hall, 515 Morrill Road, Ames, Iowa 50011, telephone: 515-294-7612, hotline: 515-294-1222, email: eooffice@iastate.edu.

## **Disclaimer Notice**

The contents of this report reflect the views of the authors, who are responsible for the facts and the accuracy of the information presented herein. The opinions, findings and conclusions expressed in this publication are those of the authors and not necessarily those of the sponsors.

The sponsors assume no liability for the contents or use of the information contained in this document. This report does not constitute a standard, specification, or regulation.

The sponsors do not endorse products or manufacturers. Trademarks or manufacturers' names appear in this report only because they are considered essential to the objective of the document.

## **Iowa DOT Statements**

Federal and state laws prohibit employment and/or public accommodation discrimination on the basis of age, color, creed, disability, gender identity, national origin, pregnancy, race, religion, sex, sexual orientation or veteran's status. If you believe you have been discriminated against, please contact the Iowa Civil Rights Commission at 800-457-4416 or the Iowa Department of Transportation affirmative action officer. If you need accommodations because of a disability to access the Iowa Department of Transportation's services, contact the agency's affirmative action officer at 800-262-0003.

The preparation of this report was financed in part through funds provided by the Iowa Department of Transportation through its "Second Revised Agreement for the Management of Research Conducted by Iowa State University for the Iowa Department of Transportation" and its amendments.

The opinions, findings, and conclusions expressed in this publication are those of the authors and not necessarily those of the Iowa Department of Transportation.

### Technical Report Documentation Page

<b>1. Report No.</b> IHRB Project TR-771	<b>2. Government Accession No.</b>	<b>3. Recipient's Catalog No.</b>	
<b>4. Title and Subtitle</b> Performance Evaluation of Very Early Strength Latex-Modified Concrete (LMC-VE) Overlay		<b>5. Report Date</b> October 2024	
		<b>6. Performing Organization Code</b>	
<b>7. Author(s)</b> Kejin Wang (orcid.org/0000-0002-7466-3451), Bharath Melugiri Shankaramurthy (orcid.org/0000-0001-7521-8440), Anand Anand (orcid.org/0000-0001-9980-3038), Yogiraj Sargam (orcid.org/0000-0001-9980-3038), Katelyn Freeseaman (orcid.org/0000-0003-0546-3760), Brent Phares (orcid.org/0000-0001-5894-4774)		<b>8. Performing Organization Report No.</b> InTrans Project 19-688	
<b>9. Performing Organization Name and Address</b> Institute for Transportation Iowa State University 2711 South Loop Drive, Suite 4700 Ames, IA 50010-8664		<b>10. Work Unit No. (TRAIS)</b>	
		<b>11. Contract or Grant No.</b>	
<b>12. Sponsoring Organization Name and Address</b> Iowa Highway Research Board Iowa Department of Transportation 800 Lincoln Way Ames, IA 50010		<b>13. Type of Report and Period Covered</b> Final Report	
		<b>14. Sponsoring Agency Code</b>	
<b>15. Supplementary Notes</b> Visit <a href="https://intrans.iastate.edu">https://intrans.iastate.edu</a> for color pdfs of this and other research reports.			
<b>16. Abstract</b> <p>Conventional bridge deck overlays made with high-performance concrete (HPC) and low-slump dense portland cement concrete (PCC) generally require a 72-hour wet curing time before they can be opened to traffic. Shorter opening times are desired to reduce the high cost of traffic control for heavily traveled urban highways. To meet this need, high early strength latex-modified concrete (LMC-VE) overlays are designed to open to traffic within 3 to 6 hours of placement. Research indicates that LMC-VE overlays are less prone to shrinkage-related problems and more resistant to chloride penetration than other early strength overlays. The high initial cost can be offset by the reduced need for traffic control and the extension in bridge deck service life by an additional 30 years, reaching a total service life of over 75 years.</p> <p>In September 2019, the Iowa Department of Transportation placed Iowa's first LMC-VE bridge deck overlay on the IA 15 bridge over Black Cat Creek in Emmet County. In this research, the overlay construction activities were thoroughly documented, and LMC-VE specimens were cast in the field to investigate a range of mechanical and durability properties in the laboratory. Additionally, the field overlay's performance was monitored for 50 months through frequent field visits and testing. Lastly, a life-cycle cost analysis (LCCA) was performed to assess the economic value of the LMC-VE overlay relative to other overlay types. The laboratory tests indicated that the LMC-VE mix reached 2,827 psi at 3 hours, which is sufficient for quickly opening a pavement to vehicular traffic, and exhibited sufficient long-term compressive and flexural strength, good chloride penetration resistance and high surface resistivity, comparable shrinkage and initial sorptivity to PCC, and mixed results for freeze-thaw durability. During field monitoring, the overlay exhibited some thin cracks, slight spalling/abrasion in a few localized areas, a slight decrease in friction over time, comparable initial and secondary sorptivity to HPC, and a good substrate-overlay bond. The LCCA results suggest that the high life-cycle cost of the LMC-VE overlay outweighs the lower user costs. However, when annual average daily traffic (AADT) values are above 3,300, the LMC-VE overlay could be a better alternative. The results of this research are expected to serve as a benchmark and assist in decision-making related to the selection of overlay alternatives for future bridge deck applications in Iowa.</p>			
<b>17. Key Words</b> bridge deck overlays—field monitoring—high early strength latex-modified concrete (LMC-VE)—laboratory investigation—life-cycle cost analysis—mechanical and durability properties		<b>18. Distribution Statement</b> No restrictions.	
<b>19. Security Classification (of this report)</b> Unclassified.	<b>20. Security Classification (of this page)</b> Unclassified.	<b>21. No. of Pages</b> 143	<b>22. Price</b> NA





# **PERFORMANCE EVALUATION OF VERY EARLY STRENGTH LATEX-MODIFIED CONCRETE (LMC-VE) OVERLAY**

**Final Report  
October 2024**

**Principal Investigator**

Kejin Wang, Professor

Department of Civil, Construction, and Environmental Engineering, Iowa State University

**Co-Principal Investigators**

Brent Phares, Research Associate Professor

Department of Civil, Construction, and Environmental Engineering, Iowa State University

Katelyn Freeseaman, Former Acting Director  
Bridge Engineering Center, Iowa State University

**Research Assistants**

Bharath Melugiri Shankaramurthy, Yogiraj Sargam, and Anand Anand

**Authors**

Kejin Wang, Bharath Melugiri Shankaramurthy, Anand Anand,  
Yogiraj Sargam, Katelyn Freeseaman, Brent Phares

Sponsored by  
Iowa Highway Research Board and  
Iowa Department of Transportation  
(IHRB Project TR-712)

Preparation of this report was financed in part  
through funds provided by the Iowa Department of Transportation  
through its Research Management Agreement with the  
Institute for Transportation  
(InTrans Project 19-688)

A report from  
**Institute for Transportation**  
**Iowa State University**  
2711 South Loop Drive, Suite 4700  
Ames, IA 50010-8664  
Phone: 515-294-8103 / Fax: 515-294-0467  
<https://intrans.iastate.edu>



## TABLE OF CONTENTS

ACKNOWLEDGMENTS .....	xi
EXECUTIVE SUMMARY .....	xiii
Background and Problem Statement.....	xiii
Major Findings and Conclusions .....	xiv
Recommendations .....	xvi
1. INTRODUCTION .....	1
1.1 Problem Statement .....	1
1.2 Objectives and Approach .....	1
1.3 Scope of the Study .....	2
2. LITERATURE REVIEW .....	4
2.1 Polymer Modification of Cementitious Systems .....	4
2.2 Hydration of Cement in LMC .....	6
2.3 Durability and Long-Term Performance of LMC .....	7
2.4 LMC-VE .....	8
3. DOCUMENTATION OF FIELD OVERLAY CONSTRUCTION .....	20
3.1 Project Overview .....	20
3.2 Deck Inspection Prior to LMC-VE Placement .....	24
3.3 Preparation for Overlay Installation.....	24
3.4 LMC-VE Overlay Installation .....	28
3.5 Materials and Mix Proportion of the LMC-VE .....	32
3.6 Trial Mixing of the LMC-VE Prior to Pouring.....	32
3.7 Tests Conducted During Overlay Construction.....	33
4. LABORATORY TESTS AND RESULTS .....	38
4.1 Laboratory Tests and Methods.....	38
4.2 Results and Discussion .....	47
4.3 Summary of Laboratory Investigation .....	63
5. FIELD MONITORING .....	66
5.1 Field Monitoring and Test Methods .....	66
5.2 Field Monitoring Results .....	72
5.3 Chapter Summary .....	85
6. LIFE-CYCLE COST ANALYSIS.....	86
6.1 LCCA Approach .....	86
6.2 Overlay Alternatives .....	87
6.3 Analysis and Results .....	87
6.4 Chapter Summary .....	94
7. CONCLUSIONS AND RECOMMENDATIONS .....	96
7.1 Major Findings and Conclusions .....	96

7.2 Recommendations .....	101
REFERENCES .....	103
APPENDIX A .....	107
APPENDIX B .....	111
APPENDIX C .....	115

## LIST OF FIGURES

Figure 2.1. Special truck used to mix/discharge LMC .....	5
Figure 2.2. Influence of curing temperature on the strength development of two batches (SB1 and SB2) of LMC-VE.....	6
Figure 2.3. Simplified model of the formation of the latex-cement co-matrix.....	7
Figure 2.4. Use of LMC-VE in the United States.....	9
Figure 2.5. Strength development in LMC-VE, LMC-HE, and LMC.....	10
Figure 2.6. LMC-VE overlay construction (a) on a weekend (by VDOT) and (b) overnight (by KYTC) .....	11
Figure 2.7. Deck preparation prior to pouring LMC-VE.....	12
Figure 2.8. Placement of LMC-VE overlay on prepared deck surface.....	13
Figure 2.9. Poor deck condition before placing the LMC-VE overlay.....	14
Figure 2.10. Reinforcing steel cut by the milling machine being removed by powered hand saw .....	15
Figure 2.11. Fixing a punch-through by KYTC .....	16
Figure 3.1. Bridge location .....	20
Figure 3.2. Overview of the bridge.....	21
Figure 3.3. Deck cross section and bridge layout .....	21
Figure 3.4. Locations of patched material on bridge deck surface .....	24
Figure 3.5. Patch locations and cracks on bridge deck surface .....	24
Figure 3.6. Sequence of milling operation.....	25
Figure 3.7. Hydrodemolition operation .....	26
Figure 3.8. Sand-blasting of the surface .....	27
Figure 3.9. Pre-wetting of deck surface prior to overlay placement.....	28
Figure 3.10. Volumetric mobile mixer truck used for in situ mixing of concrete .....	29
Figure 3.11. First half of overlay casting.....	30
Figure 3.12. Completion of the first half of overlay casting.....	31
Figure 3.13. Second half of overlay casting .....	31
Figure 3.14. (a) Pocket penetrometer and (b) mortar sieved from LMC-VE .....	33
Figure 3.15. Setting time of mortar sieved from LMC-VE .....	34
Figure 3.16. Surface reactivity measurements of overlay 3 hours after casting .....	35
Figure 3.17. Casting test specimens during overlay construction .....	36
Figure 4.1. Mechanical strength and elastic modulus test specimens.....	39
Figure 4.2. Preparation of substrate concrete for pull-off tests at ISU's PCC Lab.....	40
Figure 4.3. LMC-VE-overlaid beam specimens sliced from the cast slab specimens.....	41
Figure 4.4. Pull-off testing equipment and typical failure modes obtained during testing.....	41
Figure 4.5. Surface resistivity measurement using four-point Wenner probe .....	42
Figure 4.6. Field-cast and field-cored specimens for sorptivity testing.....	43
Figure 4.7. Typical sorptivity test curve .....	43
Figure 4.8. Salt ponding test slabs overlaid with LMC-VE.....	44
Figure 4.9. Obtaining powdered samples from salt ponded slabs for the chloride test .....	44
Figure 4.10. Chemical testing for acid-soluble chlorides using potentiometric titration.....	45
Figure 4.11. Shrinkage testing of LMC-VE specimens .....	46
Figure 4.12. Freeze-thaw testing of the cast beam specimens .....	46
Figure 4.13. Calorimetry test results .....	48

Figure 4.14. Compressive strength of LMC-VE at different ages .....	49
Figure 4.15. Flexural strength of LMC-VE at different ages .....	49
Figure 4.16. Pull-off strength test specimen and the observed failure modes .....	50
Figure 4.17. Failure modes observed in the tested specimens .....	51
Figure 4.18. Surface resistivity development with age .....	53
Figure 4.19. Comparison between sorption behavior of substrate concrete core and LMC- VE core .....	55
Figure 4.20. Initial and secondary sorptivity values of substrate concrete and LMC-VE cores .....	56
Figure 4.21. Salt ponding test results of LMC-VE overlay in comparison with other overlays and HPC .....	57
Figure 4.22. Shrinkage test results of LMC-VE specimens .....	58
Figure 4.23. Freeze-thaw test results of LMC-VE specimens .....	59
Figure 4.24. Deterioration of LMC-VE-only (middle column) and LMC-VE-overlaid (right column) test specimens due to freeze-thaw cycles (left column) .....	60
Figure 4.25. Magnified images of freeze-thaw-related deterioration in LMC-VE-only beams .....	62
Figure 4.26. Magnified images of freeze-thaw-related deterioration in LMC-VE-overlaid beams .....	63
Figure 5.1. Performing crack and deterioration survey .....	67
Figure 5.2. British Pendulum Tester used for measuring BPN .....	68
Figure 5.3. Bridge layout showing BPN measurement locations (#1, #2, and #3) .....	68
Figure 5.4. Field SR measurement using a Wenner probe .....	69
Figure 5.5. Bridge layout showing SR measurement locations (indicated by ×) .....	70
Figure 5.6. Drilling cores for pull-off strength test in the field .....	71
Figure 5.7. Pull-off testing of the field overlay .....	71
Figure 5.8. Pull-off test locations .....	71
Figure 5.9. Crack length development in the LMC-VE overlay over time .....	73
Figure 5.10. Crack width development in the LMC-VE overlay over time .....	75
Figure 5.11. Comparison of overlay deck surface at different ages (up to 44 months) .....	76
Figure 5.12. Deteriorations observed at an overlay age of 50 months (during Trip 10) .....	77
Figure 5.13. BPN values at different overlay ages .....	79
Figure 5.14. Correction to SR for using cloth layers in field measurements .....	81
Figure 5.15. Measured SR values at different locations on the deck surface .....	82
Figure 5.16. Typical ASTM C1583 failure modes observed in pull-off tests .....	82
Figure 5.17. Comparison of pull-off test failure modes at different overlay ages (with bond failures highlighted in red dashed lines) .....	84
Figure 6.1. Steps involved in an LCCA of overlay alternatives .....	86
Figure 6.2. Costs of alternatives obtained from the deterministic analysis: (a) agency costs (b) user costs, and (c) total costs .....	91
Figure 6.3. Costs of alternatives obtained from the probabilistic analysis: (a) agency costs and (b) user costs .....	93
Figure 6.4. Determining AADT threshold for LMC-VE overlay .....	94
Figure B.1. Crack survey results from Trip 2 (overlay age of 2 months) .....	111
Figure B.2. Crack survey results from Trip 3 (overlay age of 8.5 months) .....	112

Figure B.3. Cracking and other deteriorations observed during Trip 4 (overlay age of 14 months).....	113
--	-----

## LIST OF TABLES

Table 2.1. Polymer latexes used for modifying cementitious systems .....	4
Table 2.2. Typical curing durations for different LMC types.....	9
Table 2.3. Chemical and physical properties of cements used for LMC-VE, LMC-HE, and LMC .....	10
Table 2.4. Typical overnight installation schedule for LMC-VE .....	11
Table 2.5. Mix proportions used by a few DOTs .....	17
Table 2.6. Acceptance criteria adopted by a few DOTs .....	17
Table 2.7. Cost of different overlays (\$/yd <sup>2</sup> ) .....	19
Table 3.1. Major activities documented during LMC-VE overlay construction and performance monitoring.....	22
Table 3.2. Materials and mix proportions of LMC-VE .....	32
Table 3.3. Properties of latex .....	32
Table 3.4. Details of tests conducted .....	33
Table 3.5. Details of cast specimens.....	36
Table 4.1. Mix design used for substrate concrete in slabs .....	40
Table 4.2. Oxide composition of cement .....	47
Table 4.3. Pull-off strength test results .....	50
Table 4.4. Characterizing bond strength values for overlays.....	51
Table 4.5. Values for pull-off strength testing specified by various state DOTs.....	52
Table 5.1. Summary of field visits conducted .....	66
Table 5.2. Summary of possible reasons for identified cracks on the overlay surface.....	78
Table 5.3. Summary of field pull-off strength test results .....	84
Table 6.1. Pavement overlay alternatives analyzed in this study .....	87
Table 6.2. Common project-level inputs for the LCCA .....	88
Table 6.3. LCCA inputs used for overlay alternatives.....	89
Table 6.4. Results of the probabilistic analysis.....	92
Table C1. RealCost input data .....	115



## **ACKNOWLEDGMENTS**

The research team would like to thank the Iowa Department of Transportation (DOT) and Iowa Highway Research Board (IHRB) for sponsoring this research. Special thanks are given to the project Technical Advisory Committee (TAC) members, Joseph Stanisz, Ahmad Abu-Hawash, James Nelson, Scott Neubauer, Todd Hanson, Curtis Carter, Wayne Sunday, Bill Dotzler, and Ping Lu, for their invaluable direction and assistance throughout this project. The research team also greatly appreciates the contributions of Kevin Rauk Dwaine Berte, who assisted with traffic control during the field tests, Douglas Wood and Owen Steffens, who assisted with field testing, and Theodore Huisman, who assisted with laboratory testing.



## **EXECUTIVE SUMMARY**

### **Background and Problem Statement**

High-performance concrete (HPC) and portland cement concrete (PCC) are the most commonly used bridge deck overlay materials in the state of Iowa. A three-day (72-hour) wet curing procedure is specified for these materials in the Iowa Department of Transportation (DOT) standard specifications. Due to the high cost of traffic control for heavily traveled urban highways, it is desired to reduce traffic disruptions as much as possible.

To meet this need, high early strength latex-modified concrete (LMC-VE) overlays are intended to be ready for traffic within 3 to 6 hours of placement. Previous research has indicated that an LMC-VE overlay is more durable than other early strength overlays because it is less prone to shrinkage-related problems and has a higher resistance to chloride ion penetration.

Though an LMC-VE overlay has a high initial cost, this cost can be offset by the overlay's ability to reduce traffic control expenses and extend the service life of a bridge deck by an additional 30 years, reaching a total service life of over 75 years.

Though an LMC-VE overlay has a high initial cost, this cost can be offset by the overlay's ability to reduce traffic control expenses and extend the service life of a bridge deck by an additional 30 years, reaching a total service life of over 75 years. Several states (e.g., Virginia, Ohio, Missouri, Kentucky) have explored the use of LMC-VE overlays in their bridge construction projects.

In September 2019, the Iowa DOT conducted the first trial placement of an LMC-VE bridge deck overlay in the state of Iowa. The overlay was placed on the IA 15 bridge over Black Cat Creek in Emmet County. To evaluate the performance of this overlay, the research described in this report had the following objectives:

1. Document the advantages and difficulties associated with the use of LMC-VE in bridge deck overlays before, during, and after overlay construction.
2. Evaluate the key engineering properties (compressive and flexural strength, tensile adhesion bond strength, chloride penetration resistance, and friction index) of the overlay material in the laboratory by casting numerous test specimens in the field during overlay construction.
3. Monitor the field performance of the constructed LMC-VE overlay for five years through frequent field visits, testing, and measurements.
4. Conduct a detailed life-cycle cost analysis (LCCA) of the LMC-VE overlay in comparison to polymer concrete, normal concrete, and HPC overlays.
5. Provide insights and recommendations for the use of LMC-VE overlays on Iowa bridges.

## Major Findings and Conclusions

### *Laboratory Performance of Field-Cast Specimens*

#### Fresh Concrete Properties

The LMC-VE used in the field overlay project is highly workable, having a slump of approximately 9 in. and an air content of 5.5% in the fresh state. The initial set time measured by a pocket penetrometer at a penetration resistance of 500 psi was 36 minutes.

The LMC-VE paste (made with the cement, latex, and citric acid) displayed rapid heat generation during a period spanning 5 to 10 hours after mixing. During this period, the heat of hydration of the paste increased from about 25 J/g to 180 J/g, an increase about twice that of a conventional pavement cement paste. Such rapid heat generation could be responsible for potential thermal cracking of the LMC-VE overlay.

#### Mechanical Properties

- LMC-VE developed a satisfactory compressive strength of 2,827 psi at 3 hours, which is favorable for quickly opening a pavement to vehicular traffic. The compressive strength increased to 5,952 psi by 28 days and 7,816 psi by 400 days.
- The early-age flexural strength increased from 685 psi at 3 days to 865 psi at 28 days.
- The 28-day pull-off strength testing of LMC-VE overlaid on HPC substrate beams indicated a bond strength of 283 psi (greater than the 250 psi recommended for thin epoxy overlays).

#### Chloride Intrusion Resistance

- The average surface resistivity (SR) values of laboratory-cast LMC-VE specimens were 24.9 k $\Omega$ -cm at 3 days and 70.3 k $\Omega$ -cm at 14 days.
- Because the LMC-VE specimens were water cured for only 3 days and then air cured at room temperature until they were tested, the SR values at 28 days were found to be unstable. Therefore, subsequent tests involved soaking specimens in water for 2 days before taking SR measurements.
- SR values of 61.4 k $\Omega$ -cm at 170 days, 69.0 k $\Omega$ -cm at 340 days, and 110.3 k $\Omega$ -cm at 440 days were found, indicating enhanced impermeability due to the synergistic effect of continued hydration and the development of a complex latex network within the system.
- The chloride content determined from 90-day salt ponding tests indicated average acid-soluble chloride contents of 0.36% and 0.13% in the top and bottom 1/2 in. layers, respectively. The results indicate that an LMC-VE overlay has better chloride penetration resistance than a low-slump dense concrete (LSDC) overlay but not an epoxy overlay.

## Moisture Transport

- The field-cast LMC-VE specimens cured in the laboratory for 28 days (3 days in water and 25 days in air) showed a slightly lower initial sorptivity value than the cored, laboratory-cast, 28-day-old substrate HPC specimens, whereas the secondary sorptivity of the LMC-VE specimens was much higher than that of the substrate HPC specimens.
- The field-cored LMC-VE specimens showed a lower initial sorptivity value than the HPC specimens from the existing bridge deck, whereas the secondary sorptivity of the LMC-VE specimens before the age of 8.5 months was higher than that of the HPC specimens at an age of 8.5 months. After 8.5 months, the secondary sorptivity values of the field-cored LMC-VE specimens approached those of the HPC substrate specimens.

## Other Durability Properties (Drying and Autogenous Shrinkage and Freeze-Thaw Resistance)

- After 400 days, the LMC-VE prism specimens showed autogenous and drying shrinkage values of 115 and 440 microstrain, respectively, well within the typical values for PCC.
- Field-cast, laboratory-cured beam specimens made entirely with LMC-VE (denoted as LMC-VE-only) showed relatively poor freeze-thaw resistance, contrary to previous studies. At 72 freeze-thaw cycles, these specimens experienced significant mass loss, and the relative dynamic modulus fell below 60% (the lower limit specified in ASTM C666). The rate of deterioration increased thereafter, and testing was terminated after 112 freeze-thaw cycles. Such poor freeze-thaw resistance might be related to the high secondary sorptivity of the LMC-VE, and the increasing amount of moisture absorbed in the LMC-VE as soaking time increased might be responsible for the rapid freeze-thaw deterioration.
- In contrast, beams comprised of LMC-VE overlaid on an HPC substrate showed better freeze-thaw resistance than the LMC-VE-only beams. With no considerable mass loss, the relative dynamic modulus of these specimens was above 85% at 144 freeze-thaw cycles. However, after 144 cycles the LMC-VE overlay debonded from the substrate, and testing was terminated after 144 freeze-thaw cycles.
- The failure of the LMC-VE-substrate bond of the field cast specimens was possibly due to inadequate preparation of the substrate surface in the laboratory, resulting in insufficient microtexture/roughness of the exposed coarse aggregates. However, construction of the field overlay involved more extensive surface preparation techniques, including milling, hydrodemolition, and sand-blasting, and the LMC-VE-substrate bond of the LMC-VE overlay performed well in the field.

## *Short- and Long-Term Performance of In-Service/Field Overlay*

- The LMC-VE overlay material tended to develop transverse and diagonal hairline cracks over time. The major causes of these cracks may include the rapid, high heat generation experienced during cement hydration at a very early age (5 to 10 hours after casting), the material's susceptibility to shrinkage, the effect of bridge skew angle, reflective cracking from the substrate, and high vehicular loading at an early age.
- The frequency of cracking slowed after three years.

- The in-service overlay showed slight material spalling and abrasion/erosion at a few areas on the overlay surface.
- The overlay friction index, expressed in terms of the average British Pendulum Number (BPN) values, decreased over time but remained above 55, the value deemed necessary for traffic safety.
- Up to 26 months, SR values generally increased as the overlay age increased, indicating improvement in the microstructure and pore network. At later ages, the average SR values decreased slightly, which may indicate a slight deterioration in the overlay material, possibly associated with the spalling and cracking observed.
- The LMC-VE-substrate bond failure mode changed with time. At a very early age (4 days), the failure of the pull-off specimens occurred in the LMC-VE. For specimens between 2 and 14 months old, most failures occurred at the LMC-VE overlay-substrate interface. After that time (from 14 to 50 months), all specimens tested failed at the substrate, indicating the growth of the bond strength between the LMC-VE overlay and substrate.
- Although exhibiting large variation, the strengths of most specimens at failure were greater than 250 psi, which could be classified as “very good” and adequate.

### *Life-Cycle Cost Analysis*

- While polymer concrete overlays require less maintenance during their service life, the agency cost of these overlays is considerably higher than that of PCC and HPC overlays. The agency cost of polymer overlays is heavily influenced by their initial construction cost.
- The faster time for opening to traffic in the case of polymer overlays greatly reduces the cost of traffic control and thus the user cost.
- Deterministic analysis showed that the LMC-VE overlay has the highest agency cost among the overlay alternatives (LMC-VE, LMC, PPC, low-slump PCC, and HPC), primarily due to its very high initial construction cost. However, the LMC-VE overlay has the lowest user cost due to its rapid opening to traffic. (Note that UHPC overlays were not included in this analysis.)
- Probabilistic analysis revealed that at the same probability level, the agency cost of the LMC-VE overlay is higher than that of the other overlay alternatives, while the opposite trend holds for the user cost. The LMC-VE overlay also has the highest mean net present value (NPV) for the agency cost, but the standard deviation is lower.
- The annual average daily traffic (AADT) threshold for the LMC-VE overlay was determined to be 3,300. Above this AADT, the total cost of the LMC-VE overlay is expected to be less than that of the other overlay alternatives.
- The LCCA results suggest that the life-cycle cost of the LMC-VE overlay outweighs the potential benefits, such as rapid opening to traffic. However, when AADT values are above 3,300, the LMC-VE overlay could be a better alternative.

### **Recommendations**

The results of this research are expected to serve as a benchmark and assist in decision-making related to the selection of overlay alternatives for future bridge deck applications in Iowa. Recommendations resulting from this research are presented below.

### *Control of Temperature Rise*

Calorimetry test results from the laboratory study showed rapid heat generation during hours 5 through 10 of cement hydration, and the high temperature of the LMC-VE overlay was also noticed by the investigators during the SR measurement of the field overlay 3 hours after casting. Such early, rapid heat generation resulting from the rapid hydration of calcium sulfoaluminate (CSA) cement could be responsible for the thermal cracking of LMC-VE.

It is recommended that the temperature of the LMC-VE overlay be monitored in future LMC-VE overlay practice. Concrete cooling measures, such as the use of pre-cooled aggregates, chilled mixing water, and/or a sprinkling system for curing, may be taken to further reduce concrete placement temperature.

LMC-VE mix proportions, such as the latex and citric acid contents, may be adjusted to reduce rapid heat generation within the short period of early-age cement hydration, thus minimizing the early-age cracking due to rapid heat generation from cement hydration. Supplementary cementitious materials may also be used to reduce not only the heat of hydration but also the secondary sorptivity of the concrete, thus reducing cracking and deterioration.

### *Issues Related to Shrinkage Properties*

Although the laboratory investigation showed that the shrinkage behavior of the laboratory-cured LMC-VE was similar to that of conventional pavement concrete, the field LMC-VE overlay showed a number of fine/hairline transverse cracks, which was possibly related to the shrinkage of the LMC-VE. The following measures can be considered to minimize shrinkage cracking:

- The early opening of the field overlay to traffic might have increased the likelihood of shrinkage cracks because the concrete continues to shrink after exposure to traffic loads. Therefore, one possible measure for addressing this issue is to further improve LMC-VE curing. Because LMC-VE exhibits rapid strength gain and high shrinkage at a very early age, extending the curing time and properly removing the burlap to avoid sudden temperature and moisture changes may help reduce some shrinkage-related cracking.
- Techniques for shrinkage reduction, such as the use of shrinkage-reducing agents and/or lightweight fine aggregates (LWAs) as internal curing agents, could also be considered.
- Since the extent of shrinkage varies with latex dosage, future research should consider different latex dosages in combination with the use of internal curing agents.
- Since shrinkage is significantly influenced by the high initial heat of hydration of LMC-VE, heat should be measured at the site of material placement. This could be supplemented with laboratory-based isothermal/semi-adiabatic calorimetry tests.
- Future applications of LMC-VE need to consider all of the above to ensure that the constructed overlay is free from shrinkage cracking.

### *Correlating LMC-VE Microstructure to Durability*

The laboratory investigation showed that the secondary sorptivity of the laboratory-cured LMC-VE specimens (at 28 days) was much higher than that of the conventional HPC used for overlays, and the freeze-thaw resistance of LMC-VE-only specimens was low. Small areas of spalling were observed at a few locations on the field LMCVE overlay. All of those could be attributed to improper pore structure in the LMC-VE, possibly due to chemical reactions among the cement, latex, and citric acid components in the overlay and the deicer chemicals applied to the deck surface. Future research should be conducted to investigate these physico-chemical phenomena through detailed microstructural investigation. Through a better understanding of the interactions of the material components, LMC-VE mix proportions can be optimized for a better performance.

### *Potential Cost Savings through LMC-VE Applications*

- In the LCCA, the construction cost of the LMC-VE overlay was recognized as being higher than that of the other overlay alternatives. However, an LMC-VE overlay may result in cost savings when the AADT is greater than 3,300. Above this threshold, the total life-cycle cost of an LMC-VE overlay is expected to be less than that of the other overlay alternatives.
- The use of LMC-VE as an overlay material is not preferable for AADT values lower than 3,300.



# **1. INTRODUCTION**

## **1.1 Problem Statement**

Bridge deck overlays have been used as an effective deck service life extension tool by the Iowa Department of Transportation (DOT) since the 1970s. Class HPC-O high-performance concrete (HPC) and Class O portland cement concrete (PCC) are the most commonly used materials for rigid overlays. A three-day (72-hour) wet curing procedure is specified in the Iowa standard specifications. Due to the high cost of traffic control for heavily traveled urban highways, it is highly desired to reduce traffic disruptions as much as possible by getting the work done at night or on weekends. To meet this need, thin epoxy overlays were tested recently with good success, and this treatment has been adopted as a bridge preservation tool for decks that are still in good or fair condition. However, when an overlay of considerable thickness is needed or when significant patching is required, another overlay system, a high early strength latex-modified concrete (LMC-VE) overlay, has been proven to be a better choice.

LMC-VE has been used successfully in situations where a bridge lane can be closed for 1 to 2 days, such as over a weekend, but also in situations where a lane can only be closed for 8 hours or less, as is the case with a nighttime closure (Sprinkel 1999). Researchers have indicated that compared with other early strength overlays, an LMC-VE overlay is more durable because it is less prone to shrinkage-induced problems and has a higher resistance to chloride ion penetration. When an LMC-VE overlay is placed on a hydrodemolition-prepared bridge deck surface, the service life of the deck can be expected to be over 75 years, and the high initial cost of an LMC-VE overlay can be offset by its extended service life (Martens 2015). Thus, the use of an LMC-VE overlay is an ideal choice for expedited construction. Several states (e.g., Virginia, Ohio, Missouri, Kentucky) have already explored the use of LMC-VE overlays in their bridge construction projects.

In 2018, the Iowa DOT decided to explore the use of LMC-VE overlays. In a project let on November 20, 2018 (BRFN-015-4(18)-39-32), the Iowa DOT conducted the first trial placement of an LMC-VE bridge deck overlay in the state of Iowa. This overlay was placed on the IA 15 bridge over Black Cat Creek in Emmet County, in Iowa DOT District 2. The present research project documented the entire construction procedure, thoroughly evaluated the short-term and long-term performance of the LMC-VE overlay both in the laboratory and in the field, and summarized the experience and lessons learned from this field project to not only serve as an essential tool for future bridge deck overlay decision-making but also provide design and construction guidance for future practice.

## **1.2 Objectives and Approach**

The overall goal of this research was to explore the potential use of LMC-VE in Iowa bridge deck overlays. This was achieved by studying the first application of an LMC-VE overlay in Iowa, which was placed on the IA 15 bridge over Black Cat Creek in Emmet County, and monitoring its performance both in the laboratory and in the field (i.e., when the overlay was in service). The specific approach to meet this objective included the following components:

1. Document and identify the benefits and problems associated with the use of LMC-VE during construction of the LMC-VE overlay on the selected bridge. The documentation included detailed information on the materials used, construction conditions and procedures, and quality assurance/quality control (QA/QC) methods and procedures.
2. Evaluate the key engineering properties (such as compressive and flexural strengths, tensile adhesion bond strength, chloride penetration resistance, and friction index) of LMC-VE using standard and accelerated test methods.
3. Monitor the field performance of the constructed LMC-VE overlay for up to five years.
4. Conduct a detailed life-cycle cost analysis (LCCA) of the LMC-VE overlay in comparison to different conventional rigid overlay types belonging to three broad categories: polymer concrete overlays, normal concrete overlays, and high-performance concrete overlays.
5. Analyze the research results, understand the LMC-VE overlay's performance, and provide insights and recommendations for the future use of LMC-VE overlays on Iowa bridges.

### **1.3 Scope of the Study**

The following tasks were conducted to reach the technical objectives:

1. The existing literature was reviewed to obtain detailed information on the applications of LMC-VE in US bridges, including construction procedures, material properties, and performance evaluation methods.
2. An in-depth field investigation was conducted in three stages: (1) documentation of field construction operations prior to LMC-VE overlay placement (i.e., pre-construction stage), (2) field testing and preparation of test specimens during overlay placement, with field-cast specimens safely transported in their molds/forms to the Portland Cement Concrete Research Laboratory (PCC Lab) at Iowa State University (ISU) for laboratory investigation (i.e., construction stage), and (3) short-term and long-term monitoring of the overlay's performance in the field after placement (i.e., post-construction stage). The three stages are outlined in detail below:
  - a. Pre-construction Stage: This stage included documentation of information related to (1) LMC-VE materials and mix proportions; (2) preparation of the substrate surface (via milling, hydrodemolition, sand-blasting, etc.); (3) on-site procedures related to concrete mixing, placement, finishing, creation of construction joints, and curing; (4) construction conditions (roughness of prepared substrate surface, moisture conditions, weather data, traffic loading conditions [intensity, time], etc.); and (5) QA/QC methods for evaluation.
  - b. Construction Stage: During overlay construction, different tests were conducted on site and various specimens were cast to investigate a range of overlay material properties in the laboratory (ISU's PCC Lab). Specimens were cast to understand compressive strength (cylindrical concrete specimens) and flexural strength (concrete prism specimens) development, chloride penetration resistance through surface resistivity (SR) (cylinders), salt ponding (small-scale slabs), water sorptivity (cylinders), and freeze-thaw durability (concrete beams of two types: one made completely of overlay material and one consisting of a conventional high-performance concrete substrate overlaid with LMC-VE). Field tests included measurements of concrete setting time and SR measurements on the cast overlay surface (three hours post construction).

- c. Post-construction Stage: The overlay's performance in the field was monitored in the short term (starting from four days post construction) and in the long term (up to five years post construction) through various tests, including core pull-off tests, friction index measurements, and SR measurements. The condition of the cast surface was also thoroughly documented through examination for any signs of cracking (and cracking patterns), measurement and mapping of crack dimensions, and documentation of any signs of deterioration (such as abraded surface regions, concrete spalling, etc.) through photographs and schematics.
3. A comprehensive LCCA was performed to evaluate the total economic value/cost of the construction (considering the direct costs) and maintenance (considering the user costs) of the LMC-VE overlay in comparison to an HPC overlay. Additionally, three other overlay types, including a PCC overlay, a polyester polymer concrete (PPC) overlay, and a latex-modified concrete (LMC) overlay, were also considered to evaluate different alternatives for overlay system applications in the state of Iowa. The discount rates recommended by the Federal Highway Administration (FHWA) were considered for the analysis, and a typical cash flow diagram was developed for both LMC-VE and conventional thin concrete overlays to identify potential life-cycle cost savings through LCCA.

## 2. LITERATURE REVIEW

### 2.1 Polymer Modification of Cementitious Systems

Modification of cementitious systems with polymers and monomers was first introduced as an attempt to address the limitations associated with cement concrete, such as delayed hardening, high drying shrinkage, low tensile strength, and low chemical resistance (Ohama 1995). These modifiers included (1) polymer latexes (including elastomeric latexes, thermoplastic latexes, thermosetting latexes, bituminous latexes, and mixed latexes), (2) re-dispersible polymer powders, (3) water-soluble polymers, (4) liquid resins, and (5) monomers. The most widely used of these modifiers is polymer latex. Among the wide variety of available polymer latexes (Table 2.1), styrene-butadiene rubber (SBR), a synthetic rubber latex, is the most commonly used.

**Table 2.1. Polymer latexes used for modifying cementitious systems**

Type	Characteristics
Elastomeric	Natural rubber latex or synthetic latex (styrene-butadiene, polychloroprene [neoprene], acrylonitrile-butadiene)
Thermoplastic	Polyacrylic ester, styrene-acrylic, polyvinyl acetate, vinyl acetate copolymers, polyvinyl propionate, vinylidene chloride copolymers, polypropylene
Thermosetting	Epoxy resin
Bituminous and Mixed	Asphalt, rubberized asphalt, coal tar, paraffin

Data source: ACI Committee 548 2009

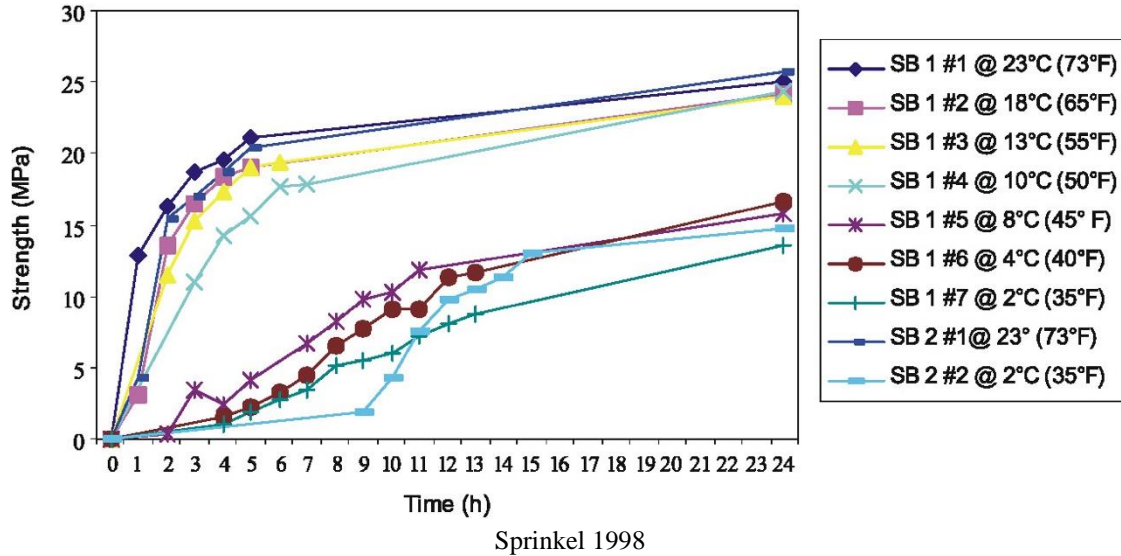
Usually, latexes contain 50% by weight of spherical polymer particles held in suspension in water by surface-active agents (Choi and Yun 2014) in dispersed form and are added to the cement mortar or concrete during mixing. A part of the mixing water is replaced with the latex emulsion, and the mixing of the concrete is usually carried out using a mobile mixer for placement (Figure 2.1). The presence of surface-active agents in the latex results in the development of large amounts of entrained air in the concrete. Hence, air-detraining agents are usually added to reduce extra air in the concrete (Choi and Yun 2014). In a typical latex, the polymer particles (produced from emulsion polymerization) range from 50 to 500 nm in size (Ohama 1995).



Theodore II et al. 2015

**Figure 2.1. Special truck used to mix/discharge LMC**

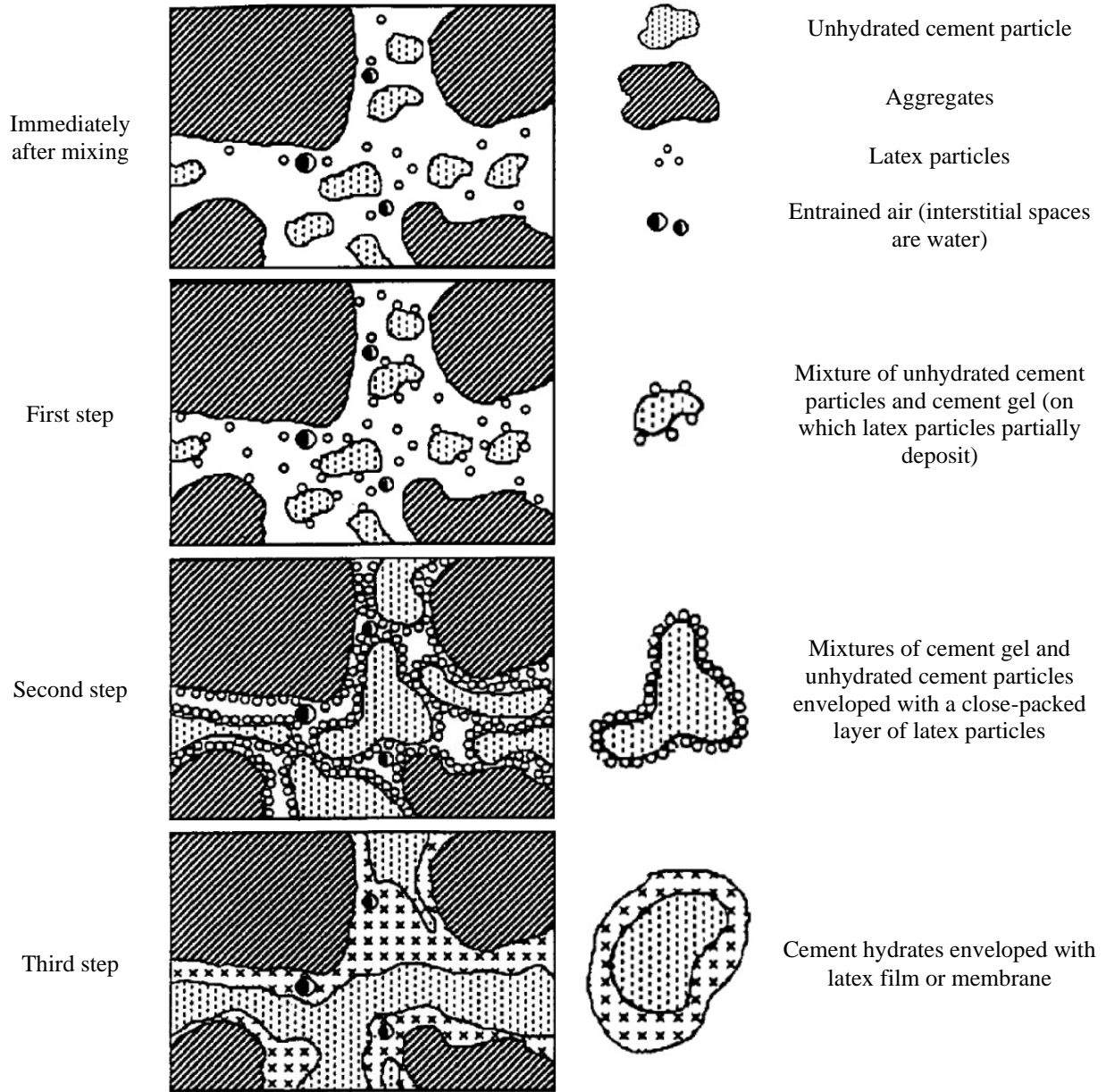
LMC was first used on a bridge deck in Virginia in 1969. The material was a PCC containing an admixture of styrene-butadiene latex particles suspended in water to replace a portion of the mixing water (Sprinkel 1999). LMC can be classified as (1) conventional LMC, (2) high early strength LMC (LMC-HE), and (3) LMC-VE. Conventional LMC overlays utilize Type I/II cement, whereas special cements are used for LMC-HE and LMC-VE. The rate of slump loss in LMC-VE is higher than in other types of LMC and hence requires the contractor to work at a faster pace. Conventional LMC has a curing period of around 72 hours and traffic is usually allowed after 4 to 7 days (Sprinkel 1999), while the curing period for LMC-VE is approximately 3 hours because it provides high early strength. However, the precise strength of LMC-VE depends on the curing temperature, a major factor in the development of compressive strength (Sprinkel 1998). This can be well understood from Figure 2.2, which shows the temperature dependence of strength development in LMC-VE. Therefore, there is a restriction on the use of LMC-VE below certain temperatures. For instance, the Virginia DOT (VDOT) restricts the application of LMC-VE below 10°C (Sprinkel 1999).



**Figure 2.2. Influence of curing temperature on the strength development of two batches (SB1 and SB2) of LMC-VE**

## 2.2 Hydration of Cement in LMC

The hydration mechanism in LMC includes the formation of a polymer-cement co-matrix phase where the cement hydration products and the polymer film are formed and penetrate into each other. This results in the development of a monolithic network, which forms a matrix of latex-modified mortar and concrete. The cement hydration reaction occurs first and is then followed by the formation of the polymer film, eventually resulting in the formation of the co-matrix phase (Ohama 1995) (Figure 2.3). As the cement particles hydrate and the mixture sets and hardens, the polymer particles become concentrated in the void spaces. As the removal of water due to cement hydration, evaporation, or both continues, the polymer particles coalesce into a polymer film that is interwoven into the hydrated cement, resulting in a mixture or co-matrix that coats the aggregate particles and lines the interstitial voids. Hence, the combination of concrete and polymers can improve the properties of both and yield cement composites with enhanced strength and durability. In the case of reactive polymers, the polymers might chemically react with calcium ions and the surfaces of the calcium hydroxide crystals in the cement paste and the silicate surfaces of the aggregates, forming chemical bonds. These chemical bonds might or might not improve the properties of the modified cement mortar or concrete. A few examples of reactive polymers include poly(vinylidene chloride-vinyl chloride), poly(styrene-acrylic ester), and polyacrylic esters.



Adapted from Ohama 1973, ACI Committee 548 2009

**Figure 2.3. Simplified model of the formation of the latex-cement co-matrix**

### 2.3 Durability and Long-Term Performance of LMC

Compared to conventional concrete, LMC shows improved performance in terms of oxygen diffusion, carbonation, chemical resistance, water penetrability, chloride penetration resistance, and freeze-thaw durability (Ohama 1995, Bordeleau et al. 1993, Yun et al. 2004, Shaker et al. 1997). The resistance to chloride and water penetration is due to the use of low water-to-cement (w/c) ratios and the formation of a plastic layer (a polymer film [Bordeleau et al. 1993]) by the latex particles within the C-S-H matrix (Yun et al. 2004). Improved freeze-thaw behavior (even in the presence of deicing salts) is due to the flexibility (i.e., LMC can easily expand and contract

during frost action) and impermeable nature of LMC (Sprinkel 1999). LMC has a relatively lower total pore volume and porosity than conventional concrete, and these properties generally decrease with an increase in the polymer-to-cement ratio (Ohama 1995). Not only do the polymer particles reduce the rate and extent of moisture movement (by blocking passages), but when microcracks form the polymer film also bridges the cracks and restricts their propagation (ACI Committee 548 2009, Shaker et al. 1997). In contrast, such strands are not present in unmodified concrete (ACI Committee 548 2009).

One of the important parameters of LMC is the latex-solid content. It has been observed that an increase in the latex-solid content can change the initial setting to a small extent and increase both the total and autogenous shrinkage but not alter the overall trend of the hydration temperature (Choi and Yun 2014). In one study (Lee and Kim 2018), a good correlation (with  $R^2 = 0.93$ ) was found between compressive strength and chloride ion penetration resistance, indicating that high-strength LMC shows high resistance to chloride ion penetration. In another study (Bordeleau et al. 1993), the scaling resistance of LMC was found to be excellent, even though the exhibited compressive strength was significantly lower than that of control mixtures.

Conventional concretes are expected to possess good freeze-thaw durability and strength if they contain acceptable air void system parameters. These include a void spacing factor of less than 0.200 mm and a specific surface greater than  $23.6 \text{ mm}^{-1}$  (Kuhlmann and Foor 1984). However, this is not the case for LMC mixtures. This can be seen in the results of a study by Clear and Chollar (1978), where it was observed that even LMC mixtures that did not meet these air void parameter requirements displayed superior performance in terms of resistance to scaling and chloride ion penetration compared to control mixtures. This finding provides a clear indication that the air void system in LMC is significantly different from that of conventional concrete (Kuhlmann and Foor 1984). In addition, it is reported in Bordeleau et al. (1993) that the use of latex normally entrains an air void system with a correct spacing factor. It was found that at proper dosages of latex, the air void spacing factor in LMC does not need to be as small as that of normal concrete for better performance (Bordeleau et al. 1993). It is believed that a latex concentration of 15% of solid polymer (by weight of cement) is the optimum ratio, taking performance versus cost for the chosen latex product into consideration.

## **2.4 LMC-VE**

In recent years, the construction of overlays has become increasingly difficult because of an enormous increase in traffic demands. Lanes cannot be closed for long periods because of the consequential traffic congestion, especially on the Interstate highway system. To minimize traffic delays, contractors often must work at night, when the ambient air temperatures are generally lower than those during the day, which increases the needed curing time of the concrete. Epoxy overlays are an alternative to time-consuming concrete overlay placement and, when used for repair, can provide 10 to 25 years of protection against chloride intrusion. However, they are very thin and follow the existing contours of the deck, and therefore they might not always be the best choice to extend a bridge's life, particularly when an overlay of considerable thickness is needed or when significant patching is required. LMC-HE overlays have been used successfully in scenarios where a lane can be closed for 1 to 2 days, such as over



a weekend. But in many situations, a bridge lane can only be closed for as little as 8 hours or less, as is the case with a nighttime closure.

To provide a fast-track option for concrete bridge deck overlays, with special attention paid to workability and strength gain, LMC-VE was developed (Choi and Yun 2014, Sprinkel 1999). As of 2019, several states have used LMC-VE, as indicated in Figure 2.4.

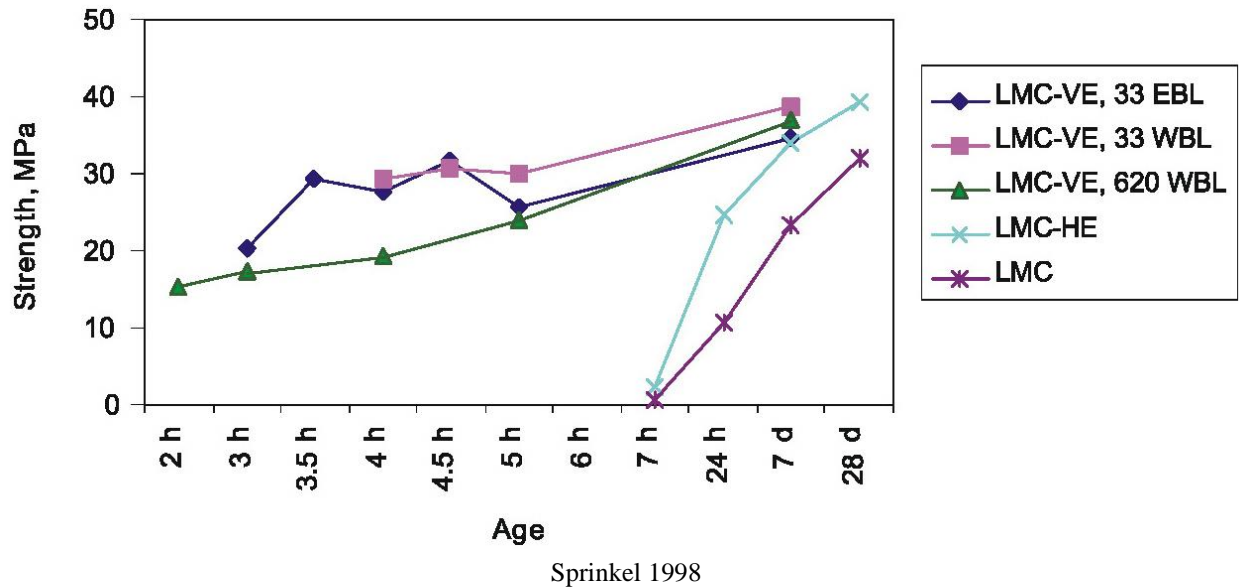


**Figure 2.4. Use of LMC-VE in the United States**

LMC-VE is produced by adding a very early strength hydraulic/portland cement to an LMC mix, which allows bridges to be opened to traffic within hours of placement while maintaining the benefits of LMC overlays (Choi and Yun 2014). For LMC-VE, the specified minimum compressive strength (ASTM C39) of 2,500 psi is achieved in as little as 3 hours at an ambient temperature range of 17°C to 24°C (62°F to 76°F). In contrast, conventional LMC overlays require 2 to 3 days or more to achieve the required strength. Typical curing durations for different LMC types are given in Table 2.2. Figure 2.5 shows the early strength benefits of LMC-VE in comparison to LMC-HE and LMC.

**Table 2.2. Typical curing durations for different LMC types**

LMC Type	Curing Duration and Type
Type I Cement LMC Mix	48 hours wet / 48 hours dry
Type III Cement LMC Mix	24 hours wet / 24 hours dry
Rapid Setting LMC Mix	3 hours wet = 2,500 psi



**Figure 2.5. Strength development in LMC-VE, LMC-HE, and LMC**

The very early strength of LMC-VE is attributed to a special blended cement that has high  $\text{Al}_2\text{O}_3$  and  $\text{SO}_3$  contents (Sprinkel 1999). For instance, the chemical compositions of cements utilized in LMC-VE, LMC-HE, and LMC by VDOT (Sprinkel 1998) are given in Table 2.3. Particular cements meeting the specific requirements are prescribed to be used for producing LMC-VE mixtures. For example, the Missouri DOT's *Bridge Special Provisions* calls for a Type HE high early strength cement, in accordance with ASTM C 1157, to be used for LMC-VE. It is to be noted that cements such as Type III fast-setting cement, which is used for LMC-HE, are not recommended for LMC-VE because the concrete does not set fast enough to reach the needed strength in 6 hours and therefore does not facilitate overnight work, and the use of such a cement has also been reported to result in higher shrinkage cracking. In addition, pozzolanic material or portland pozzolan cements should not be used for LMC-VE (Wenzlick 2006).

**Table 2.3. Chemical and physical properties of cements used for LMC-VE, LMC-HE, and LMC**

Chemical Composition	LMC-VE	LMC-HE	LMC
$\text{SiO}_2$ (%)	14.55	20.82	21.3
$\text{Al}_2\text{O}_3$ (%)	13.15	4.44	4.4
$\text{Fe}_2\text{O}_3$ (%)	1.25	2.12	4.3
$\text{CaO}$ (%)	42.33	62.33	63.7
$\text{MgO}$ (%)	2.14	3.24	3.0
$\text{SO}_3$ (%)	14.96	4.40	2.7
Ignition loss (%)	1.99	0.90	0.5
Blaine fineness ( $\text{kg}/\text{m}^3$ )	775	504	365

### 2.4.1 Installation

Figure 2.6 shows examples of LMC-VE overlay construction on a weekend and overnight.



Theodore II et al. 2015

**Figure 2.6. LMC-VE overlay construction (a) on a weekend (by VDOT) and (b) overnight (by KYTC)**

A typical weekend construction sequence for an LMC-VE overlay starts with the closure of a lane at 9 p.m. By midnight of the first night, the concrete surface is removed by milling, and any needed patch areas are removed with pneumatic hammers. The patching is completed by 2 a.m., and the lane opens to traffic at 5 a.m. Between 9 p.m. and midnight of the second night, the surface is prepared by shot-blasting, and the deck is pre-wetted. During the placement of the overlay, a fog spray that increases the relative humidity is used to prevent shrinkage cracking, and the work is completed by 2 a.m. The lane opens to traffic at 5 a.m. The sequence is repeated until all lanes are overlaid. A typical overnight schedule for an LMC-VE overlay placement is shown in Table 2.4. Figure 2.7 and Figure 2.8 provide a pictorial representation of an LMC-VE overlay installation sequence adapted from Theodore II et al. (2015).

**Table 2.4. Typical overnight installation schedule for LMC-VE**

Time	Task
7:00 p.m.	Close traffic lanes
8:00 p.m.	Milling operation
9:00 p.m.	Hydro and cleanup
12:00 p.m.	Prep of deck
2:00 a.m.	Pour LMC-VE
3:00 a.m.	Curing
6:00 a.m.	Cleanup and open to traffic



(a) Bridge deck after surface milling



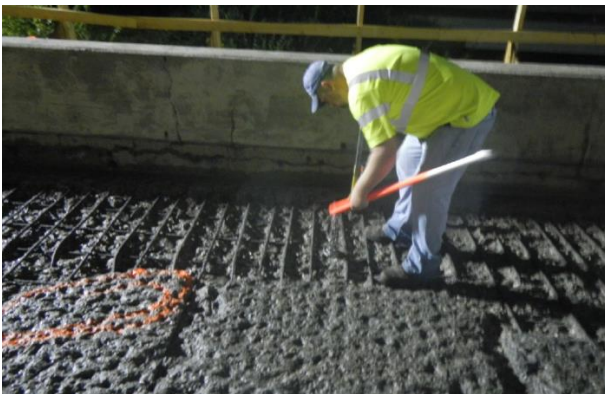
(b) Vertical perimeter of overlay work being sawed



(c) Hydrodemolition to remove distressed concrete



(d) Vacuum truck cleaning concrete debris from the deck after hydrodemolition



(e) Chain dragging after hydro-blasting to inspect remaining concrete for soundness and reveal locations that require jackhammering



(f) Jackhammering to remove unsound or delaminated concrete detected by the chain drag method after hydro-blasting; resulting debris collected by vacuum truck

Theodore II et al. (2015)

**Figure 2.7. Deck preparation prior to pouring LMC-VE**

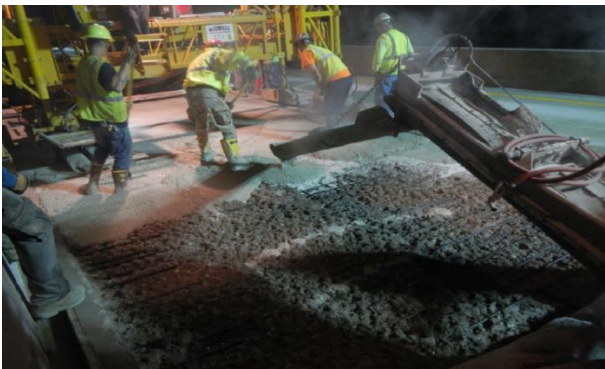




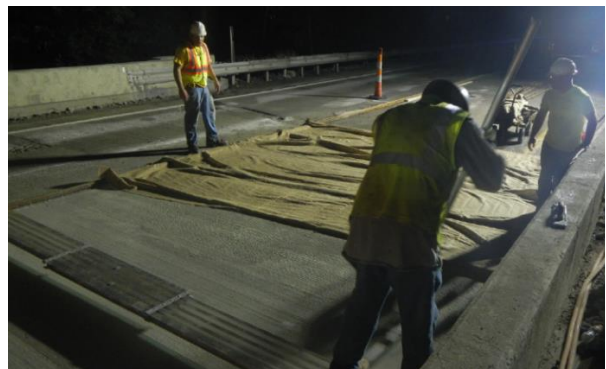
(a) Bridge deck after hydro-blasting and vacuuming showing patched concrete remaining above the upper mat of reinforcing steel



(b) Workers placing plastic sheets on prepared deck to prevent contamination of the prepared surface prior to overlay placement



(c) LMC being placed with Bidwell paving machine in the background



(d) Worker tining LMC overlay to provide surface texture. Note the wet burlap used to cover the overlay during curing.



(e) Finished bridge deck

Theodore II et al. (2015)

**Figure 2.8. Placement of LMC-VE overlay on prepared deck surface**

### 2.4.2 Problems Associated with Installation

A major factor that affects the life of an overlay is the strength of its bond with the existing deck concrete. Hence, the condition of the existing deck concrete plays an important role in providing an adequate bond with the overlay and must be examined prior to the beginning of the overlay work. Distresses, if present, need to be addressed. Figure 2.9a and Figure 2.9b show instances of distresses that existed on two bridge decks in Kentucky before LMC-VE overlay work was conducted by the Kentucky Transportation Cabinet (KYTC) (Theodore II et al. 2015). The riding surfaces of the decks exhibited extensive spalling and transverse cracking, with one deck exhibiting exposed reinforcement steel on the surface.



(a) Portion of a deck surface showing spalling on the riding surface (marked with arrows)



(b) Deck surface showing exposed reinforcement steel (marked with an arrow)

Theodore II et al. 2015

**Figure 2.9. Poor deck condition before placing the LMC-VE overlay**

In bond strength tests, failures in the base concrete just below the bond interface typically indicate damage caused by concrete removal operations such as the use of milling machines. When failure occurs in the base concrete, the bond strength is not measured but can be considered to be at least as high as the tensile strength of the base concrete (Sprinkel 1998). One of the best options to prevent debonding failure is to use the hydrodemolition process for the removal of deteriorated and unsound concrete. This process provides an excellent bonding surface between the existing substrate and the LMC-VE overlay. Water jets are usually used for hydrodemolition, and since high water pressure is applied to remove the deteriorated concrete, hydrodemolition is a more efficient method than the use of jackhammers for removing deteriorated concrete (Choi and Yun 2014). It is recommended that the substrate surface be hydro-blasted to achieve a rough bonding surface any time an LMC-VE overlay is used, and the overlay should be limited to a maximum thickness of 3 in. in order to avoid problems associated with its bonding to the substrate (Wenzlick 2006). Additionally, a strict evaporation rate specification should be included in the special provisions for the mix to facilitate finishing of the concrete surface and avoid shrinkage cracking.

During the milling process, the milling machine might cut the reinforcement steel of the bridge deck. In such a scenario, the cut reinforcement steel needs to be removed using equipment such as a powered hand saw (Figure 2.10).



Theodore II et al. 2015

**Figure 2.10. Reinforcing steel cut by the milling machine being removed by powered hand saw**

Another key issue that may be encountered due to hydrodemolition is the occurrence of a punch-through, which must be fixed alongside the already ongoing overlaying work. One such incident (Figure 2.11a) was observed by the KYTC as a result of hydro-blasting during LMC-VE overlay work (Theodore II et al. 2015). Efforts to remove unsound concrete using jackhammers (Figure 2.11b) further expanded the hole to a size of 3 x 5 ft. Extra reinforcing steel in the void area and a plywood sheet at the bottom of the deck were placed to allow for casting of a partial deck repair. USG Duracal, a patching compound with a 3,200 psi break strength and a two-hour cure time, was used to fix the hole. The compound was poured to just below the upper reinforcing steel level, as shown in Figure 2.11d.





(a) Punch-through in deck, post hydrodemolition



(b) Repairing punch-through by jackhammering to remove loose concrete



(c) Duracal patching compound being mixed to fix the punch-through



(d) Patching material being applied to fill the punch-through

Theodore II et al. 2015

**Figure 2.11. Fixing a punch-through by KYTC**

#### *2.4.3 Mix Proportions and Acceptance Criteria*

The mix proportions used and the acceptance criteria adopted for LMC-VE by a few DOTs are given in Table 2.5 and Table 2.6, respectively.



**Table 2.5. Mix proportions used by a few DOTs**

DOT	Quantity (lb/yd <sup>3</sup> )			Water	Max. w/c
	Min. Cement (Type)	FA	CA		
Virginia	658 (CTS Cement Manufacturing Corp.)	1600	1168	205 (includes 52% water)	137 0.40
Ohio	658 (CTS Rapid Set)	1501	1170	206 (Styron/Dow Modifier A)	154 0.42
Missouri	658	FA:CA=50–55: 50–45		24.5 (gal/yd <sup>3</sup> )	158 (max) 0.40
Arkansas*	-	-	-	-	0.40
Indiana	658 (rapid set)	1600	1300	208	155 0.42

\* Proportions per bag of cement: 94 lb cement, 3.5 gal latex admixture, 210 to 255 lb natural sand, 168 to 208 lb coarse aggregate, and 8 to 22 lb water

**Table 2.6. Acceptance criteria adopted by a few DOTs**

Property	Virginia	Missouri	Arkansas	Indiana
Slump (in.)	4–6	3–6	6–9	7–10
Air (%)	3–7	0–6.5	3–8	0–7
Laboratory CS at 2 hours (psi)	≥ 2500	-	-	-
Field CS at traf (psi)	≥ 2500	≥ 3200	≥ 3000 (at 6 hours)	≥ 2500 (at 3 hours)
Laboratory CS at 1 day (psi)	≥ 3500	-	-	≥ 3500
Laboratory CS at 28 days (psi)	≥ 3500	-	4000	-
Pull-off strength at 28 days (psi)	-	No specified requirement	-	-

CS = Compressive strength

#### 2.4.4 Limitations

LMC-VE might exhibit very high heat of hydration at an early age because of its inherent rapid hardening and very large binder quantity, and it could be susceptible to autogenous shrinkage because of its relatively low w/c ratio (Choi and Yun 2014, Yun et al. 2007). Rapid hydration at an early age can cause cracking and decrease durability. The high temperature caused by rapid hydration can also induce thermal cracking, and the factors associated with early-age shrinkage, including autogenous shrinkage, can result in shrinkage cracking. Thus, the possibility of early-age cracking can be greater for LMC-VE than for ordinary portland cement (OPC) concrete (Choi and Yun 2014). Studies have indicated that the autogenous shrinkage of LMC-VE increases with an increase in latex-solid content, and the pattern appears to follow a logarithmic increase (Choi and Yun 2014, Yun et al. 2007). It is expected that the influence of this autogenous shrinkage on early-age deformation can be significant.

Various types of cracking have been observed in LMC-VE overlays by previous researchers (Choi and Yun 2014):

1. *Transverse cracking*: Transverse cracking is typically due to high shrinkage, high heat of hydration, and inadequate curing at an early age. Transverse cracking due to concrete material and construction issues can typically be visible seven days after concrete placement.
2. *Longitudinal cracking*: Longitudinal cracking is rarely observed in LMC-VE overlays.
3. *Map cracking*: General causes for map cracking are known to be shrinkage cracking, alkali-silica reaction, and freeze-thaw reaction. Map cracking in LMC-VE is most likely caused by early-age shrinkage and propagates within 15 days (Yun and Choi 2014). Map cracking may also occur due to debonding failure between the overlaid concrete and the existing substrate, and since it is related to serious deterioration in the substrate, it is not easy to prevent by improving the material properties of the LMC-VE.

Debonding can occur due to a large overlay thickness, the stresses between the overlay and the original substrate as a result of differential expansion and contraction, and a relatively smooth substrate surface texture left by the milling operation (Wenzlick 2006). Hence, LMC-VE bridge deck overlays should be kept to a maximum thickness of 3 in. In addition, hydro-blasting following milling is critical for creating a more irregular surface for better bonding between the overlay and the concrete substrate.

The costs of LMC-VE bridge deck overlays are 25% to 53% higher than those of conventional concrete bridge deck overlays, which restricts their usage.

#### *2.4.5 Advantages*

LMC-VE overlays provide a reliable driving surface and reduce user delays. The use of LMC-VE overlays for bridge deck repair can help avoid long lane closures in very high traffic areas (Wenzlick 2006). These overlays are intended to be ready for traffic within 3 to 6 hours of placement. On projects with complicated construction staging because of multiple lanes of heavy traffic, the fast-setting characteristics of LMC-VE overlays can accelerate the time between stages. Additional time can be saved if the decks do not require extensive repair and can use hydro-blasting (Wenzlick 2006). These time savings can offset the increased construction costs for LMC-VE overlays.

In terms of durability, LMC-VE incorporates all of the properties of conventional LMC but also performs relatively better. According to Sprinkel (1999, 2005), chloride permeability tests (AASHTO T 277) have shown that LMC-VE is significantly less permeable to chloride ions than LMC and therefore could be more durable. At 28 days, the permeability of conventional LMC overlays was determined to be low while that of LMC-VE overlays was determined to be low to very low. After 1 year, the permeability of LMC overlays was low while that of LMC-VE overlays was very low. In an evaluation of the first LMC-VE overlay in Virginia after 9 years of service, Sprinkel (1999) found that the bond strength was adequately high and the chloride permeability was still negligible, indicating long-term protection (Sprinkel 1999). Like other concrete overlays, LMC-VE overlays achieve high bond strengths with the appropriate selection and use of surface preparation equipment and procedures, mixture proportions, and placement and curing procedures. Compared to conventional LMC overlays, LMC-VE overlays are less prone to cracking because they undergo less shrinkage and therefore can be more durable. More

importantly, LMC-VE overlays cost about 75% of what conventional LMC overlays cost (Sprinkel 1999).

Similar to the life-cycle cost of LMC, which has a higher initial production cost, the life-cycle cost of LMC-VE should be compared to the sum of the initial production cost of conventional concrete plus the cost of the expected repair works during the service life of the structure, especially for structures exposed to severe/aggressive environments (Shaker et al. 1997). Moreover, the biggest advantage of LMC-VE is that it develops a compressive strength over 21 MPa within 3 hours after placement, thus shortening traffic closure times. Therefore, LMC-VE has the advantage of minimizing user costs due to traffic disruptions (Choi and Yun 2014).

Another cost consideration is that LMC-VE overlays cost about 75% of what conventional LMC overlays cost (Sprinkel 1999). The special cement required for LMC-VE overlays, however, costs four times as much as the Type I and II cements used for conventional LMC overlays. Although this adds approximately \$90 per cubic yard of concrete, the costs are more than offset by the large savings in the cost of traffic control and the time savings accrued through the use of LMC-VE. It is expected that DOTs that spend \$5 million per year on deck rehabilitation can save up to \$1.25 million per year by using LMC-VE overlays. LMC-VE (and LMC-HE) overlays can be placed for approximately 25% less than conventional LMC overlays. One example of a cost comparison that considered different overlay installations in Virginia (Sprinkel 1998) is summarized in Table 2.7. The table shows that LMC-VE overlays are cost-effective, considering both the reduction in the cost of overlay construction and the minimized inconvenience to motorists (Sprinkel 1998).

**Table 2.7. Cost of different overlays (\$/yd<sup>2</sup>)**

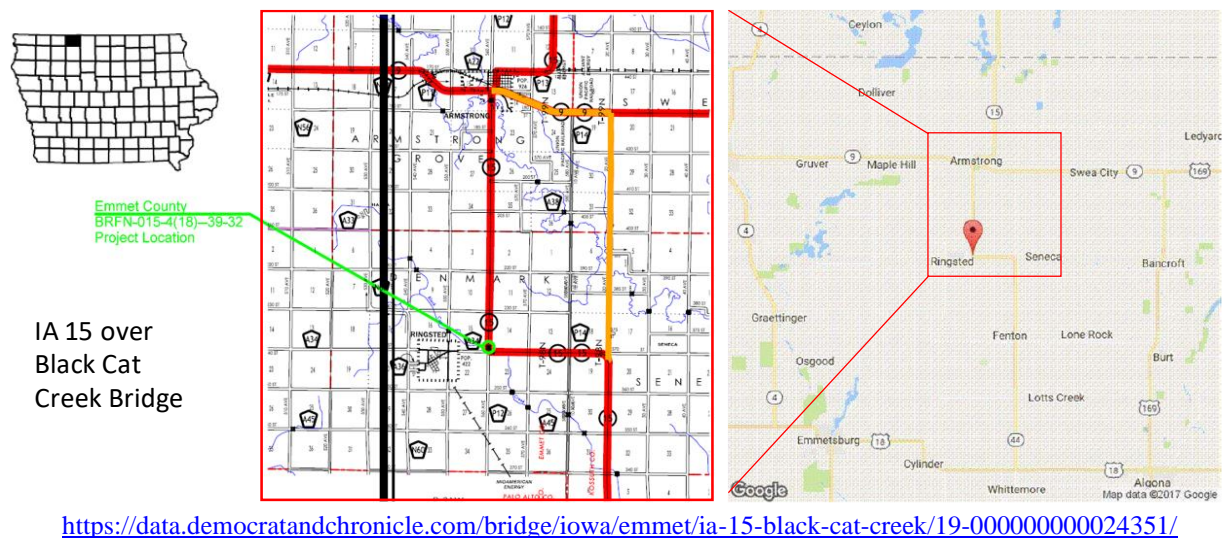
	<b>Epoxy</b>	<b>LMC</b>	<b>LMC-VE</b>	<b>LMC-HE</b>
Treatment	24	61	65	61
Miscellaneous	0	23	23	23
Traffic	8	46	8	8
Total	32	130	96	92
Life (years)	15	30	30	30
Life cycle	47	130	96	92
% Control	36	100	74	71

Source: Sprinkel 1998

### 3. DOCUMENTATION OF FIELD OVERLAY CONSTRUCTION

#### 3.1 Project Overview

The IA 15 bridge over Black Cat Creek, 6.4 miles south of IA 9 in Emmet County, Iowa, was selected for the first trial placement of an LMC-VE bridge deck overlay in Iowa. The bridge (Bridge ID 3248.5S015) was built in 1991 and has a single span 93 ft in length and 40 ft in width. It is a two-way traffic bridge, with an average daily traffic of 1,030, with 14% truck traffic. Figure 3.1 shows the location of the bridge.



**Figure 3.1. Bridge location**

The IA 15 bridge over Black Cat Creek consists of prestressed concrete beams with galvanized steel intermediate diaphragms and a cast-in-place concrete deck. Both abutments are integral concrete and are supported on steel H-piling. The most recent repair of this bridge occurred on October 8, 2013, according to an Iowa DOT report of a routine inspection conducted on July 3, 2017. Figure 3.2 shows an overview of the bridge, and Figure 3.3 presents the deck profile and the layout of the bridge.



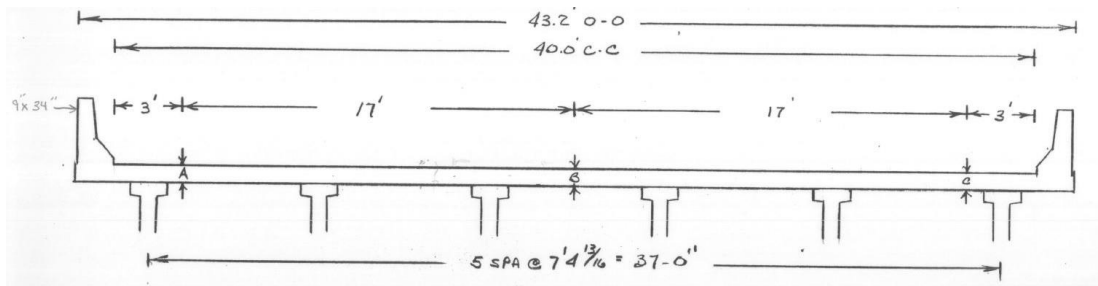
(a) Old deck surface



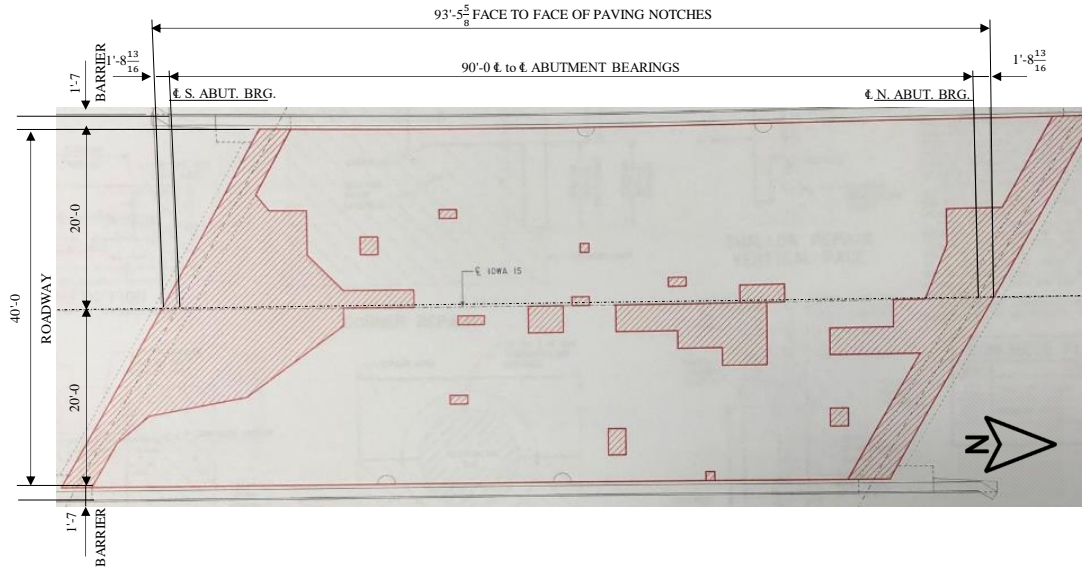
(b) Side profile of the bridge

Iowa DOT inspection report, July 3, 2017

**Figure 3.2. Overview of the bridge**



(a) Cross section of the bridge deck



(b) Bridge layout and dimensions

Iowa DOT inspection report, July 3, 2017

**Figure 3.3. Deck cross section and bridge layout**

As mentioned in Chapter 1, the main tasks of the present research project were to document the construction procedure and monitor the long-term performance of the LMC-VE overlay on the IA 15 bridge over Black Cat Creek. Table 3.1 shows a timeline of the related activities.

**Table 3.1. Major activities documented during LMC-VE overlay construction and performance monitoring**

<b>Project Timeline</b>	<b>Year</b>	<b>Date</b>	<b>Major Activities</b>	<b>Notes</b>
Pre-construction Stage	2019 (Start Year)	8/26/2019	Deck inspection before LMC-VE construction	Cracks and patches were mapped and photographed.
		8/26/2019	Deck milling	Complete milling operation was observed and documented. Photographs and videos were captured.
		8/28/2019	Hydrodemolition	Hydrodemolition operation was documented. Photographs and videos of activities were captured. Aggregate exposed post hydrodemolition was measured.
		9/5/2019	Sand-blasting and pre-wetting	The operation was documented. Photographs and videos were captured.
Construction Stage	2019 (Start Year)	9/5/2019	First half of LMC-VE overlay installation (Starting at 10:45 p.m.)	Complete overlay pouring and casting operations were documented. Photographs and videos were captured. Setting time was measured on site. Specimens to determine mechanical strength (compressive, flexural, and bond strength) and durability performance (SR, salt ponding, sorptivity, freeze-thaw, shrinkage) were cast. Initial shrinkage measurements were taken, and all specimens were transferred to ISU's PCC Lab (except 3 cylinders that were field cured for 3 days).
		9/5/2019	Wet burlap removal (Four hours after first cast)	Photographs were captured.
		9/6/2019	Second half of LMC-VE overlay installation (Starting at 4 a.m.)	Installation and related procedures were documented via photographs and videos.
		9/6/2019	Wet burlap removal (Four hours after second cast)	Photographs were captured.

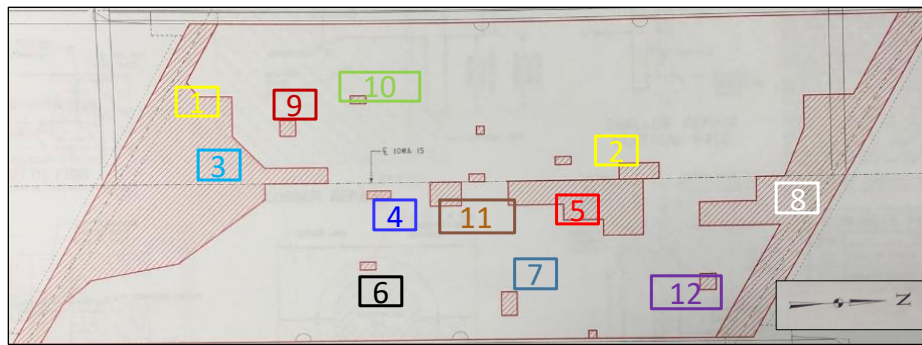
Project Timeline	Year	Date	Major Activities	Notes
Post-construction Stage (Field Testing and Monitoring of Short- and Long-Term Overlay Performance)	2019 (Start Year)	9/10/2019	Field monitoring Trip 1 (Age: 4 days)	Surface resistivity, friction index, and pull-off tests were performed. The pull-off tests' broken cores were brought to the laboratory for sorptivity tests.
		11/04/2019	Field monitoring Trip 2 (Fall trip, age: 60 days)	A crack survey (mapped and photographed) and SR, friction index, and pull-off tests were conducted. The pull-off tests' broken cores were brought to the laboratory for sorptivity tests.
	2020 (Year 1)	05/20/2020	Field monitoring Trip 3 (Spring trip, age: 8.5 months)	A crack survey (mapped and photographed) and SR, friction index, and pull-off tests were conducted. The pull-off tests' broken cores were brought to the laboratory for sorptivity tests.
		11/02/2020	Field monitoring Trip 4 (Fall trip, age: 14 months)	A crack and deterioration survey (mapped and photographed) and SR, friction index, and pull-off tests were conducted.
	2021 (Year 2)	05/12/2021	Field monitoring Trip 5 (Spring trip, age: 20 months)	A crack and deterioration survey (mapped and photographed) and SR, friction index, and pull-off tests were conducted.
		11/08/2021	Field monitoring Trip 6 (Fall trip, age: 26 months)	A crack and deterioration survey (mapped and photographed) and SR, friction index, and pull-off tests were conducted.
	2022 (Year 3)	05/19/2022	Field monitoring Trip 7 (Spring trip, age: 32 months)	A crack and deterioration survey (mapped and photographed) and SR, friction index, and pull-off tests were conducted.
		10/28/2022	Field monitoring Trip 8 (Fall trip, age: 38 months)	A crack and deterioration survey (mapped and photographed) and SR, friction index, and pull-off tests were conducted.
	2023 (Year 4)	05/23/2023	Field monitoring Trip 9 (Spring trip, age: 44 months)	A crack and deterioration survey (mapped and photographed) and SR, friction index, and pull-off tests were conducted.
		11/06/2023	Field monitoring Trip 10 (Fall trip, age: 50 months) (Last Field Trip)	A crack and deterioration survey (mapped and photographed) and SR, friction index, and pull-off tests were conducted.



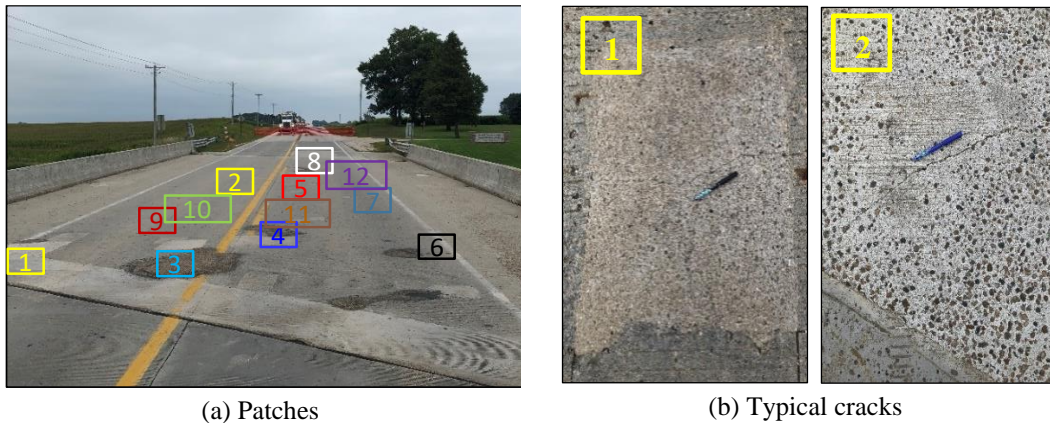
### 3.2 Deck Inspection Prior to LMC-VE Placement

Prior to construction (on August 26, 2019), the existing bridge surface was visually inspected for the presence of cracks, scaling, spalling, and other signs of damage. The locations of any prior patching were mapped and photographed. The information would later serve as a reference for the long-term performance monitoring of the installed LMC-VE overlay.

As shown in Figure 3.4, several patches and several fine cracks were observed on the deck, but there were few/no large cracks or instances of severe joint deterioration, scaling, or spalling. The shaded areas in the figure indicate the partial-depth repair areas required for the present project. Figure 3.5a shows patch locations, and Figure 3.5b presents some cracks found on the surfaces of the patches.



**Figure 3.4. Locations of patched material on bridge deck surface**



**Figure 3.5. Patch locations and cracks on bridge deck surface**

### 3.3 Preparation for Overlay Installation

Preparation for installation of the LMC-VE overlay consisted of (1) milling of the existing deck surface, (2) hydrodemolition, and (3) sand-blasting, which were mainly used to improve the bond between the new overlay and the substrate concrete.



### 3.3.1 Milling

Figure 3.6a shows an overview of the milling process. The surface of the deck was milled, and the resulting debris was placed in a dump truck. Any remaining debris was cleared by a skid steer loader that followed the milling machine. Figure 3.6b shows a comparison between the milled and the unmilled surfaces of the deck. The corners and edges were milled using a micro miller, as shown in Figure 3.6c. Figure 3.6d shows the final deck surface after the milling operation was completed. The entire milling procedure was completed over a duration of 2 hours on August 26, 2019.



(a) Overview of milling process



(b) Milled and unmilled surfaces



(c) Micro milling at the edges



(d) Deck surface after completion of milling

**Figure 3.6. Sequence of milling operation**

### 3.3.2 Hydrodemolition

Hydrodemolition was conducted to remove all unsound concrete from the milled surface. It was performed by CLC Hydro Services from August 28 to September 2, 2019. Figure 3.7a shows an overview of the operation. The hydro pressure used was 14,700 psi, above that required for typical overlay demolition work, which is 13,000 psi. The hydrodemolition speed was controlled by the rate of water that was used, which was 25 gallons per minute, lower than the required rate of 55 gallons per minute. The debris created by the process was collected by a skid steer loader, as shown in Figure 3.7a. Any remaining loose particles were then removed by manual power washing. This washing exposed the epoxy-coated reinforcement bars, as shown in Figure 3.7b.

The hydrodemolition and power washing provided a rough and exposed aggregate surface, as shown in Figure 3.7c. Figure 3.7d shows the Class A removal at different locations where excess substrate concrete was removed above and, in some cases, below the reinforcement bars. Both the milling and hydrodemolition operations together removed a total depth of 3 in. from the existing deck.



**Figure 3.7. Hydrodemolition operation**

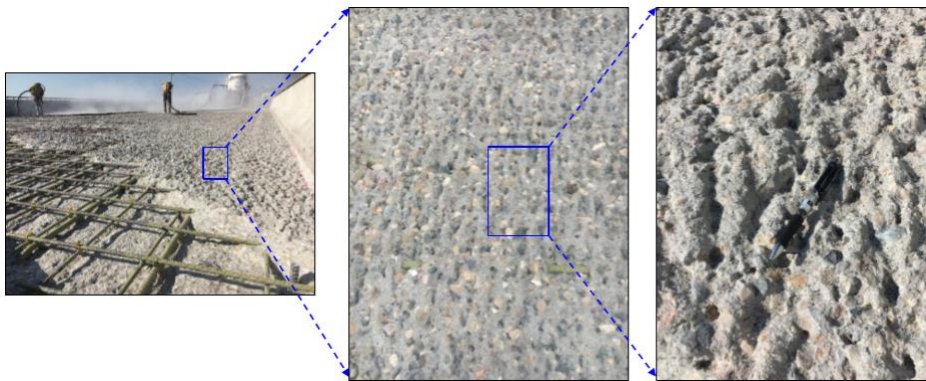
### 3.3.3 Sand-Blasting

Prior to overlay placement, the prepared surface was cleaned thoroughly via sand-blasting. Sand-blasting was performed at noon on the same day of but prior to overlay placement. Figure 3.8a shows the manual sand-blasting process, which left the textured surface shown in Figure 3.8b.





(a) Overview of sand-blasting operation

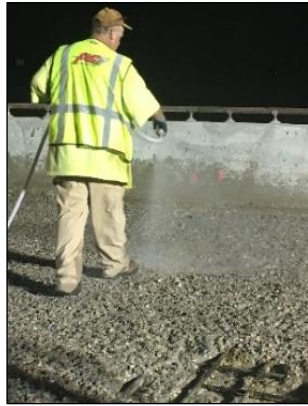


(b) Microtexture of sand-blasted surface

**Figure 3.8. Sand-blasting of the surface**

### *3.3.4 Surface Wetting*

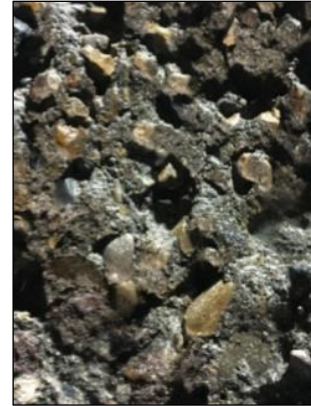
The sand-blasted surface was wetted with water to keep the surface saturated for the LMC-VE casting, as shown in Figure 3.9. The wetted surface was covered with polyethylene sheeting until the time of overlay placement.



(a) Water sprayed on surface



(b) Pre-wetted rebar



(c) Pre-wetted substrate

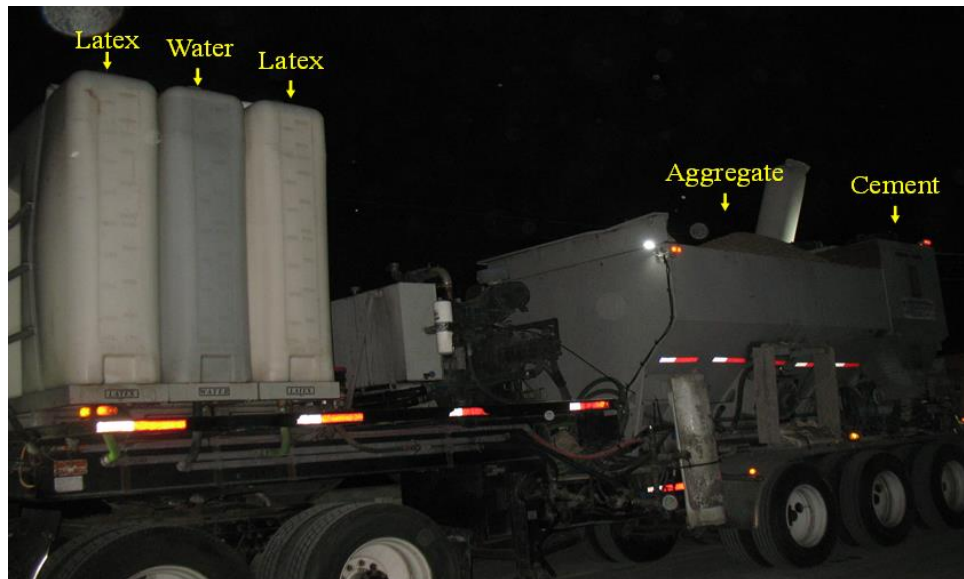
**Figure 3.9. Pre-wetting of deck surface prior to overlay placement**

### **3.4 LMC-VE Overlay Installation**

The overlay was cast in two passes (or in two different pours). The first pass began at 10:45 p.m. on September 5, 2019, and ended at 1:20 a.m. on September 6, 2019. The actual ambient temperatures measured at the nearest town were 54°F (low) and 82°F (high) on September 5, 2019, and 60°F (low) and 76°F (high) on September 6, 2019. The LMC-VE materials were mixed using the volumetric mobile mixer truck shown in Figure 3.10a, which was then backed onto the deck in front of the finishing machine. All of the required materials were preloaded into the mixer truck in designated containers, as shown in Figure 3.10b.



(a) Mobile mixing truck



(b) Preloaded materials in different containers mounted on the mixing truck

**Figure 3.10. Volumetric mobile mixer truck used for in situ mixing of concrete**

Immediately after being dispensed from the mixer, the concrete was poured from one end of the deck surface to the other (from north to south). The poured concrete was spread manually and then finished with a Bidwell finishing machine (screed), as shown in Figure 3.11a. The LMC-VE was highly flowable and was self-consolidating.

As the paver progressed, the cast overlay surface was immediately covered with a clean, single layer of presoaked burlap to prevent any loss of moisture from the concrete surface, as shown in Figure 3.11b. Fog was manually sprayed over the wet burlap surface immediately and continuously to ensure prevention of moisture loss (Figure 3.11b). This was an especially important step because the rate of hydration is particularly fast in LMC-VE, and any moisture loss would result in high shrinkage and the formation of shrinkage cracks.



The cast surface was moist cured (Figure 3.11e) for 4 hours according to Section 150447.03.C.5.b of the special provisions (SP-150447), after which the wet burlap was removed (Figure 3.11f).

Figure 3.12a shows the finished and cured surface of the LMC-VE overlay after 4 hours, and Figure 3.12b shows the cast and uncast surfaces of the deck.



(a) Overview of the overlay casting operation



(b) Cast surface covered with presoaked burlap



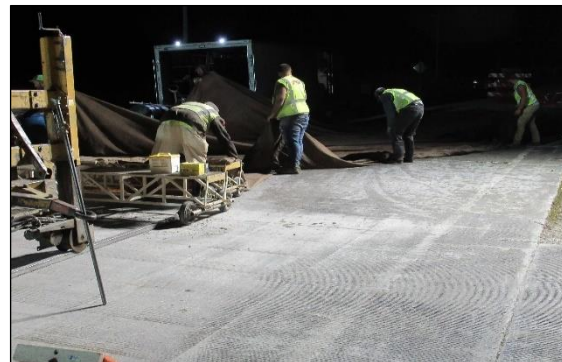
(c) Fogging over the wet burlap cover



(d) Wet burlap kept for 4 hours of wet curing



(e) Overlay cast on half of the deck surface



(f) Wet burlap removal after 4 hours

**Figure 3.11. First half of overlay casting**



(a) Overlay surface after wet burlap removal



(b) Cast versus uncast surface

**Figure 3.12. Completion of the first half of overlay casting**

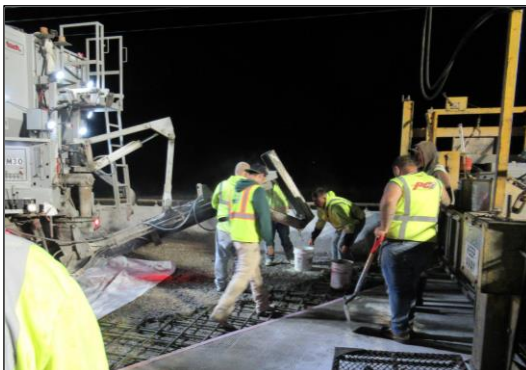
Casting of the second half of the LMC-VE overlay began around 5:45 a.m. and ended at about 7:30 a.m. on September 6, 2019. The LMC-VE was made using the same mix proportions and was poured using the same procedures as those used to cast the first half of the overlay, and pouring proceeded from north to south. As shown in Figure 3.13a, construction vehicles had already moved onto the first half of the overlay, which had been poured only about 3.5 hours earlier. After the pouring, the overlay was similarly wet cured for 4 hours (Figure 3.13d).



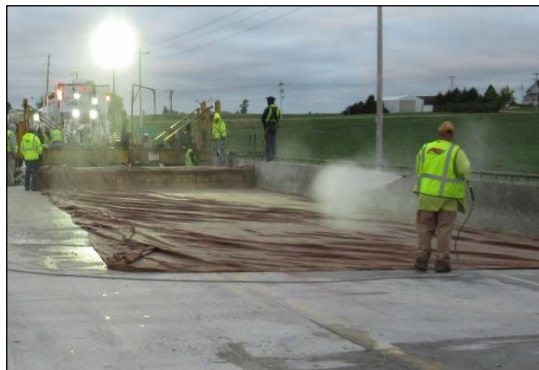
(a) Preparation for second pour



(b) Beginning of second pour



(c) Pouring on second half of the deck surface



(d) Fogging over wet burlap

**Figure 3.13. Second half of overlay casting**

### 3.5 Materials and Mix Proportion of the LMC-VE

The materials and mix proportions of the LMC-VE used in this research project (provided by Modified Concrete Suppliers, LLC of Indianapolis, Indiana) are given in Table 3.2. The properties of the latex used (provided by Trinseo of Midland, Michigan) are given in Table 3.3. As mentioned previously, the LMC-VE materials were mixed on site in a mobile mixing truck (Figure 3.10a) just before pouring.

**Table 3.2. Materials and mix proportions of LMC-VE**

Material	Type	Specific Gravity	Volume (ft <sup>3</sup> )	Weight (lb/yd <sup>3</sup> )
Cement	CTS Rapid Set, Juarez, Mexico	2.98	3.54	658
Sand	1-4110, Hallet Mat, Emmetsburg, 2101	2.71	9.07	1533
Coarse aggregate	0839-1/2" Martin Marietta, Moore A76004	2.62	7.42	1213
Latex	Trinseo (Dow) Mod A, Midland, Michigan	1.01	3.30	208 (24.5 gal)
Water	City	1.00	2.32	145 (as needed)
Air	(Estimated @5%)	-	1.35	-
Citric acid	(1/2% to 1% by wt of a bag of cement)	-	-	-

Note: CTS Rapid Set cement contains approximately 90 to 100 wt% calcium sulfoaluminate (CSA) cement and < 0.1 wt% crystalline silica (quartz).

**Table 3.3. Properties of latex**

Test	Unit	Lower Limit	Upper Limit	Value
Solids	%	47.0	49.0	49.0
pH	-	9.0	11.0	10.0
200 mesh residue (per 900 mL)	G	-	0.500	0.001
Brookfield viscosity (#1 spindle @10 rpm)	cP	5	40	31
Particle size	Nm	175	205	185
Surface tension	mN/m	22.0	31.0	28.0
Freeze thaw stability	g	-	0.10	0.00
Shipping temperature	°C	10.0	30.0	25.0
Butadiene content	%	30.0	40.0	34.8
Density	lb/gal	8.40	8.60	8.55

### 3.6 Trial Mixing of the LMC-VE Prior to Pouring

Prior to the beginning of the actual pouring of the LMC-VE overlay, a trial mix was prepared by the contractor on the evening of September 5, 2019, to confirm the fresh slump, air content, and 3-hour compressive strength of the concrete. The trial mix was prepared using the same mix proportions provided in Table 3.2, and three trial specimens were cast in the field immediately after concrete mixing. The trial mix had a slump of approximately 9 in. and an air content of 5.5% in the fresh state and an average 3-hour 40-minute compressive strength of 2,827 psi (i.e., 2,916 psi for Specimen 1, 2,738 psi for Specimen 2, and 2,827 psi for Specimen 3).



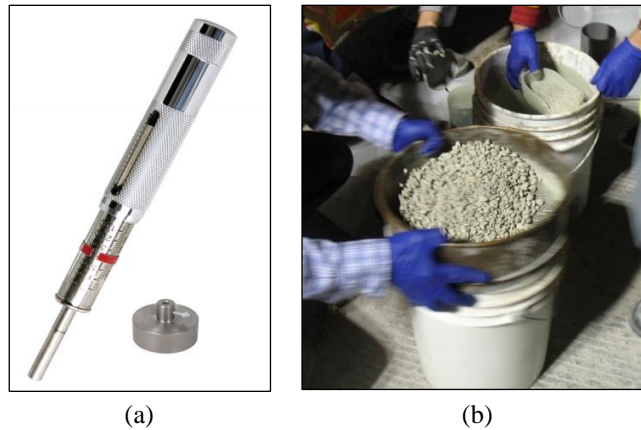
### 3.7 Tests Conducted During Overlay Construction

Various tests were conducted in the field and in the laboratory to gain an understanding of the performance of LMC-VE. Table 3.4 summarizes the types of tests conducted.

**Table 3.4. Details of tests conducted**

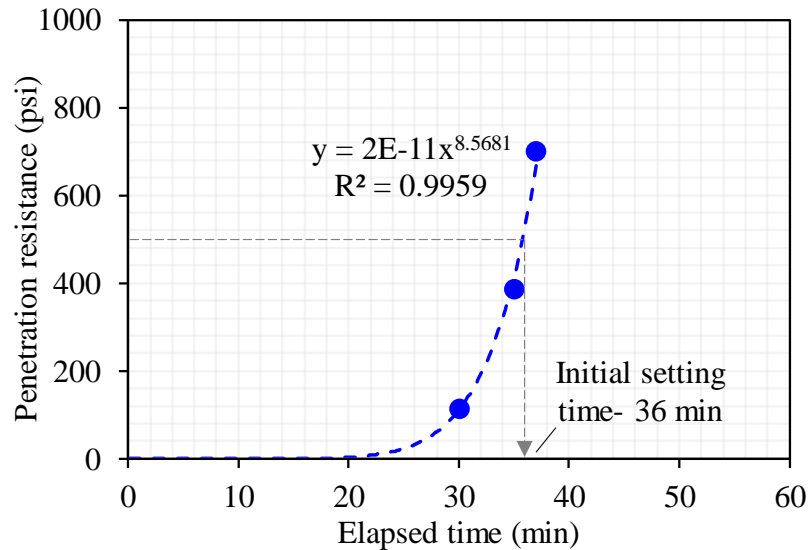
	Tests	Purpose
Field tests	Setting time	For measurement of initial and final setting time of mortar
	Surface resistivity (SR)	Electrical test to understand resistance of LMC-VE to chloride intrusion
	Pull-off strength	For evaluating strength of bond between substrate and LMC-VE
	British Pendulum Test	For surface roughness/friction measurement
Laboratory tests	Mechanical strength	To evaluate development of compressive and flexural strengths with age
	Isothermal calorimetry	To understand heat evolution due to hydration
	Pull-off strength	To evaluate strength of bond between substrate and LMC-VE
	Shrinkage	To measure drying, autogenous, and restrained shrinkage
	SR	Electrical test to understand resistance of LMC-VE to chloride intrusion
	Water sorptivity	Non-electrical test to obtain information on the pore structure and resistance of LMC-VE to chloride intrusion
	Salt ponding	Non-electrical test to understand resistance of LMC-VE to chloride intrusion
	Freeze-thaw	To evaluate resistance of LMC-VE to freeze-thaw deterioration

The setting time of the LMC-VE was measured on site during the overlay construction. The measurements were obtained according to ASTM WK27337 using a pocket penetrometer, shown in Figure 3.14a. The measurements were made on fresh mortar that was sieved from the LMC-VE using a #4 sieve, as shown in Figure 3.14b.



**Figure 3.14. (a) Pocket penetrometer and (b) mortar sieved from LMC-VE**

A pocket penetrometer is a simple device that provides results that are comparable with those of other tests, such as the Vicat needle and Gillmore needle (Rupnow 2013). Using a pocket penetrometer, the initial setting time was measured as the time required to achieve a penetration resistance of 500 psi, and the final setting time corresponded to a penetration resistance of 4,000 psi using extrapolation from the obtained data points, as shown in Figure 3.15.



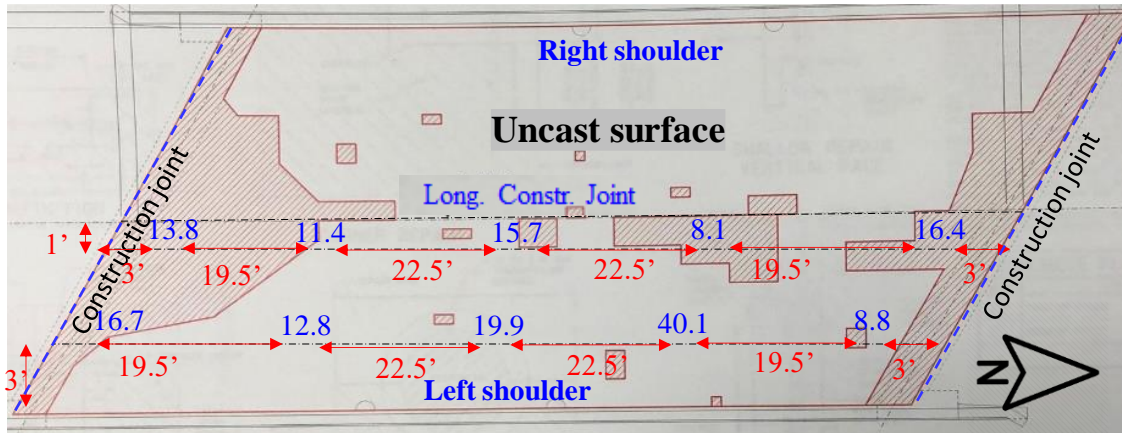
**Figure 3.15. Setting time of mortar sieved from LMC-VE**

### 3.6.2 Surface Resistivity

About 3 hours after the first pour of the LMC-VE overlay, the SR of the overlay was measured on site using a handheld four-point Wenner probe (Proceq Resipod). The testing was done in accordance with AASHTO T 358. Because the freshly cast overlay was very moist, the measurements were taken by directly placing the four electrodes of the device on the surface at the selected locations (Figure 3.16a). Measurements were taken at various locations on the left shoulder and close to the longitudinal construction joint of the deck surface. At each location, two measurements were made. The test locations and the average of the two SR measurements at each location are shown in Figure 3.16b. The distances of the locations (in feet) with respect to the construction joints are given in red numbers, and the SR values (in kΩ-cm) are given in blue numbers. The SR measurements near the longitudinal construction joint varied from 8.1 to 16.4 kΩ-cm, and those on the left shoulder varied from 8.8 to 40.1 kΩ-cm. (At the time of the first SR measurement, it was noticed that the LMC-VE overlay covered by wet burlap felt very warm due to the heat released by rapid cement hydration.)



(a) On-site SR measurements



(b) SR measurement of overlay 3 hours after casting

**Figure 3.16. Surface reactivity measurements of overlay 3 hours after casting**

### 3.6.3 Field Sample Preparation

Specimens for most of tests listed in Table 3.4 were cast in the field during overlay construction (Figure 3.17). Table 3.5 provides some details on the cast specimens. The cast specimens, along with their molds, were then brought to Iowa State University's Portland Cement Concrete Research Laboratory on the same day. The specimens were retained in their molds for one day. After being removed from their molds, the specimens were then moist cured in a standard curing room ( $23 \pm 3^\circ\text{C}$  [ $73 \pm 5^\circ\text{F}$ ] and  $95 \pm 3\%$  relative humidity [RH]) for three days. Thereafter, they were placed in a room at  $23 \pm 3^\circ\text{C}$  until their testing ages. Additionally, three cast cylinder specimens were left in their plastic molds at the field site for three days before they were brought back to the laboratory for testing.



**Figure 3.17. Casting test specimens during overlay construction**

**Table 3.5. Details of cast specimens**

Test	Specimen Dimensions (in. x in.)	Testing Age	Total Specimens
Compressive strength (cylinder)	4 x 8	(3 hours), 12 hours, 1 day, 3 days, 7 days, 28 days	18
Flexural strength (beam)	3 x 3 x 11	1 day, 3 days, 7 days, 28 days	8
Elastic modulus (cylinder)*	-	-	-
Bond strength/Pull-off (slab)	12 x 12 x 3.5	28 days	3
Surface resistivity (cylinder)*	-	3 hours, 12 hours, 1 day, 3 days, 7 days, 28 days	-
Salt ponding (slab)	12 x 12 x 3.5	142 days	2
Drying shrinkage (beam)	3 x 3 x 11	-	3
Autogenous shrinkage (beam)	3 x 3 x 11	-	3
Freeze-thaw (beam)	3 x 4 x 16	28 days	4

\* Cylinders that were cast for testing compressive strength were also used for these tests.

After the overlay was placed, regular field visits were conducted and the long-term performance of the LMC-VE overlay was monitored for five years. The results of the laboratory testing of

these field-cast specimens and the long-term field monitoring of the overlay are presented in Chapters 4 and 5, respectively.

## 4. LABORATORY TESTS AND RESULTS

As mentioned previously, the setting time of the LMC-VE was tested at the field site, and the results are presented in Chapter 3. To evaluate the hardened LMC-VE properties, samples were cast in the field and then tested in the Portland Cement Concrete Research Laboratory at Iowa State University. The hardened LMC-VE properties evaluated included mechanical properties (e.g., compressive, flexural, and pull-off bond strength) and durability properties (e.g., SR, water sorptivity, shrinkage, chloride penetration, and freeze-thaw resistance). All results from the hardened concrete property tests are presented in this chapter. Information on the LMC-VE materials and mix proportions can be found in Section 3.5.

In addition, small amounts of cementitious materials, latex, and citric acid were brought from the field site and were used for chemical analysis of the cement and to mix pastes for the heat of hydration tests. These test results are also presented in this chapter.

### 4.1 Laboratory Tests and Methods

Immediately after casting in the field, all specimens were covered with wet rags and left to sit for 3 hours, after which the specimens were transferred in their molds to ISU's PCC Lab. The specimens were retained in their respective molds for 24 hours and were then removed from their molds. The specimens were then moist cured for 3 days in a moisture room maintained at a temperature of  $23\pm3^{\circ}\text{C}$  and a relative humidity of  $95\pm3\%$ . Thereafter, the specimens were placed in a room maintained at  $23\pm3^{\circ}\text{C}$  (i.e., air cured at room temperature) until their testing ages. In the laboratory, a few paste mixes were also prepared using the same materials and mix proportions as those used for the field LMC-VE. These mixes were used to perform isothermal calorimetry to understand the heat evolution pattern resulting from the hydration reaction.

#### 4.1.1 Chemical Composition

The chemical composition of the rapid-set cement (CTS Rapid Set) used for the overlay was analyzed at the Materials Analysis and Research Laboratory (MARL) at Iowa State University using x-ray fluorescence.

#### 4.1.2 Isothermal Calorimetry

Calorimetry is the measurement of heat and the rate of heat generation. A semi-isothermal calorimeter measures heat and the rate of heat generation at a constant temperature. In this study, a PTC-1 calorimeter was used to perform the calorimetry tests. The calorimeter contains eight separate channels, each of which holds a single specimen during the test. Each channel has an aluminum sample holder, which rests on a heat flow sensor that is placed on a common heat sink consisting of a large block of aluminum. On the other side of the heat sink is another heat flow sensor and a 129 g aluminum block. The aluminum block is used as a reference to reduce the noise signal in the conduction calorimeter. When a sample is placed in the unit, the heat produced by hydration flows rapidly to its surroundings. The main route for heat exchange



between the sample and the surroundings is through the heat flow detector. The heat flow, which causes a temperature difference across the sensor, creates a voltage signal proportional to the amount of heat flow. This voltage signal is then converted to the rate of heat evolution by applying a calibration factor based on the reference material (aluminum) (Wang et al. 2020b, Sargam et al. 2019a).

#### 4.1.3 Mechanical Strength

The compressive strength of LMC-VE was evaluated at specimen ages of 3 hours, 12 hours, 1 day, 3 days, 7 days, and 28 days. Testing was done using standard 4 × 8 in. cylinder specimens (Figure 4.1a) in accordance with ASTM C39. An average of three specimens were measured at each testing age. Flexural strength was evaluated at specimen ages of 3, 7, and 28 days. Testing was done on 3 × 3 × 11 in. beam specimens (Figure 4.1b) using the third-point bending test in accordance with ASTM C78. An average of three specimens were measured at each testing age.



(a) Compressive strength test specimens

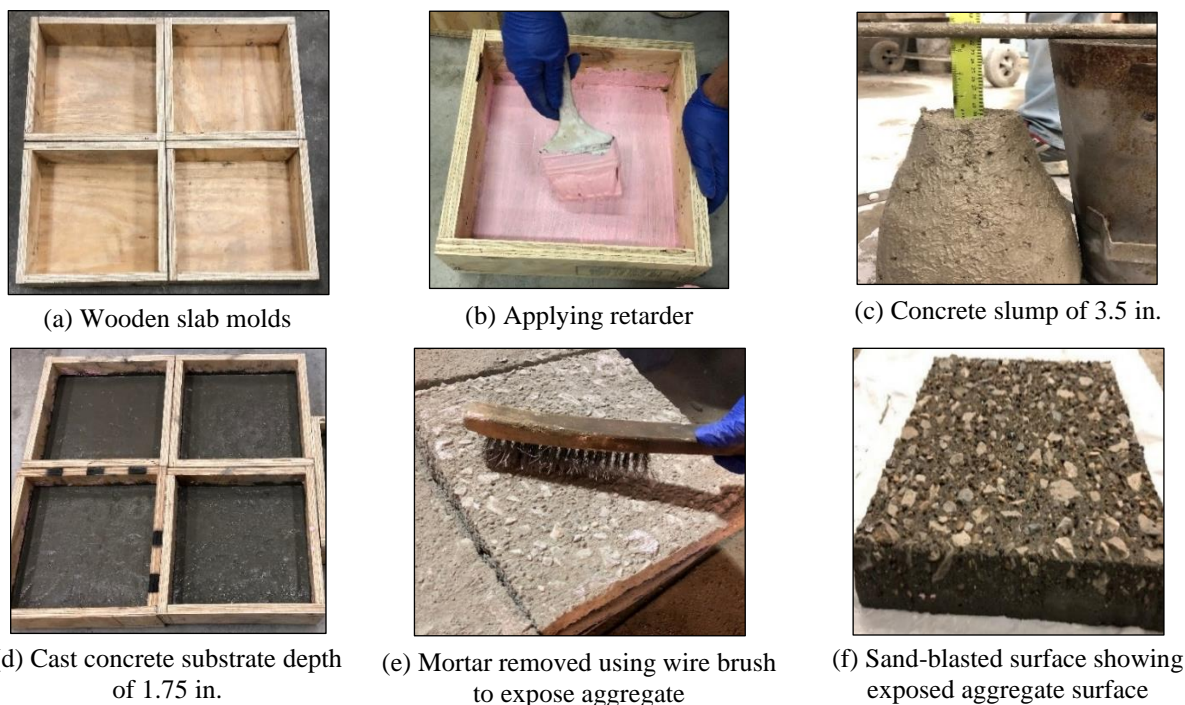


(b) Flexural strength test specimens

**Figure 4.1. Mechanical strength and elastic modulus test specimens**

#### 4.1.4 Pull-Off Strength

To perform pull-off strength tests in the laboratory (ASTM C1583), a substrate concrete mixture was prepared six months prior to the LMC-VE overlay application and was cast in 12 × 12 × 1.75 in. (l × b × h) slab molds. These substrate slabs were cast using the same concrete mix proportions used for the actual bridge (Class D mix). Figure 4.2 (a–f) shows the preparation of the substrate concrete, and Table 4.1 provides the details of the mix proportions used to prepare the substrate slabs. Note that a retarder solution was added to one surface of the formwork to inhibit the hardening of the surface of the concrete. The prepared substrate mix had a slump of 3.5 in., a unit weight of 140.8 lb/ft<sup>3</sup>, and a fresh air content value of 9%. One day after casting, the slabs were removed from their molds, and the mortar at the bottom surface of the cast slab that was in contact with the retarder was brushed off using a metal wire brush to expose the aggregates for the purpose of providing a better bond with the overlay material. The brushed surface was further sand-blasted (by the Iowa DOT) to expose a sufficient surface area of the aggregates with the intention of enhancing the bonding between the LMC-VE overlay and the substrate.



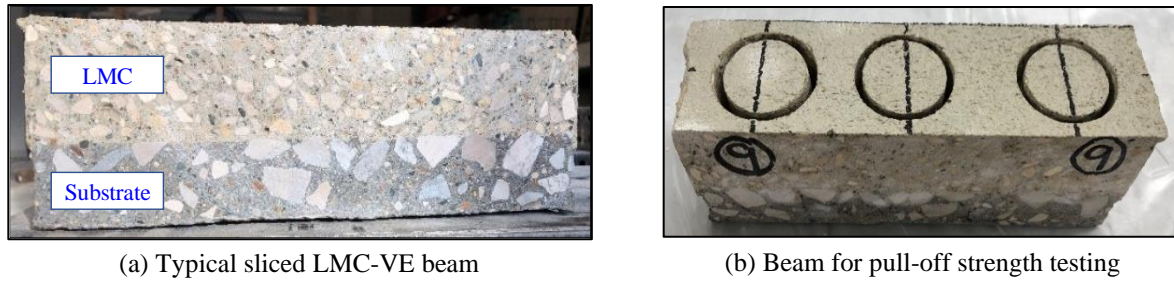
**Figure 4.2. Preparation of substrate concrete for pull-off tests at ISU's PCC Lab**

**Table 4.1. Mix design used for substrate concrete in slabs**

Material	Proportion (lb/yd <sup>3</sup> )	Batch Weight (lb)
Cement	710	33.25
Sand	1,696	79.42
Coarse aggregate (D57)	1,130	52.91
Water	291.1	13.63
Air-entraining agent	210.2	9.84
Water reducer (ml/yd <sup>3</sup> )	629.8	29.49

These substrate slabs were then overlaid with LMC-VE to a depth of 1.75 in. (to simulate the average thickness of the LMC-VE overlay in the field) during construction of the field overlay. The overall dimensions of the slabs, including both the substrate and LMC-VE overlay, were 12 × 12 × 3.5 in. (l × b × h). Prior to placing the overlay material over the substrate concrete, a thin layer of mortar (sieved from the LMC-VE) was applied to the substrate's surface to ensure a better bond between the overlay and substrate concretes. The overlaid slabs were cured in the moisture room for 3 days and then air cured until a specimen age of 28 days. After 28 days, the slabs were sliced to prepare beams with dimensions of 11 × 3 × 3.5 in. (l × b × d). A typical sliced beam is shown in Figure 4.3a. The prepared beams were divided into two sets. One set of beams was used to determine pull-off strength, and the other set of beams was utilized to determine freeze-thaw performance.

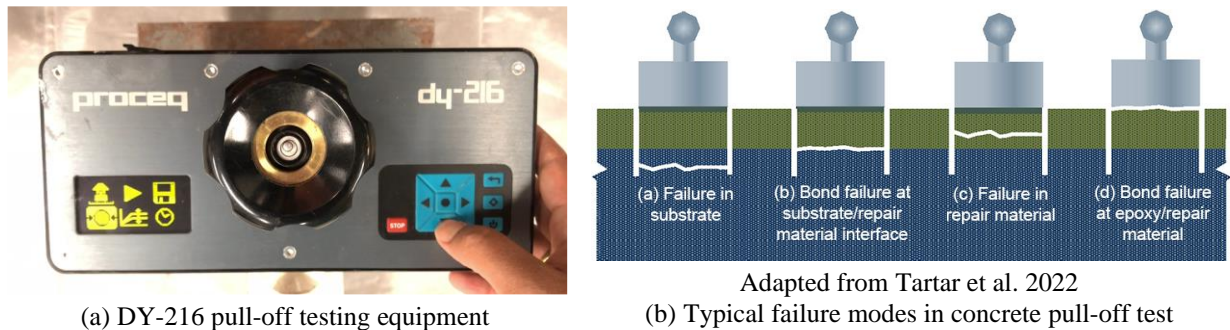




**Figure 4.3. LMC-VE-overlaid beam specimens sliced from the cast slab specimens**

The pull-off test was performed using Proceq DY-216 pull-off test equipment (Figure 4.4a). The testing was done in accordance with ASTM C1583 as per the following procedure:

1. Three shallow cores were drilled to a depth of 3 in. on each specimen, as shown in Figure 4.3b.
2. The top surfaces were brushed using sandpaper to remove any dirt and loose material that was present.
3. A puck was glued to each of the three locations using high-strength epoxy.
4. The pucks were left undisturbed for 4 to 5 hours. Once the pucks were firmly adhered to the surface, the pucks were screwed to the pull-off test equipment and a load was applied until failure occurred.
5. The strength value and the specimen failure mode (Figure 4.4b) were recorded.

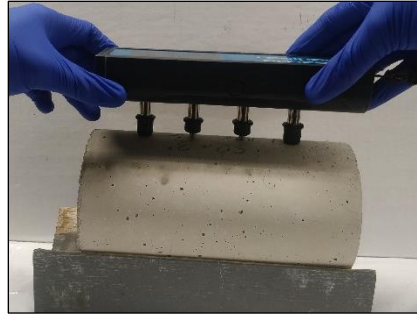


**Figure 4.4. Pull-off testing equipment and typical failure modes obtained during testing**

#### 4.1.5 Surface Resistivity

Surface resistivity was measured using a handheld four-point Wenner probe (Proceq Resipod), shown in Figure 4.5. The testing was done on standard 4 × 8 in. cylinder specimens in accordance with AASHTO T 358. For each specimen, the four electrodes of the Resipod were dipped in water (to ensure good contact between the electrodes and the specimen surface) and pressed against the specimen's surface to obtain the SR reading in  $k\Omega\text{-cm}$ . Testing was done at 1, 3, 7, 14, and 28 days. Specimens were tested in saturated surface wet condition until 3 days of age, after which only the surfaces of the specimens were wetted before testing. This was because the specimens were wet cured for only 3 days, after which the specimens were air cured in a

room at  $23 \pm 3^\circ\text{C}$ . However, the air cured specimens gave fluctuating/unstable readings at 28 days. Therefore, further measurements at later ages (170 days, 340 days, and 440 days) were taken after the cylinders had been soaked in water for 2 days to ensure stable SR readings. An average of eight values were measured for each cylinder specimen, and an average of three cylinders were measured at each testing age.

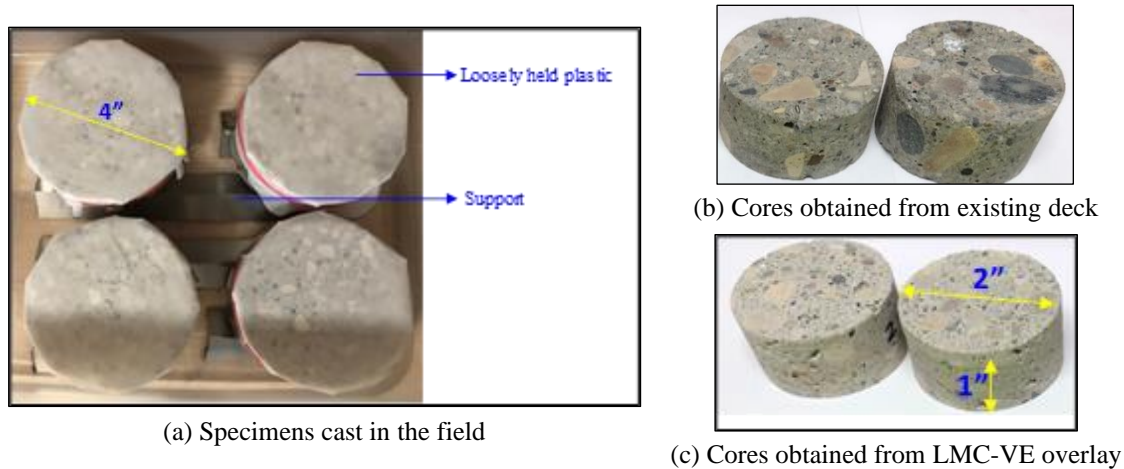


**Figure 4.5. Surface resistivity measurement using four-point Wenner probe**

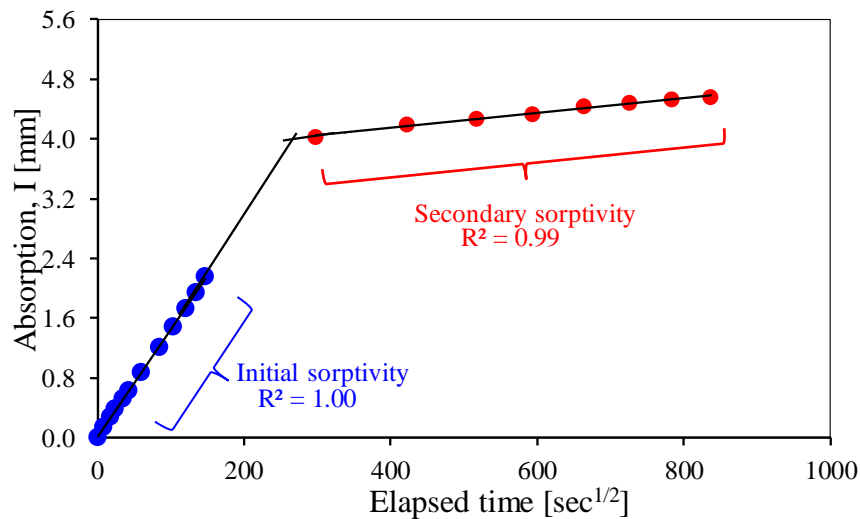
#### *4.1.6 Water Sorptivity*

The sorptivity (i.e., water absorption) test was performed on  $4 \times 2$  in. ( $d \times h$ ) LMC-VE specimens sliced from  $4 \times 8$  in. ( $d \times h$ ) cast cylinders at an age of 28 days, as shown in Figure 4.6a. The test was performed in accordance with ASTM C1585. The top and bottom 2 in. of the standard  $4 \times 8$  in. cylinders were discarded prior to obtaining the sorptivity test specimens. An average of only those initial (0 to 6 hours) and secondary (1 to 8 days) sorptivity test results that had a correlation coefficient (R value) greater than 0.98 were considered, as per the recommendations in the standard. An average of four specimens that were cut from two cylinders was considered to be the average sorptivity at each age.

Similarly, the sorptivity test was also performed on smaller  $2 \times 1$  in. ( $d \times h$ ) specimens cut from the cores obtained for the pull-off tests performed on the bridge deck in the field at different ages after overlay placement. After pull-off testing, these cores were sliced to obtain the LMC-VE portions from the failed cores (Figure 4.6c) for sorptivity testing. Similar smaller sized test specimens were also prepared using cores collected from the existing HPC deck (Figure 4.6b) for the purpose of comparison. A typical sorptivity test curve of a conventional concrete showing bilinear sorption behavior is shown in Figure 4.7.



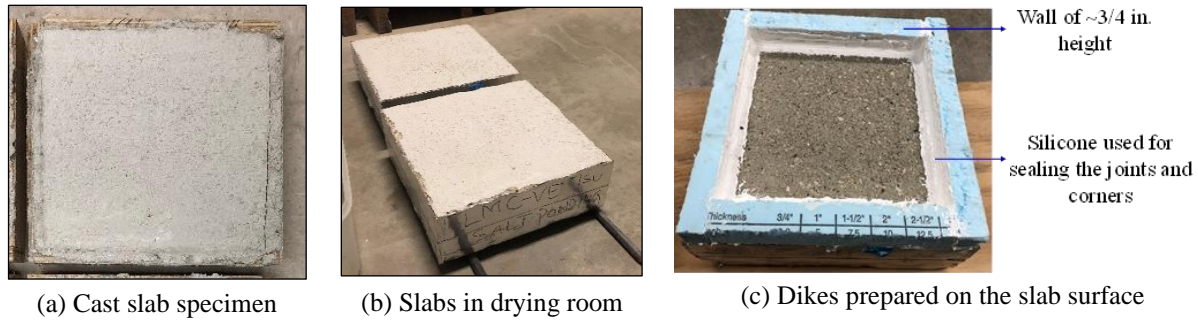
**Figure 4.6. Field-cast and field-cored specimens for sorptivity testing**



**Figure 4.7. Typical sorptivity test curve**

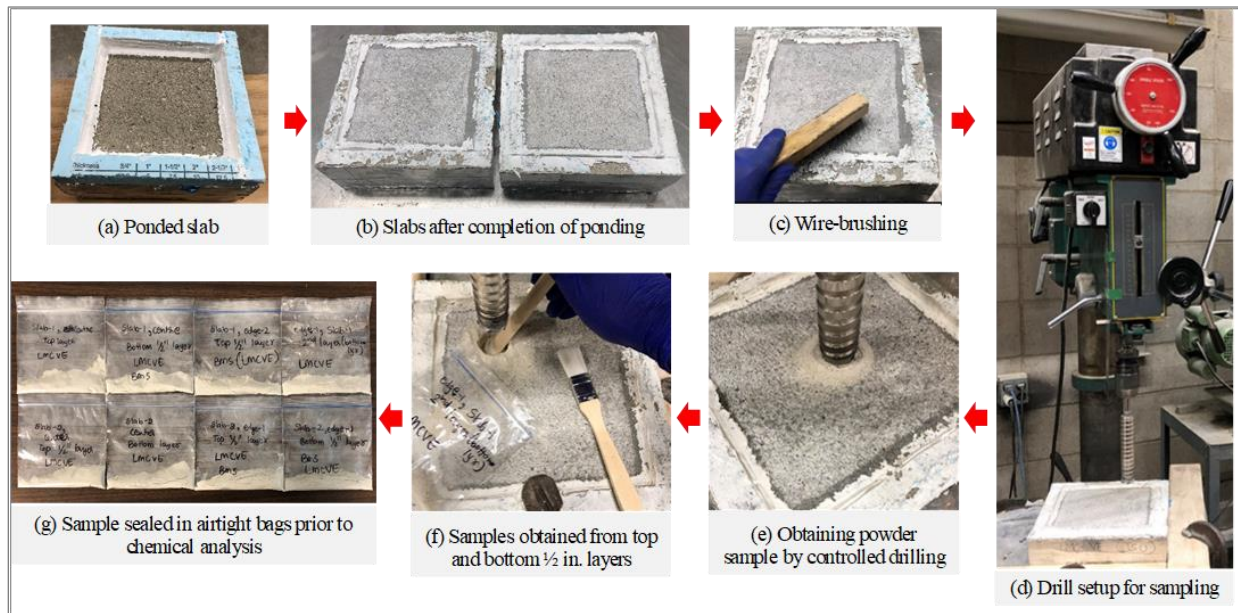
#### 4.1.7 Salt Ponding

The salt ponding test was performed on cast  $12 \times 12 \times 3.5$  in. ( $l \times b \times h$ ) LMC-VE slab specimens in accordance with AASHTO T 259. The substrate for each of the slab specimens was prepared as shown in Figure 4.2, and these specimens were overlaid with the LMC-VE used in the field, as shown in Figure 4.8a. The prepared slabs were cured in a moist curing room for 3 days, as explained above, and then air cured until an age of 14 days. After 14 days, the slabs were moved to a drying room (Figure 4.8b) maintained at room temperature and an RH of 50%, where the slabs were kept for the next 28 days. After 28 days (i.e., a total 42 days since casting), dikes were made using Styrofoam at the top surface to hold the salt solution, as shown in Figure 4.8c. The slabs were then ponded with 3% NaCl solution for 90 days to evaluate the performance of the overlaid LMC-VE to the natural ingress of chloride ions.



**Figure 4.8. Salt ponding test slabs overlaid with LMC-VE**

After 90 days of ponding, the Styrofoam dikes from the slabs were removed (Figure 4.9b), and any salt crystals on the slab surfaces were brushed off using a steel wire brush (Figure 4.9c). Powder samples were then directly collected from the slabs at two different depths, 0 to 0.5 in. (top layer) and 0.5 to 1 in. (bottom layer), using a modified drill setup (Figure 4.9d). The powder samples were collected using a brush and spatula (Figure 4.9f) and were stored in airtight plastic bags to prevent contact with atmospheric moisture (Figure 4.9g) until the day of the chemical testing.

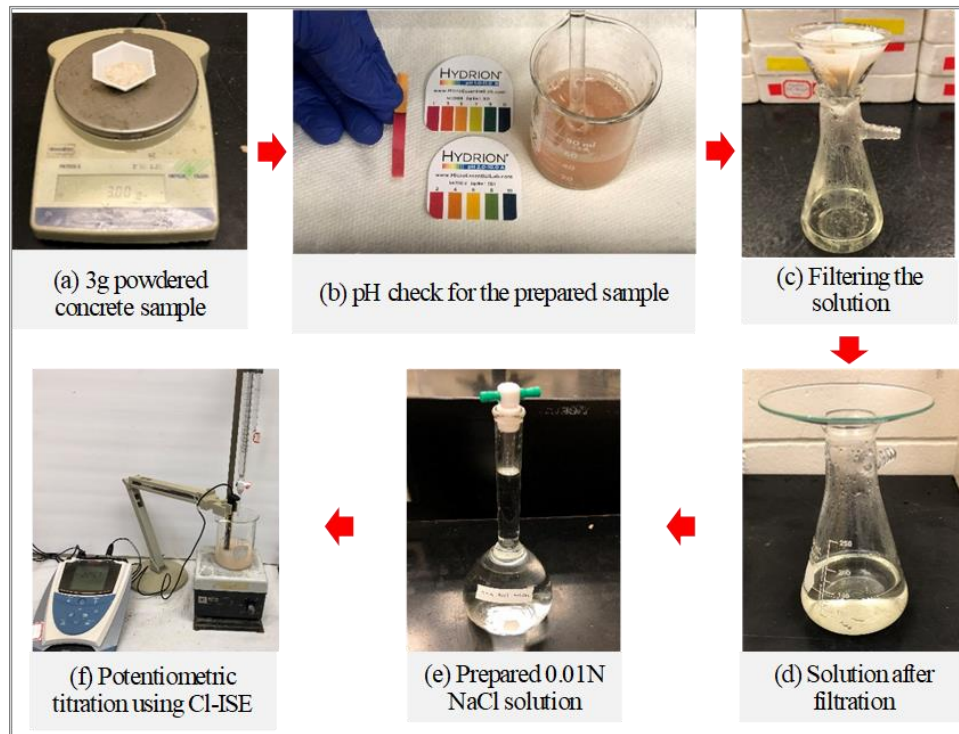


**Figure 4.9. Obtaining powdered samples from salt ponded slabs for the chloride test**

Figure 4.10 provides an overview of the chemical analysis performed to determine the presence of acid-soluble chlorides in the obtained powder samples in accordance with AASHTO T 260. Potentiometric titration (Figure 4.10f) was conducted using an ion selective electrode (ISE) (Hach Sension+ 9652C) for chlorides ( $\text{Cl}^-$ ) along with Hach Chloride Ionic Strength Adjustment (ISA) Powder Pillows. Because the electrode was new, it was immersed in 0.01N NaCl solution for a week before being used for the analysis. The end point of titration was determined by recording the quantity of standard 0.01N silver nitrate ( $\text{AgNO}_3$ ) that needed to be added to the



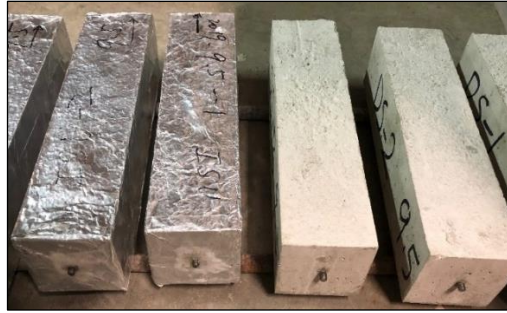
sample solution to bring the voltmeter reading (mV) to the equivalence point, which had earlier been determined by immersing the electrode in distilled water.



**Figure 4.10. Chemical testing for acid-soluble chlorides using potentiometric titration**

#### *4.1.8 Shrinkage*

Drying and autogenous shrinkage measurements were made on  $3 \times 3 \times 11$  in. ( $b \times h \times l$ ) LMC-VE beam specimens (Figure 4.11a) using length change values measured using a comparator with a digital display (Figure 4.11b) in accordance with ASTM C157. For drying shrinkage testing, the first reading was taken after demolding the specimens 1 day after casting, whereas for autogenous shrinkage measurements, the initial reading was taken at the occurrence of initial set. An average of the readings from three specimens was taken and was recorded as the average shrinkage value at each testing age.



(a) Shrinkage test specimens



(b) Shrinkage measurement

**Figure 4.11 Shrinkage testing of LMC-VE specimens**

#### 4.1.9 Freeze-Thaw Testing

Freeze-thaw testing was performed on cast LMC-VE-only beams (i.e., beams made entirely of LMC-VE) and on sliced beams (i.e., beams sliced from LMC-VE-overlaid slabs prepared as explained above). The cast (Figure 4.12a) and sliced (Figure 4.12b) beams had dimensions of  $3 \times 4 \times 16$  in. ( $l \times b \times h$ ) and  $12 \times 3 \times 3.5$  in. ( $l \times b \times h$ ), respectively. Specimens were wet cured for 3 days and air cured thereafter and were tested for freeze-thaw resistance at a specimen age of 28 days. Testing was performed according to ASTM C666 using a freeze-thaw chamber, as shown in Figure 4.12c. The test beams were evaluated for their mass loss, relative dynamic modulus, and deterioration (via visual inspection) after every 36 cycles until failure.



(a) LMC-VE-only beam



(b) LMC-VE-overlaid beam



(c) Overview of the freeze-thaw chamber with test beams

**Figure 4.12. Freeze-thaw testing of the cast beam specimens**

## 4.2 Results and Discussion

### 4.2.1 Chemical Composition

The chemical composition of the rapid-set cement (CTS Rapid Set) used in the overlay was analyzed using x-ray fluorescence, and the results are given in Table 4.2. For additional information, refer to Appendix A.

**Table 4.2. Oxide composition of cement**

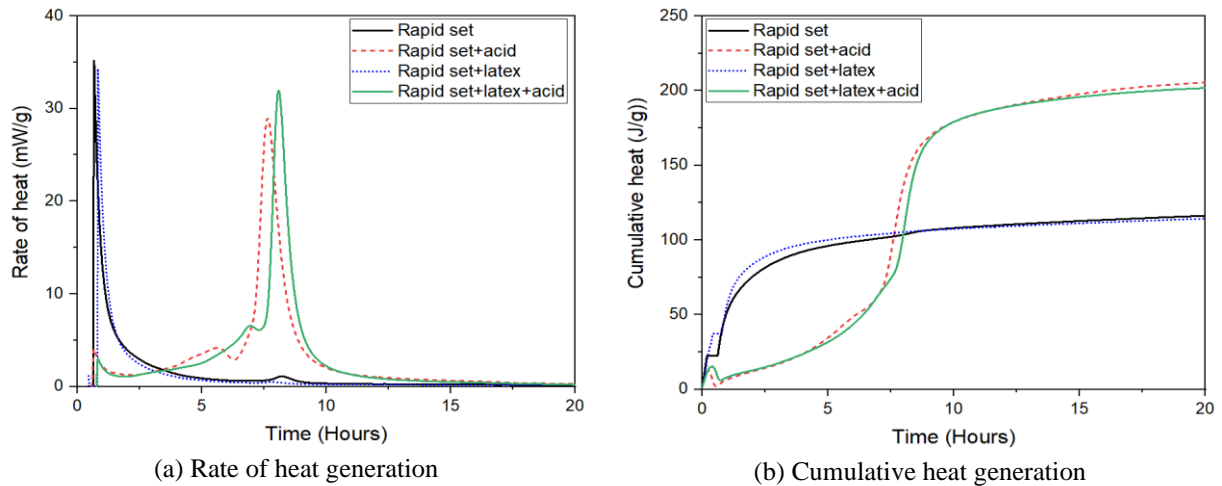
Composition	CaO	SO <sub>3</sub>	Al <sub>2</sub> O <sub>3</sub>	MgO	SiO <sub>2</sub>	FeO	Na <sub>2</sub> O	K <sub>2</sub> O	Others*
Oxide %	49.18	17.92	16.69	1.13	12.06	0.90	0.12	0.74	1.25

\*Others: P<sub>2</sub>O<sub>5</sub> + TiO<sub>2</sub> + MnO + SrO

### 4.2.2 Isothermal Calorimetry

Isothermal calorimetry was performed (at 20°C) to analyze the effect of citric acid and latex on the hydration kinetics of the rapid-set cement used in the LMC-VE overlay. Figure 4.13 shows the rate of heat generation and cumulative heat curves. From Figure 4.13a, it can be observed that the heat signature of the rapid-set cement consisted of a sharp peak without any dormant period. This signifies that the initial hydration occurred very quickly, and consequently the setting of the cement was also faster. This observation is consistent with the setting time results presented in Section 3.2.2. The addition of latex did not cause a significant change in the heat signature of the rapid-set cement. However, the addition of citric acid led to an increased dormant period and shifting of the peak rate of heat generation towards the right. This suggests that the hydration of the rapid-set cement was delayed in the presence of citric acid, which acted as a retarding admixture. The hydration-retarding effect of citric acid was also evident in the mixture containing both rapid-set cement and latex.

The cumulative heat curves in Figure 4.13b show features similar to those observed in the rate of heat generation curves. The addition of latex did not exhibit a significant effect on the cumulative heat of rapid-set cement (for the measured duration). For the mixes containing citric acid, the cumulative heat was lower than that of the mixes without citric acid until 7.5 hours, after which the trend was reversed. At that point, a substantial difference in the cumulative heat of the two types of mixes (with and without citric acid) could be observed. During a period spanning 5 to 10 hours after mixing, the heat of hydration of the pastes with citric acid rapidly increased from about 25 J/g to 180 J/g, an increase about twice that of a conventional pavement cement paste. Such rapid heat generation could cause thermal cracking if the concrete were subjected to a large temperature drop after being exposed to a low-temperature environment. After 10 hours, the rate of heat generation of the LMC-VE paste (a mixture of rapid set cement, latex, and citric acid) became much steadier. At 20 hours, the cumulative heat of the paste with rapid set cement, latex, and citric acid was around 200 J/g.

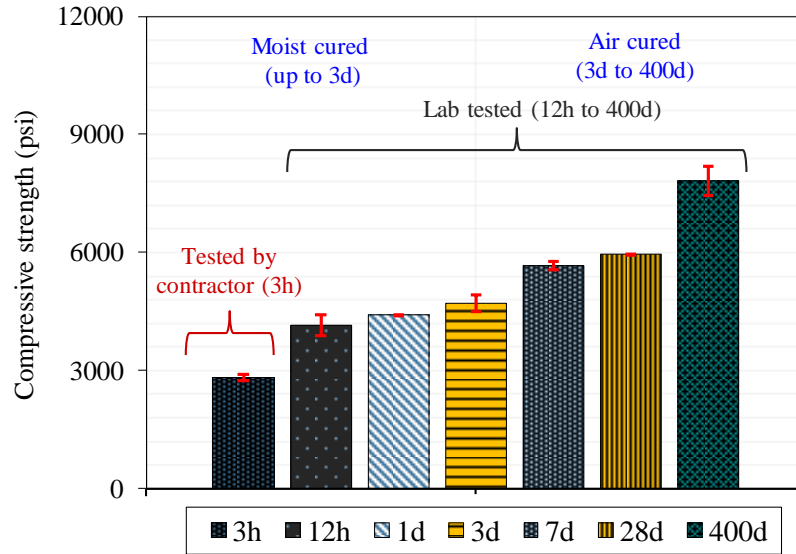


**Figure 4.13. Calorimetry test results**

#### 4.2.3 Compressive Strength

LMC-VE is expected to have a compressive strength high enough to allow opening to traffic in a short time (as early as 3 hours). Accordingly, the LMC-VE in this project was expected to have a minimum compressive strength of 3,000 psi at 3 hours. As shown in Figure 4.14, the overlay concrete had a slightly lower average compressive strength when measured by the contractor at approximately 3 hours (i.e., at 2 hours 40 minutes) on the same day as but prior to placement of the overlay concrete. However, the compressive strength measured at 12 hours in the laboratory (i.e., 4,151 psi) exceeded the minimum strength requirement of 3,000 psi. The compressive strength further increased to 4,413 psi at 24 hours and then to 4,711 psi at 3 days. It is important to note that the cast specimens were water cured only for 3 days and were air cured thereafter. A sudden increase in the average compressive strength value from 4,711 psi at 3 days to 5,667 psi at 7 days (i.e., an approximately 20% increase) could thus be attributed to the air curing, which facilitated strength development. As specimens continued to air cure, a slight increase in the compressive strength was again observed, with a 28-day average compressive strength of 5,952 psi. At 400 days, the recorded average compressive strength was 7,816 psi, which indicated that though the LMC-VE test specimens contained rapid-set cement, the concrete continued to develop strength over the long term under air cured conditions. Overall, within the timeframe of testing (i.e., from 3 hours to 400 days), the compressive strength values increased by a factor of three.

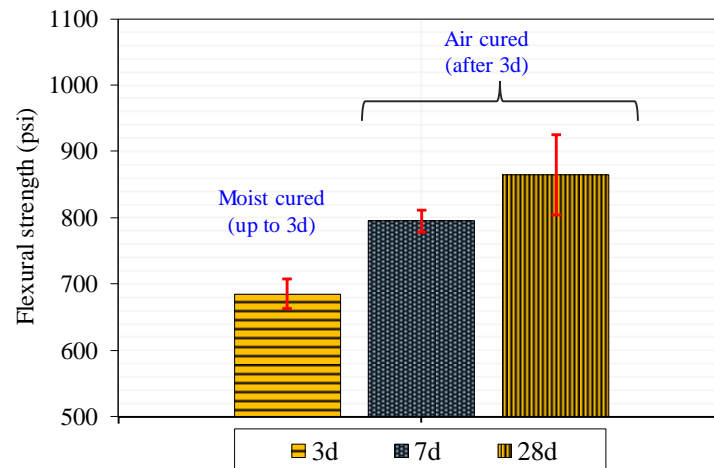




**Figure 4.14. Compressive strength of LMC-VE at different ages**

#### 4.2.4 Flexural Strength

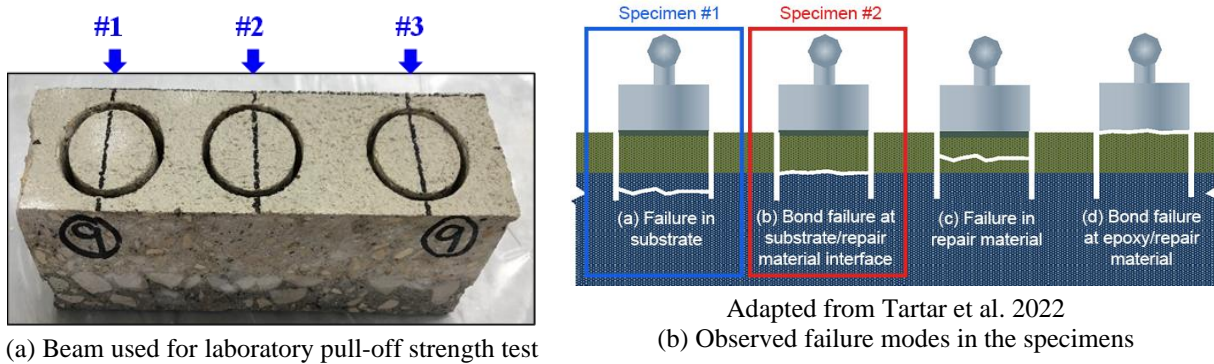
The development of the flexural strength of the LMC-VE beam specimens with time, measured using three-point bending, is shown in Figure 4.15. As early as 3 days, the specimens showed an average flexural strength of 685 psi, which was about 14.5% of the compressive strength at 3 days. The average flexural strength increased to 795 psi at 7 days (14% of the compressive strength at 7 days) and then increased to 865 psi at 28 days (14.5% of the compressive strength at 28 days).



**Figure 4.15. Flexural strength of LMC-VE at different ages**

#### 4.2.5 Pull-Off Strength

In the laboratory, the pull-off strength test was performed only at a specimen age of 28 days. The test beams were sliced from slabs that were overlaid in the field (with the substrate concrete cast in laboratory, as explained in Section 4.1.4). Three pull-off tests were performed on each test beam, as shown in Figure 4.16a. In one of the three tests conducted (specifically on Specimen 3), a result could not be obtained because the specimen broke during the test preparation. The failure modes observed along with the results of the other two tests are shown in Figure 4.16b and Table 4.3, respectively.

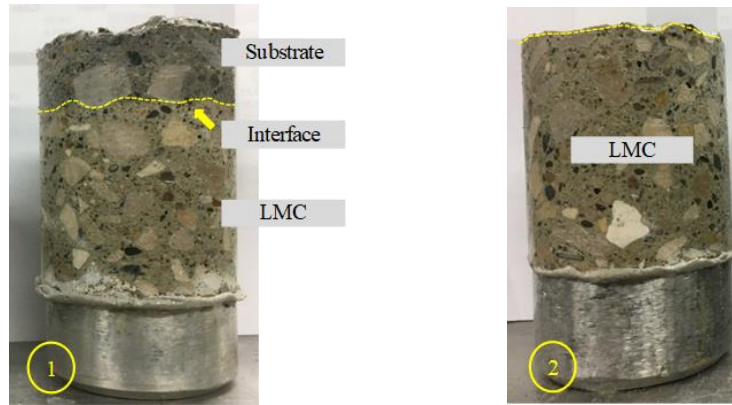


**Figure 4.16. Pull-off strength test specimen and the observed failure modes**

**Table 4.3. Pull-off strength test results**

Specimen	Strength at Failure (psi)	Failure Mode per ASTM
1	325.7	A (substrate failure)
2	282.7	B (bond failure)
3	Specimen failed during preparation stage	

Specimen 1 failed at the substrate, as shown in Figure 4.17a, and exhibited a failure strength of 325.7 psi. Specimen 2 failed at the bond, as shown in Figure 4.17b, and exhibited an LMC-VE-substrate bond strength of 282.7 psi. Specimen 3 failed during specimen preparation prior to the test. When a specimen shows a substrate failure, it suggests that the overlay-substrate bond strength is higher than the substrate strength. Therefore, the data in Table 4.3 indicate that the LMC-VE overlay-substrate bond strength was higher than 282.7 psi at the repair age of 28 days. Similar results for the bond strength between the LMC-VE and the substrate concrete were reported in a study by Sprinkel (1998), where the bond strength values for cores obtained from two different project locations were observed to be 248 psi and 276 psi, respectively.



(a) Failure in the substrate in Specimen 1    (b) Failure at the bond in Specimen 2

**Figure 4.17. Failure modes observed in the tested specimens**

During the pull-off strength testing, failure can occur in the overlay material, in the substrate concrete, or at the interface (i.e., bond) between the overlay and substrate. A complete (100%) failure at the interface provides an indication of the actual bond strength. However, in reality, such failures might not always occur. Based on the results obtained for a given pull-off test, the bond strength can be classified into different categories, as indicated in Table 4.4 (Sprinkel 2000). Specifications for pull-off strength values from some DOTs for certain types of overlay systems are listed in Table 4.5, and these values can be used in a comparison with the LMC-VE pull-off strength test results obtained in this research. Based on the information in Table 4.4 and Table 4.5, in general it can be understood that a bond strength value over 250 psi indicates an adequately bonded overlay system.

**Table 4.4. Characterizing bond strength values for overlays**

<b>Strength Value (psi)</b>	<b>Category</b>
≥ 300	Excellent
250 to 299	Very good
200 to 249	Good
100 to 199	Fair
0 to 99	Poor

Source: Sprinkel 2000

**Table 4.5. Values for pull-off strength testing specified by various state DOTs**

Overlay Type	Specifying State DOT	Minimum Specified Pull-Off Strength Value	Additional Remarks
Multi-layer polymer concrete overlay	Iowa	Avg. of 250 psi (24 hours) regardless of depth of failure	<ul style="list-style-type: none"> <li>• Tested according to ACI 503R, Appendix A, VTM 92</li> <li>• &lt; 250 psi indicates that additional surface preparation is necessary</li> </ul>
Thin polymer overlay system	Illinois	250 psi (24 hours)	Tested according to ACI-503-R pull-off test
Type III Epoxy polymer overlay	Nebraska	250 psi (after 24 hours minimum)	Tested according to ASTM C1583
Epoxy overlay system	North Carolina	250 psi @ 75° at 24 hours	Tested according to ASTM C1583

Source: Dahlberg and Phares 2016

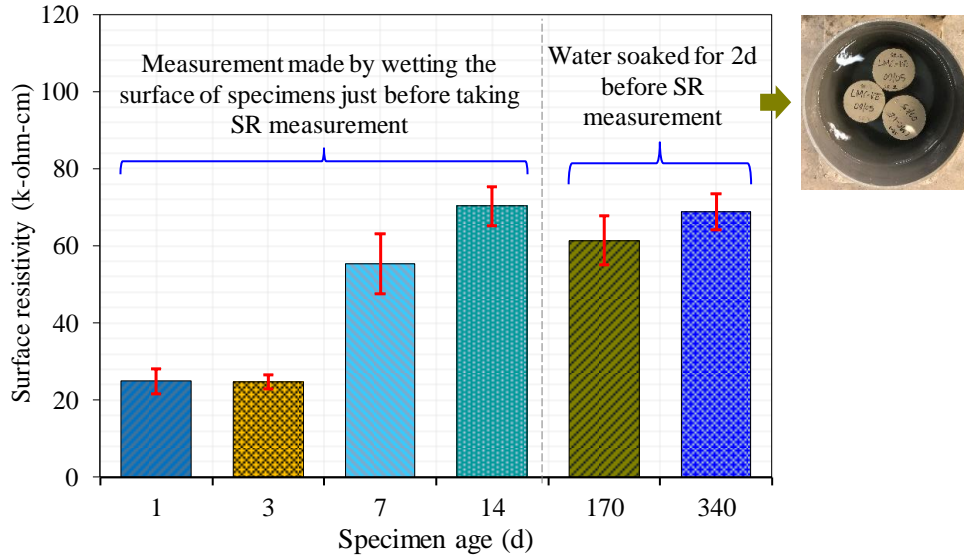
Based on the above discussion and the obtained strength value from Specimen 2, it can be understood that the true bond strength between the LMC-VE and the substrate in the laboratory was over 250 psi (i.e., approximately 283 psi). Since Specimen 1 failed at the substrate and indicated a strength value over 282.7 psi (i.e., 325.7 psi), it can again be inferred that the LMC-VE-substrate bond in the laboratory was strong and could be classified as “very good” based on the information in Table 4.4 (Sprinkel 2000).

#### 4.2.6 Surface Resistivity

The SR test measures the ability of a material to resist the transport of conductive ions (such as  $\text{Cl}^-$ ) through the pore solution in a cementitious system. Therefore, the chemical makeup of the pore solution influences the resistivity measurement to a great extent (Ramezani pour et al. 2011, Tibbetts et al. 2020, Melugiri-Shankaramurthy et al. 2016, Milla et al. 2021, Sargam et al. 2019b). Cementitious systems with enhanced pore connectivity do not hinder the movement of ions through them, and hence such systems show low SR values compared to systems that have reduced pore connectivity (Sargam et al. 2019b; Melugiri-Shankaramurthy et al. 2018, 2021). A comparison of SR values therefore provides an indication of the durability of a system against the ingress of deleterious ions into the system (Milla et al. 2021, Melugiri-Shankaramurthy et al. 2021).

In this study, SR measurements were taken at different specimen ages to understand the development of resistivity due to the continued hydration, development of latex film, and resulting pore refinement. Figure 4.18 shows the SR measurements taken on  $4 \times 8$  in. LMC-VE cylinder specimens. As early as 1 day, water cured LMC-VE specimens showed an average SR value of 24  $\text{k}\Omega\text{-cm}$ . With continued water curing from 1 day to 3 days, no change was observed in the measured SR values, indicating no further development in the average SR value. However, the average SR value increased more than twofold from a measured value of 24  $\text{k}\Omega\text{-cm}$  at 3 days to 56  $\text{k}\Omega\text{-cm}$  at 7 days. A further increase in the average SR value to 70  $\text{k}\Omega\text{-cm}$  was observed at 14 days. It is important to note that all of the LMC-VE specimens were water cured for only 3

days and then were air cured at room temperature until the specimens were tested. The pattern observed in the measured SR values from 1 day to 14 days thus indicates the importance of air curing for the development of a refined pore structure within LMC-VE, which is different than that of conventional binder-based concrete systems.



**Figure 4.18. Surface resistivity development with age**

Further attempts to measure SR values after 14 days using the same procedure described above yielded fluctuations in the measurements, and hence no stable constant value could be recorded at 28 days. This could be because the specimens were very dry, and even wetting the four electrodes of the Wenner probe (by immersion in water) was not sufficient to obtain constant measurements. Hence, for the later-age, long-term measurements (i.e., at 170 and 340 days), the LMC-VE specimens were soaked in water at room temperature for 2 days, after which the specimens were removed from the water, any excess water was wiped from the specimens' surfaces, and SR measurements were taken and recorded. After the measurements were recorded, the specimens were returned to the room and air cured at room temperature thereafter. The soaking of the specimens in water together with the wetting of the electrodes of the Wenner probe ensured stable SR measurements.

However, a comparison of the average SR measurements at 14 days and 170 days indicated a slight decrease in the average SR value from 70 kΩ-cm at 14 days to 63 kΩ-cm at 170 days. This was possibly due to soaking the specimens in water, which resulted in water penetration into the top surface layer of the specimens to a small extent and thereby facilitated movement of not only the ions in the pore solution but also the ions in the water that was used to soak the specimens. Careful observation of the error bars at 14 days and 170 days also indicates that the difference was not very significant. A small increase in the SR value was recorded at 340 days compared to 170 days. For the measurement at 340 days, the specimens were again presoaked in water for 2 days prior to testing. The average SR value at 340 days (69 kΩ-cm) measured from the specimens that underwent the two-day water saturation process was very close to the SR value determined at 14 days from the specimens that did not undergo the 2-day water saturation

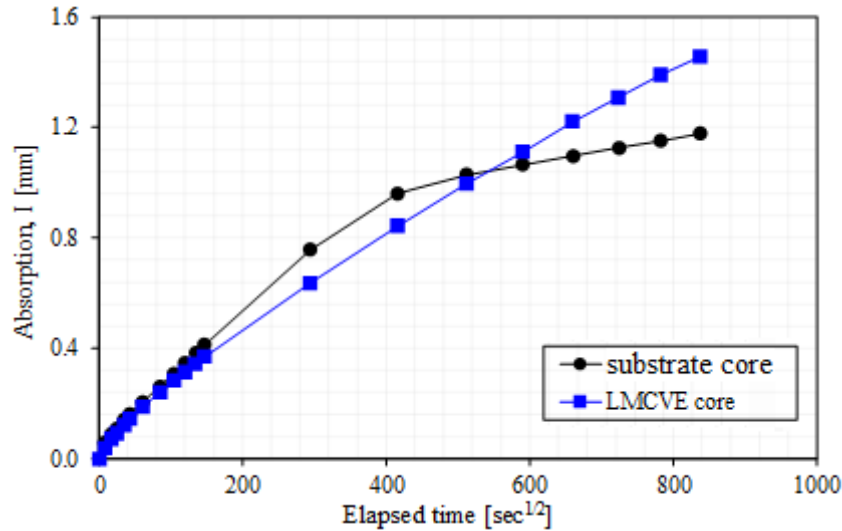
process. Though the measurements were again taken on water-soaked specimens, an increase in the average SR value at 340 days compared to that measured at 170 days indicates possible cement hydration as a result of water slightly intruding into the specimen during the 2 days of water immersion.

#### 4.2.7 Sorptivity

Absorption is one of the key moisture transport mechanisms in cementitious systems, and the water sorptivity test measures the absorption characteristics of unsaturated porous systems (Hall and Tse 1986, Hall 1989). The initial sorptivity value is determined as the slope of the linear fit line of the data points from the beginning of the test (except time zero) up to a point where a clear change of slope or curvature is noticed, while the secondary sorptivity is determined as the slope of the linear fit line of the data points thereafter until the end of the testing period (Alderete et al. 2020). Initial sorptivity takes place at a relatively faster rate than secondary sorptivity (Alderete et al. 2020, Neithalath 2007). However, according to ASTM C1585, the slope of the least squares linear fit line for the measurements taken during the first 6 hours is referred as to initial sorption ( $S_i$ ), and the slope of the least squares linear fit line for the measurements taken from 1 to 8 days is referred to as secondary sorption. A comparison of sorptivity values enables an understanding of the pore connectivity in a cementitious system (Zhutovsky and Hooton 2019) and, to some extent, provides insights into the resistance of the system against moisture-induced deterioration mechanisms caused by freeze-thaw cycles and sulfate attack (Bentz et al. 2001, Sen Li et al. 2020, Hall and Yau 1987).

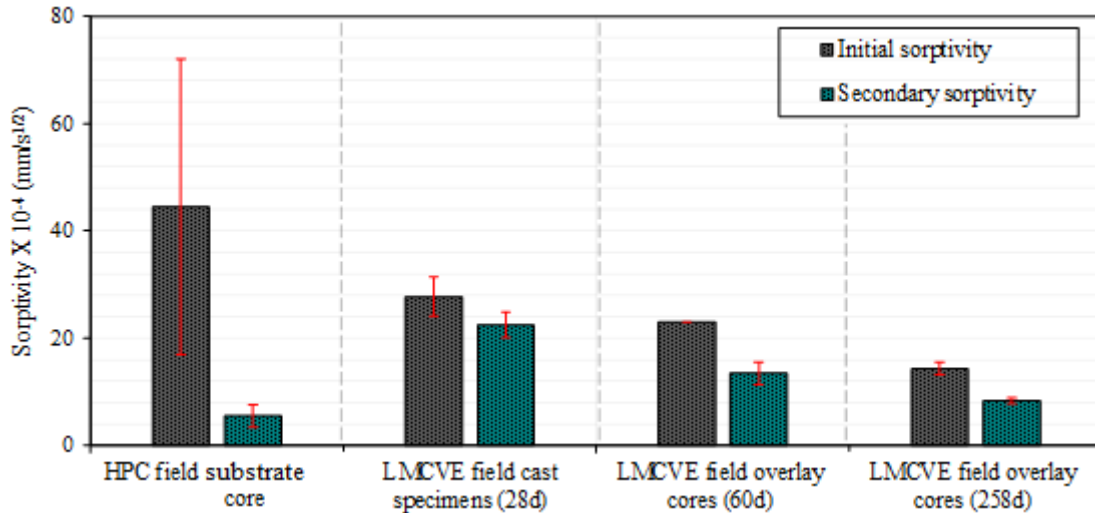
Figure 4.19 gives a comparison of typical overall sorptivity curves for substrate HPC and LMC-VE overlay specimens. A clear difference in curvature can be observed between the curves. The substrate concrete attained saturation more quickly than LMC-VE, whereas LMC-VE took a longer time to saturate and hence underwent prolonged water absorption. This indicates higher pore connectivity in the substrate concrete compared to the relatively less connected pore network in LMC-VE. Thus, moisture movement in LMC-VE took place at a relatively slower rate compared to the substrate concrete initially, resulting in a longer transition time between the initial and secondary sorptivity regimes (Alderete et al. 2020). After 3 days, however, the water absorption of the substrate became steady while the water absorption of the LMC-VE continued to increase over the testing time. At the end of test (after an elapsed time of 8 days), the absorption of the substrate was slightly lower than 12 mm while the absorption of the LMC-VE was about 14.4 mm. Such an increase in water absorption could be responsible for the moisture-induced deterioration, like freeze-thaw damage, as discussed later.





**Figure 4.19. Comparison between sorption behavior of substrate concrete core and LMC-VE core**

A comparison of the initial and secondary sorptivity values shown in Figure 4.20 indicates the clear difference in the sorption characteristics of the substrate concrete and LMC-VE. A comparison of the average initial sorptivity values indicates that the substrate concrete had a significantly higher initial sorptivity value of  $44 \times 10^{-4} \text{ mm/s}^{1/2}$ , whereas LMC-VE had lower initial sorptivity values at all tested ages, with the highest average initial sorptivity value being  $28 \times 10^{-4} \text{ mm/s}^{1/2}$  at 28 days for the field-cast specimens. Moreover, the LMC-VE specimens obtained from cores taken directly from the field overlay had lower initial sorptivity values compared to not only the substrate concrete but also the field-cast LMC-VE specimens. This indicates that the LMC-VE specimens obtained directly from the field overlay had a relatively finer pore network compared to both the substrate concrete and the field-cast LMC-VE specimens. A finer pore network enhances the resistance of the system to moisture movement (El-Dieb and Hooton 1995, Khan and Lynsdale 2002), whereas a larger and coarser pore network decreases the resistance of the system to moisture movement (Henkensiefken et al. 2009). Hence, LMC-VE with a finer pore network could be expected to have enhanced durability in terms of moisture transport. Additionally, the substrate concrete showed higher variability in terms of sorptivity values (indicated by longer error bars) compared to the LMC-VE specimens (which had shorter error bars), indicating the better quality and uniformity of the latter. A comparison of only the LMC-VE sorptivity values over time indicates a marked reduction in both the initial and secondary sorptivity values, suggesting that a refinement in the pore structure might be taking place due to a certain amount of continued cement hydration and the formation of a latex network.

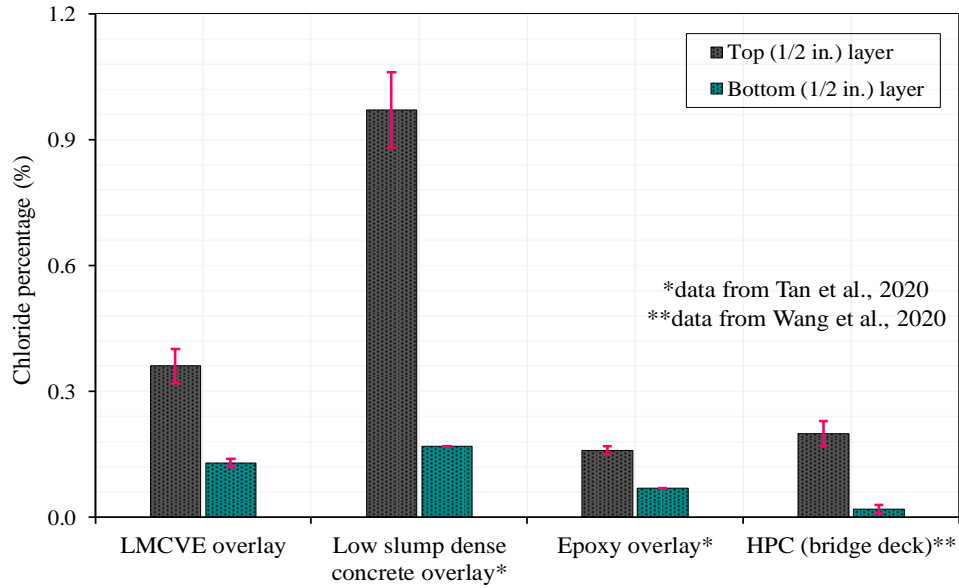


**Figure 4.20. Initial and secondary sorptivity values of substrate concrete and LMC-VE cores**

#### 4.2.8 Salt Ponding

The salt ponding test is a long-term test that is typically performed by ponding a 3% NaCl solution on the surface of concrete slabs for a total duration of 90 days in accordance with AASHTO T 259. With the salt solution on the top surface (within dikes made of either cement mortar or some impermeable material such as thick Styrofoam), an impermeable coating (such as epoxy or aluminum tape) on the side surfaces, and an uncovered bottom surface (exposing the bottom of the slab to the conditions of the drying room), the salt solution is allowed to permeate through the depth of the concrete test specimen. Thus, the test simulates a natural, unaccelerated intrusion of deleterious ions such as chlorides into the system. At the end of the 90 days of ponding, the solution is removed from the surface and the surface is left to dry in the drying room (maintained at  $23 \pm 2^\circ\text{C}$  and 50% RH). The dried slab surfaces are then brushed off using a steel wire brush to clear off crystallized salt (if any). Powdered concrete test samples are then obtained at different depths from the prepared slabs, after which the samples are subjected to potentiometric titration against a 0.01N standard silver nitrate solution using a chloride ISE to determine acid-soluble chloride contents at various depths in the ponded slab specimens.

In this study, the tested slabs consisted of an HPC substrate overlaid with LMC-VE. These slabs were subjected to ponding before powdered samples were obtained at two depth levels: 1/16 to 1/2 in. and 1/2 to 1 in. The obtained samples were then subjected to titration to obtain the chloride content percentages. Samples were also obtained from a reference LMC-VE cylinder that was not ponded with salt solution. The results obtained for the LMC-VE-overlaid specimens are shown in Figure 4.21. In the same figure, the chloride ingress behavior of LMC-VE is compared with that of two other overlay types, a low-slump dense concrete (LSDC) overlay and an epoxy overlay (Tan et al. 2020), and an HPC (Wang et al. 2020a) from the published literature to better understand where the performance of LMC-VE stands among the given systems.



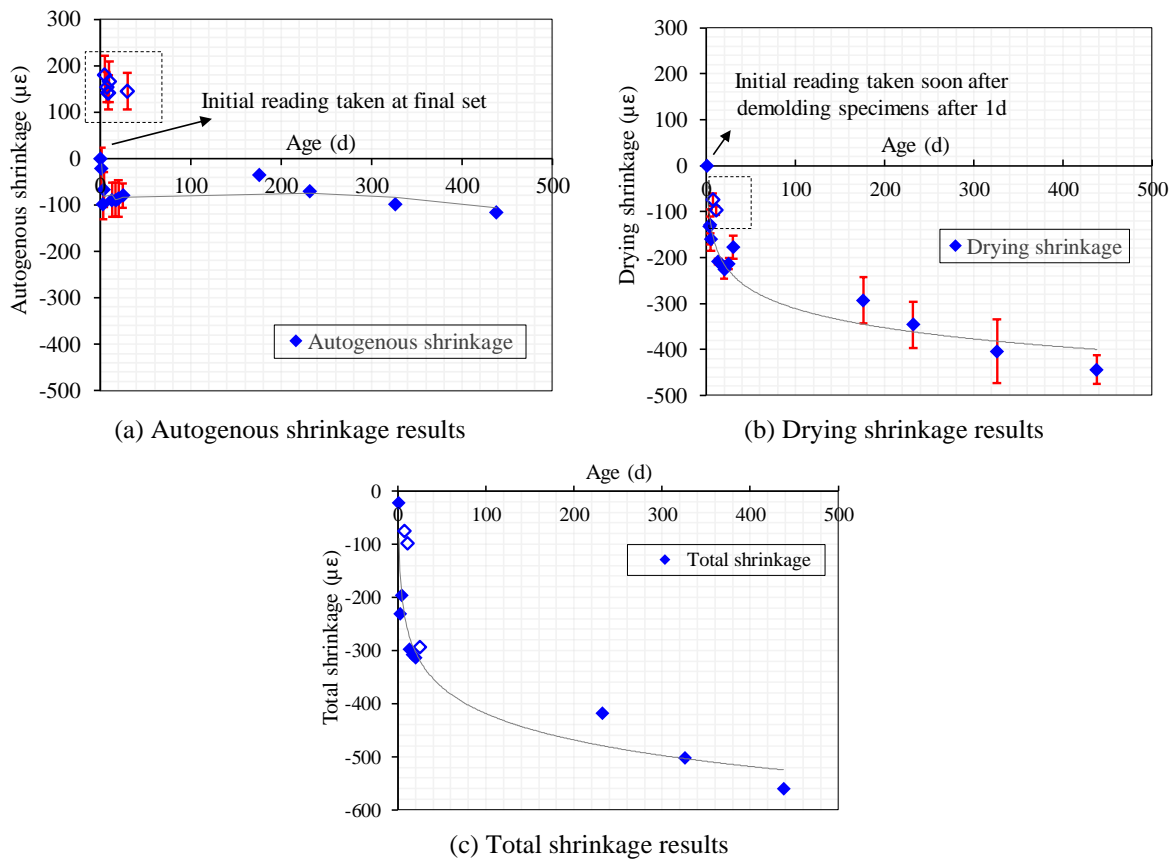
**Figure 4.21. Salt ponding test results of LMC-VE overlay in comparison with other overlays and HPC**

The results for the LMC-VE test specimens indicated an average chloride content of 0.36% in the top 1/2 in. layer and 0.13% in the bottom 1/2 in. layer. These chloride percentage values were observed to be slightly higher than that obtained from the epoxy overlay system but lower than that obtained from the LSDC overlay system. Thus, the performance of LMC-VE with respect to chloride ingress could be anticipated to be in between these two overlay systems. Also, LMC-VE was seen to slightly underperform compared to the typical bridge deck HPC, which had lower chloride percentage values in both the top and bottom 1/2 in. layers of the salt-ponded concrete specimens. However, the chloride intrusion resistance of the specimens obtained directly from the field LMC-VE overlay might be relatively better than that of the field-cast specimens because the sorptivity test results showed that the specimens obtained from the field LMC-VE overlay cores performed better than the field-cast LMC-VE specimens.

#### 4.2.9 Shrinkage

Due to its incorporation of rapid-set cement, LMC-VE has been reported to have issues related to shrinkage because it has a high heat of hydration, resulting in high early-age thermal deformations (Yun et al. 2014). In addition, the chances of autogenous shrinkage are higher in LMC-VE than in other concrete systems due to its use of lower water-to-binder (w/b) ratios, leading to a higher chance of early-age cracking. The magnitude of the autogenous shrinkage further increases with an increase in latex content (Yun et al. 2014). In this study, autogenous shrinkage was measured using the initial comparator readings taken at the initial set of the concrete, whereas drying shrinkage was measured using the initial readings taken soon after the specimens were demolded after 24 hours of casting.

Figure 4.22a and Figure 4.22b show the autogenous and drying shrinkage results, respectively, up to a specimen age of 440 days. Figure 4.22c shows the corresponding total shrinkage results. From the figures, it can be observed that after 440 days, the autogenous shrinkage is more or less constant whereas the LMC-VE specimens are still undergoing drying shrinkage. At the end of 440 days, the magnitude of the autogenous shrinkage was observed to be 115 microstrain whereas that of the drying shrinkage was observed to be 440 microstrain. A similar magnitude of autogenous shrinkage (close to 120 microstrain) was reported in a study by Yun et al. (2014), where it was observed that LMC-VE specimens that were cast and then immediately cured at 20°C and 50% RH underwent most of their shrinkage within the first 24 hours. A few data points in Figure 4.22 between 4 and 12 days (highlighted in dashed boxes) were observed to be outliers. These outliers were possibly due to slight variations in the temperature and humidity of the drying room where the shrinkage specimens were placed.



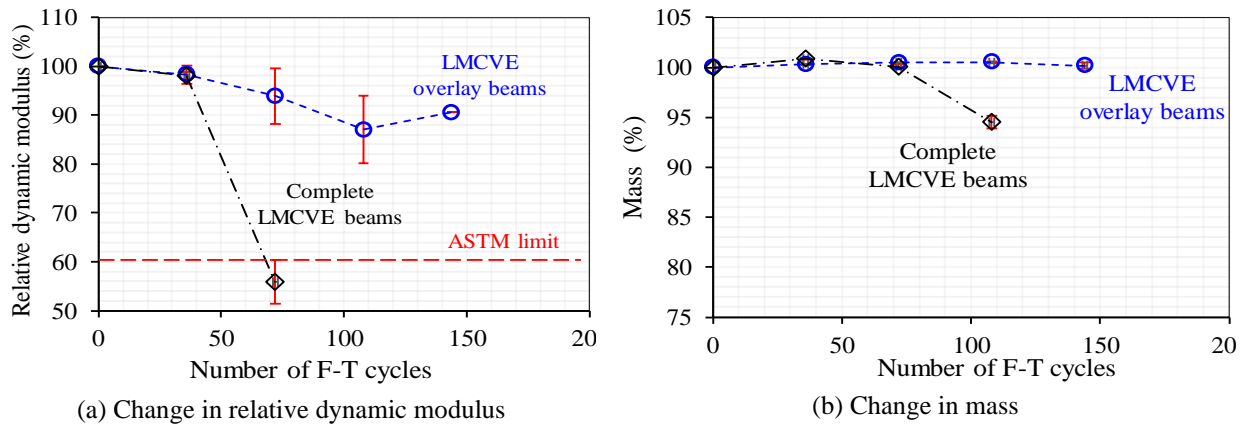
**Figure 4.22. Shrinkage test results of LMC-VE specimens**

#### 4.2.10 Freeze-Thaw Resistance

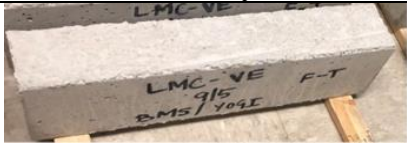






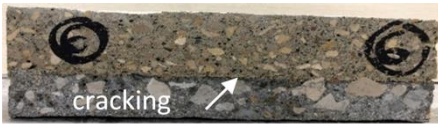

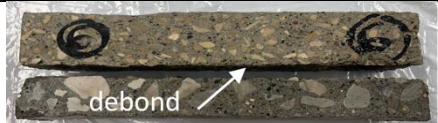
As explained in Section 4.1.9, freeze-thaw testing was conducted on LMC-VE-only beams (beams made entirely of LMC-VE) and LMC-VE-overlaid beams (beams with LMC-VE overlaid on an HPC substrate). Depending on the type of the specimen utilized for testing, a typical freeze-thaw test provides an understanding of the specimen's pore features (such as pore

connectivity and permeability), the mechanical strength of the matrix, and the bond strength/adhesion of the material to the substrate (Yun et al. 2004, Liu et al. 2020).

As the freeze-thaw cycles progressed, the mass loss, relative dynamic modulus, and deterioration (via visual inspection) of the specimens were monitored every 36 cycles until failure. Figure 4.23a and Figure 4.23b show the changes in the relative dynamic modulus values and the mass of both types of LMC-VE test specimens. Figure 4.24 shows a comparison of the rate and extent of visible deterioration of both specimen types as the freeze-thaw cycles proceeded.



**Figure 4.23. Freeze-thaw test results of LMC-VE specimens**

No. of Freeze-Thaw Cycles	LMC-VE-Only Beams	LMC-VE-Overlaid Beams
0	 (a) Before freeze-thaw cycles	 (b) Before freeze-thaw cycles
36	 (c) Surface layer becoming deteriorated	 (d) No visible damage on surface or interface
72	 (e) More deterioration of surface layer	 (f) No visible damage on surface or interface
108	 (g) Significant deterioration at surface layer and corners	 (h) Visible crack at the interface
144	 (i) Extremely damaged specimen	 (j) Specimen separated due to bond failure

**Figure 4.24. Deterioration of LMC-VE-only (middle column) and LMC-VE-overlaid (right column) test specimens due to freeze-thaw cycles (left column)**

From Figure 4.23 and Figure 4.24, it is clear that the LMC-VE-only beams underwent faster deterioration compared to the LMC-VE-overlaid beams. As early as 36 freeze-thaw cycles (Figure 4.24c), pieces from the surface layers of the LMC-VE-only beams started to fall off, exposing the interior concrete. After 72 freeze-thaw cycles, surface layer deterioration could be seen in more than 40% of the LMC-VE-only specimens, as shown in Figure 4.24e. As a result, the average relative dynamic modulus of these specimens decreased to a value of approximately 54% (lower than the ASTM C666 limit of 60% for stoppage of the test). Though at the end of 108 freeze-thaw cycles the surface layers in these beams had completely deteriorated, most of the interior concrete remained intact (with a mass loss of approximately 6%), as shown in Figure 4.24g. The deteriorated specimens had uneven surfaces and protruding aggregate particles, which made it impossible to measure the relative dynamic modulus at 108 freeze-thaw cycles and later. The LMC-VE-only beams completely deteriorated after 144 freeze-thaw cycles and the specimen matrix no longer remained intact, as shown in Figure 4.24i. Research has indicated that

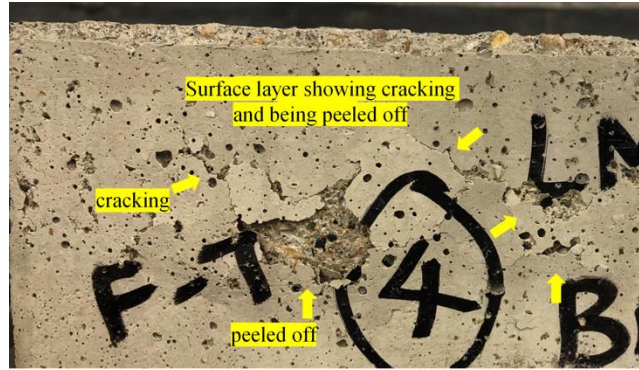


only CSA concrete with a low w/b ratio ( $<0.5$ ) displays a comparable freeze-thaw resistance to portland cement concrete (Bukhari and Khanzadeh 2023). As mentioned previously, the increasing water absorption of LMC-VE at a later age could be responsible for moisture-induced deterioration such as freeze-thaw damage. At present, the research on the freeze-thaw performance of latex modified CSA concrete is very limited (Lin et al. 2018).

In contrast, the LMC-VE-overlaid beams displayed better performance in terms of higher relative dynamic modulus and lower mass loss values within the timeframe of testing. The LMC-VE-overlaid specimens showed no signs of visible deterioration until the completion of 72 freeze-thaw cycles, as shown in Figure 4.24b, Figure 4.24d, and Figure 4.24f. Consequently, no mass loss was observed for any of the LMC-VE-overlaid beams in this period. As a result, the relative dynamic modulus of the specimens remained high (approximately 95% and higher) until the end of 72 freeze-thaw cycles. After the completion of 108 cycles, cracks appeared at the interface of the LMC-VE and the substrate, as indicated in Figure 4.24h. The effect of this cracking was reflected in the slightly lower magnitudes of the relative dynamic modulus values after 108 cycles. After the completion of 144 freeze-thaw cycles, the LMC-VE-substrate interface failed completely, resulting in the separation of the LMC-VE overlay and the substrate concrete. After 144 freeze-thaw cycles, no significant reduction in the measurable parameters was observed apart from the bond failure; i.e., the relative dynamic modulus remained above 85%, the mass loss was almost 0%, and no visible signs of deterioration (no significant spalling of material from the surface or corners) were noted. Therefore, the LMC-VE-overlaid specimens could be anticipated to perform well under freeze-thaw conditions.

Although the reasons for the early failure of the LMC-VE-only beams remain unknown (and need further investigation), the failure of the bond in the LMC-VE-overlaid beams could be due to the poor interface properties, which were likely a result of inadequate surface preparation of the substrate (i.e., the laboratory-cast HPC). Various efforts were made to ensure a good bond between the LMC-VE and the laboratory-cast HPC, such as (1) application of retarder to the mold surface (Figure 4.2b) in which the substrate concrete was cast followed by manual wire brushing 24 hours after casting to remove the mortar portion and expose the aggregate surfaces to enhance the surface roughness, (2) sand-blasting of the wire-brushed surface to further increase the surface roughness, and (3) application of a thin layer of mortar sieved (using the #4 sieve) from the fresh LMC-VE before pouring the LMC-VE overlay over the hardened substrate concrete. Nevertheless, the LMC-VE-overlaid specimens exposed to freeze-thaw cycles still failed at the interface. This clearly indicates the inadequacy of these surface preparation methods, which do not seem to simulate the surface preparation techniques adopted for the actual overlay construction in the field.

Magnified images of the key features of freeze-thaw-related deformation observed in both the LMC-VE-only and LMC-VE-overlaid beam specimens are shown in Figure 4.25 (a–d) and Figure 4.26 (a–c), respectively.



(a) Beginning of surface layer degradation (marked with arrows) after 36 freeze-thaw cycles



(b) More than 40% to 50% degradation of only surface layer material after 72 cycles

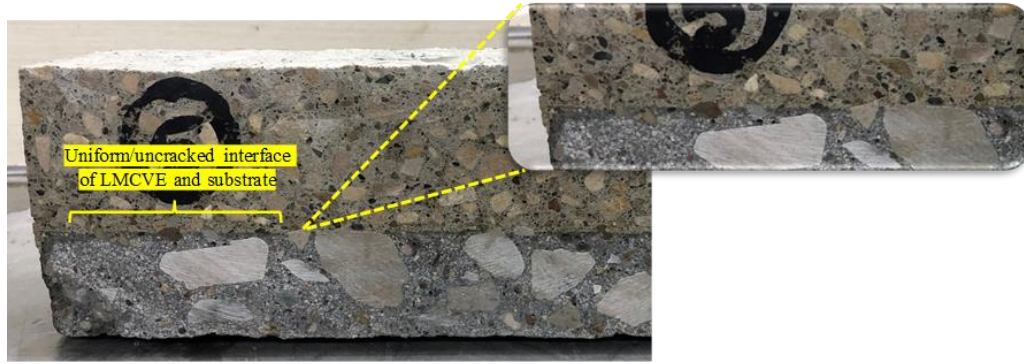


(c) Surfaces with aggregate particles exposed on the surfaces after 108 freeze-thaw cycles

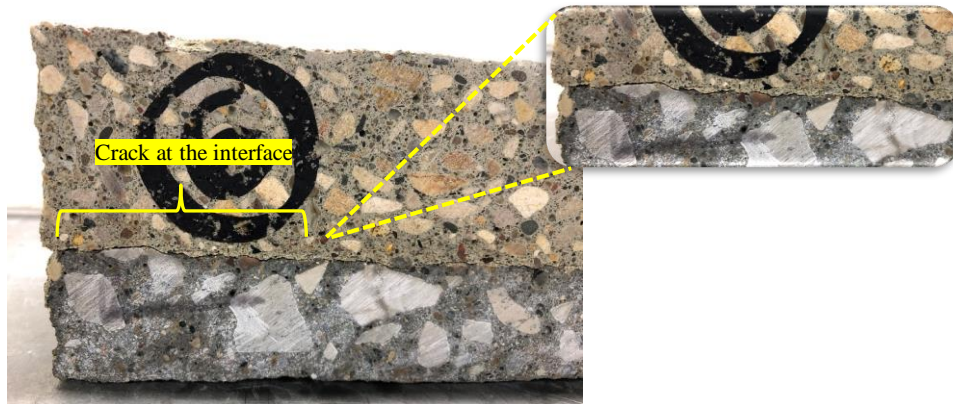


(d) Completely deteriorated beams after 144 freeze-thaw cycles

**Figure 4.25. Magnified images of freeze-thaw-related deterioration in LMC-VE-only beams**



(a) LMC-VE-overlaid beam without any visible or measurable damage after 72 freeze-thaw cycles



(b) Cracking at the interface of LMC-VE-overlaid beam at 108 freeze-thaw cycles



(c) Complete failure at the LMC-VE-substrate interface (separation of overlay and substrate) after 144 freeze-thaw cycles

**Figure 4.26. Magnified images of freeze-thaw-related deterioration in LMC-VE-overlaid beams**

### 4.3 Summary of Laboratory Investigation

This section summarizes the laboratory tests and results.

#### 4.3.1 Mechanical Properties

The mechanical properties of LMC-VE that were studied include compressive and flexural strength development of the LMC-VE and the LMC-VE-substrate bond strength via the pull-off strength test. The specimens were demolded after 1 day, cured in a standard moisture curing

room ( $23\pm3^{\circ}\text{C}$  and  $95\pm3\%$  RH) for 3 days, and then air cured under laboratory conditions ( $23\pm3^{\circ}\text{C}$ ) until the testing age. Key results were as follows:

1. LMC-VE showed a compressive strength of 2,827 psi at 3 hours, which confirms that LMC-VE can be used to accelerate the construction and opening to traffic of bridge deck overlays. The strength increased by a factor of three to 7,816 psi at 400 days.
2. An early-age flexural strength of 685 psi was recorded for LMC-VE beams at 3 days, which further increased to 865 psi at 28 days.
3. Pull-off strength tests conducted at 28 days on LMC-VE-overlaid beams indicated an LMC-VE-substrate bond strength of 283 psi (a very good bond strength value that is greater than the minimum specified pull-off strength value of 250 psi for thin epoxy overlays).

#### *4.3.2 Chloride Intrusion*

The resistance of LMC-VE to the intrusion of deleterious chloride ions was studied using the SR (electrical) and salt ponding (non-electrical) test methods. Key results were as follows:

- Cylinder samples of LMC-VE were moist cured for 3 days and air cured thereafter. The average SR values measured from the samples increased from 24.9 k $\Omega$ -cm at 3 days to 70.3 k $\Omega$ -cm at 14 days. At 28 days, the SR values measured from the air cured samples were unstable.
- After 28 days, the SR values of the LMC-VE samples were determined after the samples were soaked in water for 2 days to ensure a stable reading. With this modified test procedure, the average SR values of the LMC-VE samples were 61.4 k $\Omega$ -cm at 170 days and 110.3 k $\Omega$ -cm at 440 days, showing enhanced impermeability with time.
- The chloride content determined from the 90-day salt ponding tests showed an average chloride content of 0.36% in the top 1/2 in. layer and 0.13% in the bottom 1/2 in. layer. These values indicate that an LMC-VE overlay has a chloride penetration resistance better than that of an LSDC overlay but not as good as that of an epoxy overlay.

#### *4.3.3 Moisture Transport*

The moisture transport properties of LMC-VE were evaluated using a standard water sorptivity test. The test was performed on specimens sliced from field-cast, laboratory-cured 4 in. x 8 in. LMC-VE cylinders and on smaller specimens sliced from field-cored samples of the actual overlay at different ages. For comparison, two specimens sliced from field cores of the existing HPC deck were also tested. Key results were as follows:

1. Both the initial sorptivity and secondary sorptivity values of the LMC-VE specimens decreased when the age of the overlay increased from 2 months to 8.5 months, indicating pore refinement of the concrete over time.
2. The initial sorptivity of the field-cast and field-cored LMC-VE specimens was lower than that of the HPC specimens obtained from an existing concrete deck, whereas the secondary sorptivity of the field-cast and field-cored LMC-VE specimens was slightly higher than that of the HPC specimens before the LMC-VE specimens reached the age of 258 days. After 258



days, the secondary sorptivity values of the field-cored LMC-VE overlay specimens started approaching those of the existing HPC substrate specimens.

#### *4.3.4 Other Durability Properties*

The other durability properties that were evaluated for LMC-VE included shrinkage (both drying and autogenous) and freeze-thaw resistance. Shrinkage was investigated using standard LMC-VE beam specimens. Freeze-thaw tests were conducted using LMC-VE-only and LMC-VE-overlaid beam specimens. Key results were as follows:

1. After 400 days, the autogenous shrinkage and drying shrinkage of LMC-VE was 115 and 440 microstrain, respectively. These values are similar to those of normal-strength PCC.
2. The LMC-VE-only beams showed poor freeze-thaw resistance. Significant mass loss occurred after 72 freeze-thaw cycles, and the samples lost their prism shape and were unable to be tested after 112 freeze-thaw cycles. The relative dynamic modulus of the samples was less than 60% at 72 freeze-thaw cycles (a relative dynamic modulus of 60% is the ASTM C666 limit for stoppage of freeze-thaw testing).
3. The LMC-VE-overlaid beams showed better freeze-thaw resistance than the LMC-VE-only beams. Significant mass loss was not observed, and the relative dynamic modulus values were greater than 85% until 144 freeze-thaw cycles. However, after 144 cycles the LMC-VE-substrate interface failed, i.e., the LMC-VE overlay separated from the substrate. Therefore, freeze-thaw tests were discontinued thereafter.

Note that the failure of the bond between the LMC-VE and the substrate was possibly due to inadequate preparation of the substrate concrete surface in the laboratory, where the substrate's surface was prepared to the expose coarse aggregate using a steel brush to remove the mortar before concrete was fully set, after which sand-blasting was performed on the exposed aggregate surface. However, the field overlay placement consisted of aggressive surface preparation techniques that included milling, hydrodemolition, and sand-blasting. As can be seen in Chapter 5, the field test results indicate that the LMC-VE-substrate bond strength in the field did not change noticeably after the overlay had been in service for over a year.

## 5. FIELD MONITORING

This chapter provides information on all of the field monitoring activities that were conducted once the LMC-VE overlay placement/casting process was completed in the field. The field monitoring consisted of performing regular field tests on the LMC-VE-overlaid deck surface at different overlay ages after field construction. Initially, field visits were conducted more frequently to monitor early-age properties. Later, visits were conducted twice a year (once during the spring in May and once during the fall in November) to monitor the field performance of the LMC-VE overlay. A summary of the 11 field visits undertaken throughout this project is given in Table 5.1. Information related to all of the field visits is presented in this chapter.

**Table 5.1. Summary of field visits conducted**

Field Trip #	Field Trip Date	Overlay Age
-	September 5, 2019	Field overlay casting
1	September 10, 2019	0.1 month (4 days)
2	November 04, 2019	2.0 months (60 days)
3	May 20, 2020	8.5 months (258 days)
4	November 02, 2020	14 months
5	May 12, 2021	20 months
6	November 08, 2021	26 months
7	May 19, 2022	32 months
8	October 28, 2022	38 months
9	May 23, 2023	44 months
10	November 06, 2023	50 months (5 years)

### 5.1 Field Monitoring and Test Methods

Immediately after the LMC-VE overlay was cast in the field, the concrete was covered with a wet rag. The covered concrete surface was also continuously sprayed with water for 3 hours of wet curing. After completion of the wet curing, the concrete surface was uncovered and exposed to natural environmental conditions. The complete deck surface was cast in two stages, as explained in Chapter 3. Once the first stage of casting was completed, the SR of the LMC-VE overlay was measured on the overlay's surface using a four-point Wenner probe (the same instrument that was used for SR measurements in the laboratory) to serve as a reference SR value for future measurements.

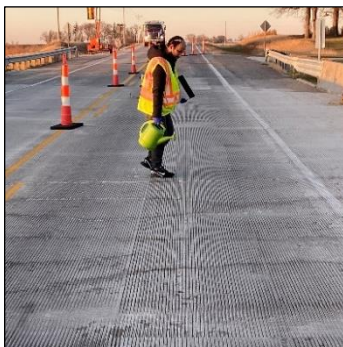
Thereafter, regular field visits were conducted to perform crack and deterioration surveys and to measure SR, friction index, and pull-off strengths at different overlay ages (starting from an early overlay age of 4 days after casting). The detailed procedures that were followed to conduct the aforementioned field tests are given in the following sections.



### 5.1.1 Crack and Deterioration Survey

Each crack and deterioration survey consisted of a careful visual examination of the overlay surface to detect, locate, and record the presence of any cracking or deterioration of the deck surface. The procedure followed to perform the survey was as follows:

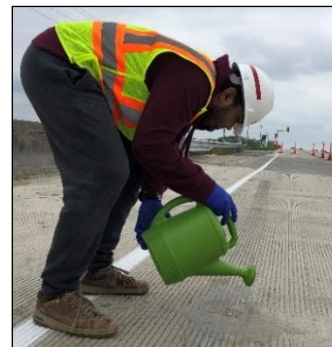
1. A transverse pass was made starting from one side of the deck while spraying water to wet a small portion of the overlay surface, as shown in Figure 5.1a.
2. Soon after the water was sprayed, careful examination was made of the wet portion of the overlay surface to identify the presence of any cracks, as shown in Figure 5.1b. The sprayed water helped to detect the cracks more clearly.
3. When a crack was identified, the location of the crack was noted, and its profile was manually drawn on the bridge layout drawing. The crack location with respect to the side railings and/or connection joints were measured and marked on the same bridge layout drawing for identification of individual cracks during subsequent field trips. The length (in feet) and width (in inches) of the cracks were also measured and recorded. The crack widths were measured using a handheld crack comparator, shown in Figure 5.1c.
4. Signs of other types of deterioration (such as spalling and abraded regions, examples of which are shown in Figure 5.1d) were also identified, mapped, and photographed.



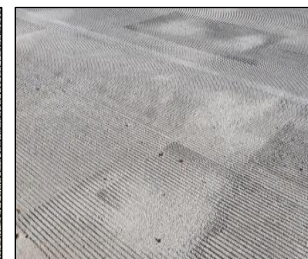
(a) Spraying water to wet small portion of overlay surface



(b) Careful examination for cracks



(c) Crack comparator used for crack width measurement



(d) Typical spalled and abraded areas on the overlay concrete

**Figure 5.1. Performing crack and deterioration survey**

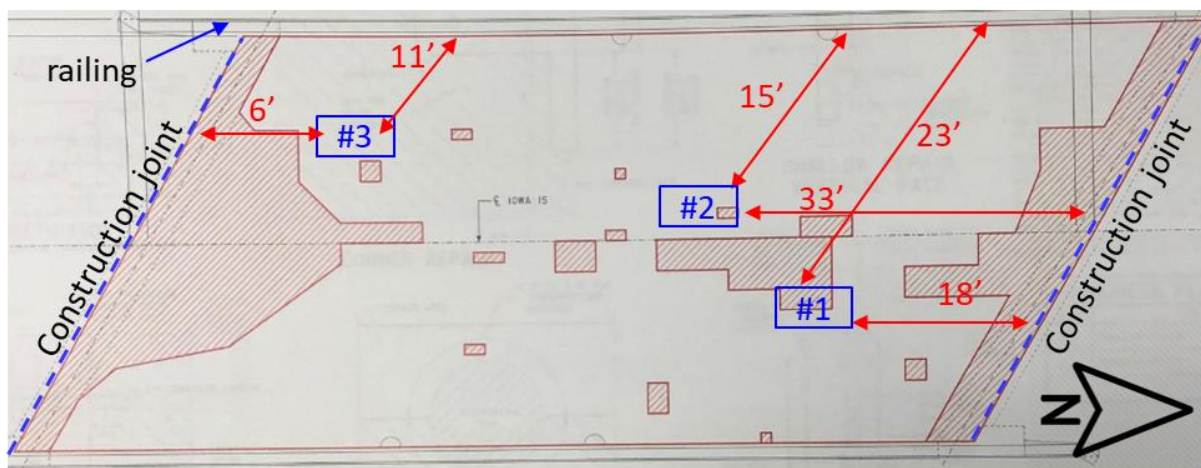
### 5.1.2 Friction Index

The friction characteristics of the overlay surface were determined by measuring the surface's British Pendulum Number (BPN) using a British Pendulum Tester, shown in Figure 5.2a. The testing was performed in accordance with ASTM E303. Immediately before measurement at each test location, the deck surface was cleared using a brush to ensure that the surface was free of loose material and dust particles, as shown in Figure 5.2b.



**Figure 5.2. British Pendulum Tester used for measuring BPN**

The BPN measurements were made at three different locations on the deck surface, as shown in Figure 5.3. (In the figure, the test locations are numbered #1, #2, and #3. The locations were mapped by measuring distances [in feet] with respect to the construction joints and/or side railings.) These testing locations were fixed, and thus the BPN measurements were made at the same three locations during each field trip.



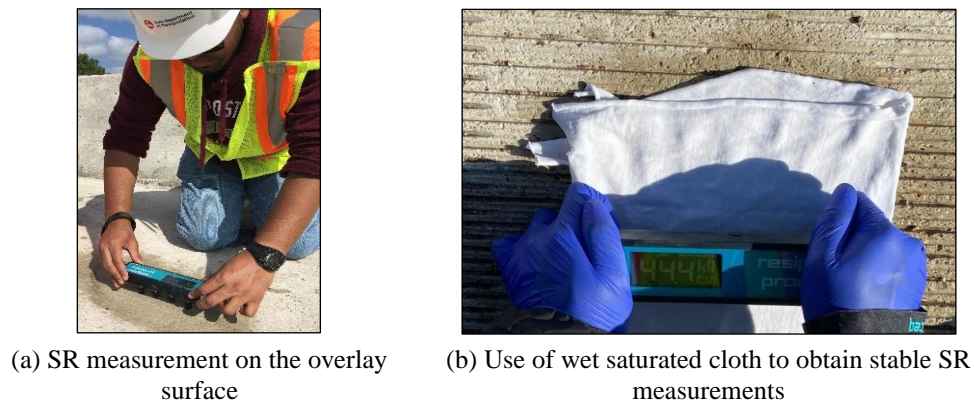
**Figure 5.3. Bridge layout showing BPN measurement locations (#1, #2, and #3)**

At each location, BPN measurements were made parallel and perpendicular to the grooves on the overlay surface (except during Trip 1, when the grooves were not yet in place). The measurements were made in dry and wet conditions of the overlay surface. (For wet

measurements, sufficient water was sprayed at the test location on the overlay surface using a handheld water sprayer, as shown in Figure 5.2c.) Hence, a total of four configurations (i.e., parallel dry, parallel wet, perpendicular dry, and perpendicular wet) were captured at each location, and an average of four BPN measurements in each configuration were taken at each test location during every field trip. A contact path length of 5 in. (for the slider) was always maintained for all BPN measurements in accordance with ASTM E303.

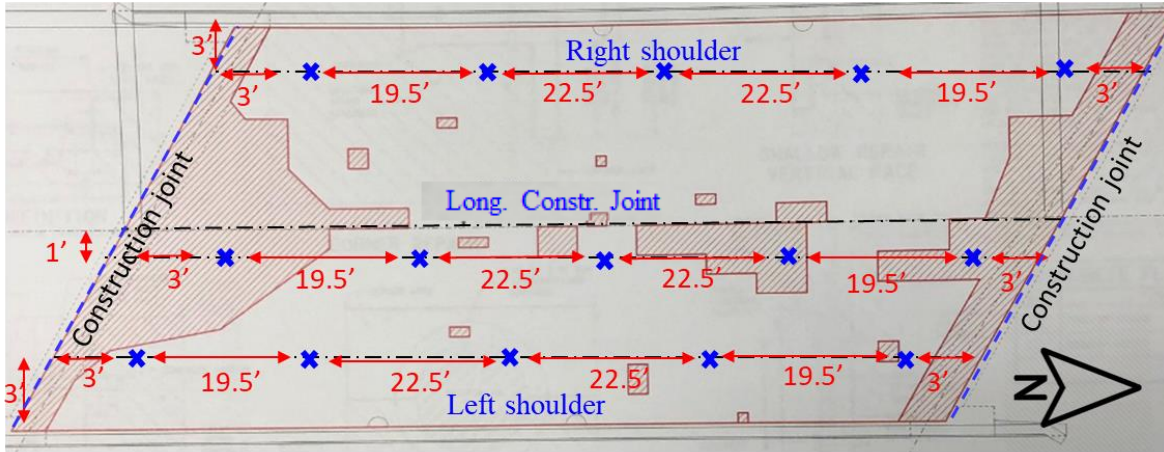
### 5.1.3 Surface Resistivity

SR measurements were made in the field using a handheld four-point Wenner probe (Figure 5.4), the same instrument that was used for SR measurements in the laboratory. On the overlay surface, the resistivity measurements were made at different locations on the right shoulder, close to the longitudinal construction joint, and on the left shoulder, as indicated in Figure 5.5. (In the figure, all testing locations are indicated by an ×.) Prior to each measurement, the deck surface was sprayed with water (using the same handheld water sprayer that was used during the BPN measurements), and the four probes of the instrument were dipped in water to ensure proper contact of the probes with the overlay surface. The four probes were pressed firmly against the overlay surface to obtain SR readings in  $k\Omega\text{-cm}$ . An average of two SR measurements were taken at each test location during each field trip. The abovementioned procedure was used for Trip 1 through Trip 3. Using the same testing procedure resulted in unstable (highly fluctuating) SR readings during Trip 2 and Trip 4 (both of which were conducted in November, i.e., in late fall). Thus, during Trip 4, an attempt was made to use a saturated/wet cloth in between the instrument probes and the wet overlay surface, as shown in Figure 5.4b. Use of the wet cloth provided not only stable SR measurements but also measurements that were repeatable. More information on this procedure is given in Section 5.2.3.



**Figure 5.4. Field SR measurement using a Wenner probe**



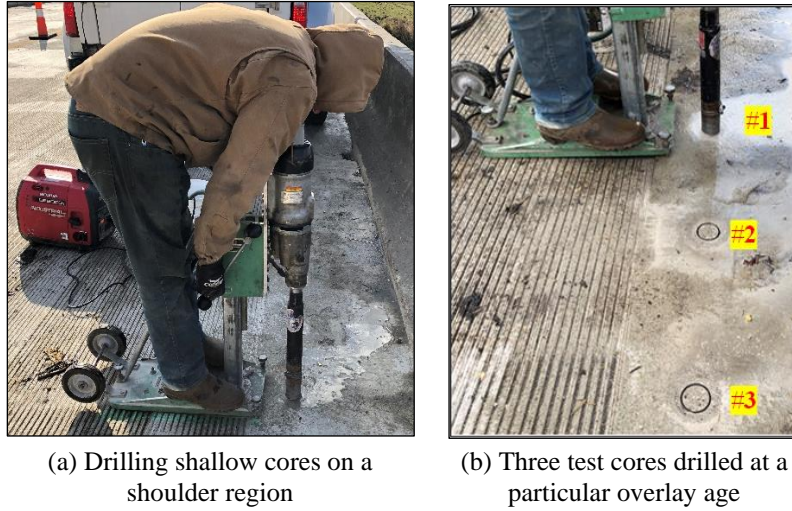


**Figure 5.5. Bridge layout showing SR measurement locations (indicated by ×)**

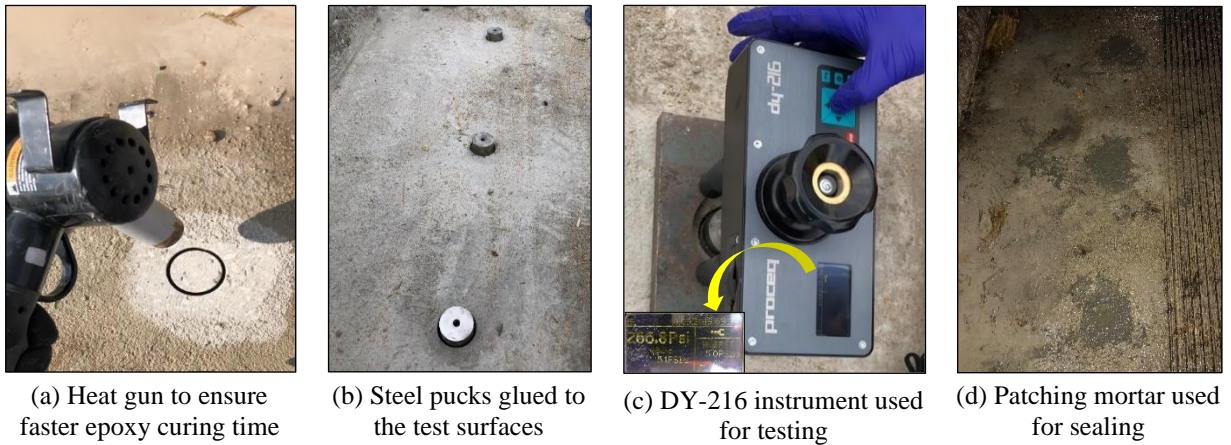
#### 5.1.4 Pull-Off Strength

Pull-off testing in the field was performed using a portable Proceq DY-216 pull-off testing device. The testing was conducted in accordance with ASTM C1583 using the following procedure:

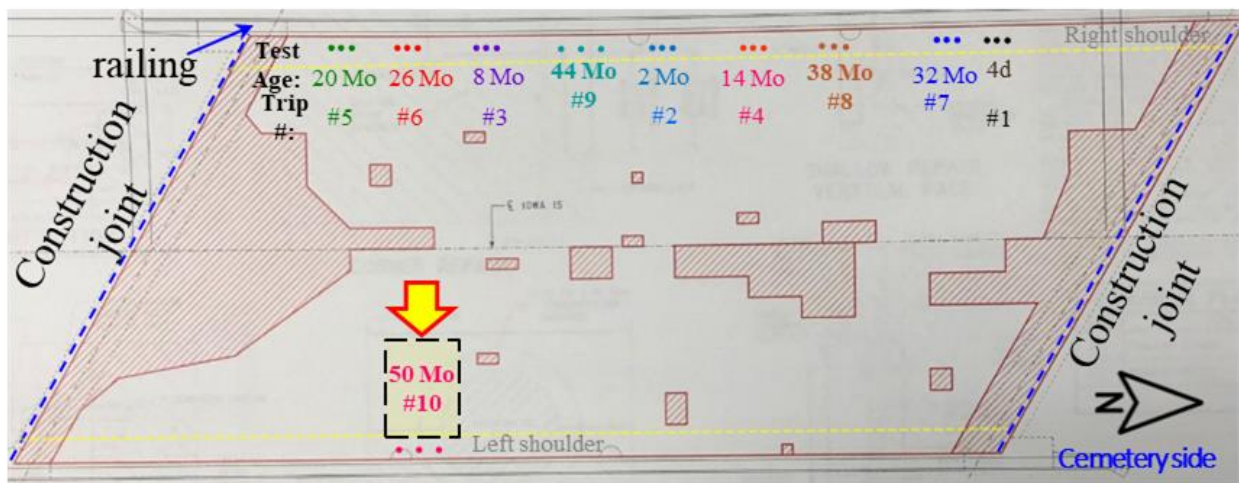
1. Three shallow cores were drilled in the shoulder region at each test location using a portable core drilling machine, as shown in Figure 5.6a and Figure 5.6b.
2. Once the core drilling was completed, the surface of each test core was brushed using sandpaper to ensure that surface was free of soft, loose particles that would prevent the steel pucks from adhering to the prepared surfaces.
3. The surface of the sandpaper-brushed test cores was blown dry using a handheld air blower/heat gun to remove wetness and dust particles, as shown in Figure 5.7a. The blow drying also helped the epoxy cure faster and stick firmly to the steel pucks. The latter was especially relevant and important during winter field trips.
4. A thin uniform coat of structural epoxy (Sikadur-31 Hi-Mod Gel, Part A and Part B in a 1:1 mix ratio) was then applied to the blow-dried test surfaces, after which the steel pucks were manually pressed against the epoxy-coated surfaces, as shown in Figure 5.7b, and held for a while to make sure they remained firmly in place. A dead weight was placed over these pucks until they were tested to ensure a stronger bond between the pucks and the overlay surface. (All of these precautions were consciously taken to avoid any possibility of epoxy failure during pull-off testing.)
5. After letting the epoxy cure (for at least 5 to 6 hours, supplemented with hot air frequently blown over the glued steel pucks using a heat gun), the pucks were screwed to the pull-off testing equipment one at a time, as shown in Figure 5.7c, after which the load was applied until failure.
6. After testing, pictures of all of the failed cores were taken, and the failure strength value (i.e., pull-off strength) and the failure mode of each core were recorded.
7. The tested locations were sealed off using a patching mortar, as shown in Figure 5.7d (with water : cement : sand proportions of 0.3:1:2.5). All tested locations are shown in Figure 5.8.



**Figure 5.6. Drilling cores for pull-off strength test in the field**



**Figure 5.7. Pull-off testing of the field overlay**



**Figure 5.8. Pull-off test locations**

## 5.2 Field Monitoring Results

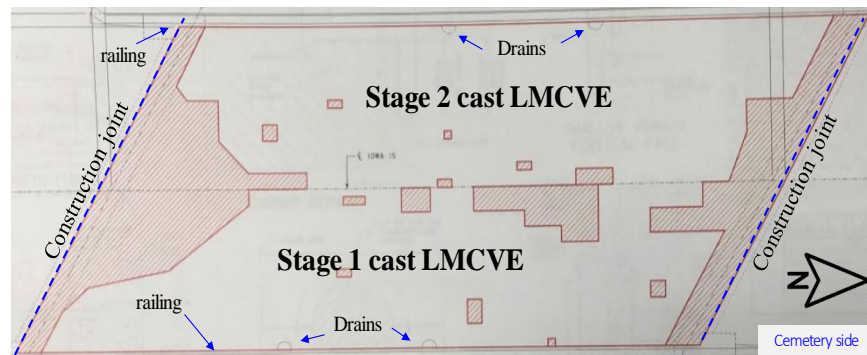
The results of the field tests that were performed from an early age of 4 days (after overlay construction) through the end of the research project (50 months) are given in Sections 5.2.1 through 5.2.4. These tests were conducted during regular field visits that were undertaken to monitor the field performance of the cast LMC-VE overlay.

### 5.2.1 Crack and Deterioration Survey

A crack survey was conducted during each visit that followed the procedure outlined in Section 5.1.1. When cracks were identified, their dimensions were measured and their locations were mapped through measurement of their distances with respect to the construction joints and/or side railings of the bridge.

This section provides information on crack identification and the growth of cracks with respect to their lengths and widths over time. The complete details about the crack survey results obtained during each visit are given first, and then a comparison between the obtained crack survey results at different overlay ages is provided. The latter helps in understanding the growth of cracks in terms of their number (i.e., total number of identified cracks), their widths (measured using a crack comparator), and their lengths.

Figure 5.9a shows the plan/layout of the bridge deck with the LMC-VE overlay, which was cast in two stages. It should be noted that a detailed crack survey was not performed at an age of 4 days and therefore is not shown. Figure 5.9 and Figure 5.10 provide a summary of the crack surveys conducted at different ages. The figures show the cracks that were identified at different locations and provide information on their lengths and widths at each age. Though the locations of these identified cracks were mapped and recorded with respect to benchmarks, as explained above, the information on the distances is not provided in this section for legibility purposes. More detailed information on the crack mapping results and the distances recorded is provided in Appendix B.



(a) Cast overlay on the bridge deck surface



[illegible][illegible]

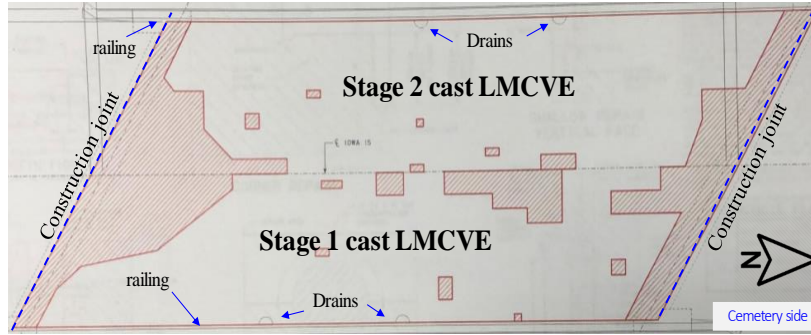
Figure 1 is a plan view of the test structure. It shows a cross-section of a concrete structure with two stages of casting. The lower portion is labeled 'Stage 1 cast concrete' and the upper portion is labeled 'Stage 2 cast concrete'. The structure is divided into several vertical sections by wavy lines representing reinforcement or joints. Dimensions are given in feet and inches. A north arrow points towards the top right.

[illegible]

\*Figure not to scale

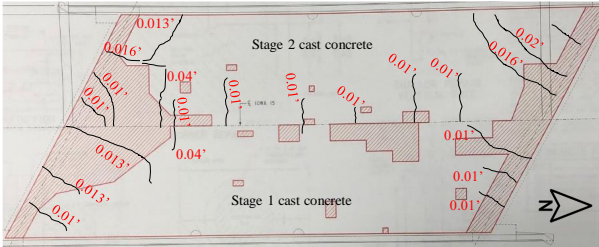
**Figure 5.9. Crack length development in the LMC-VE overlay over time**





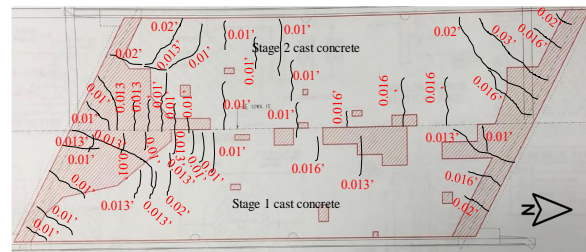
(a) Cast overlay on the bridge deck surface

#### Fall (November) Field Trips

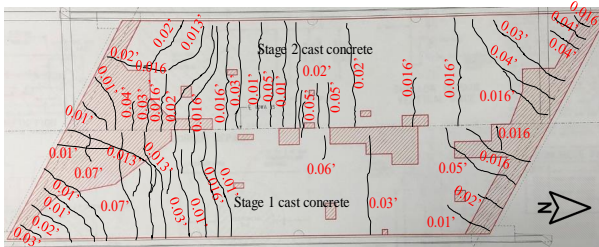


(b) Trip 2 (overlay age of 2 months)

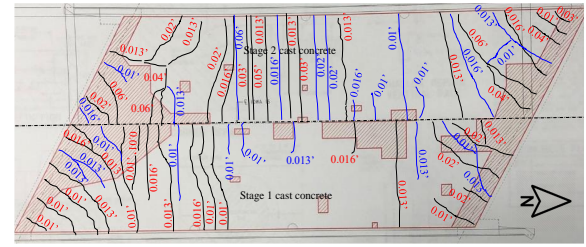
#### Spring (May) Field Trips



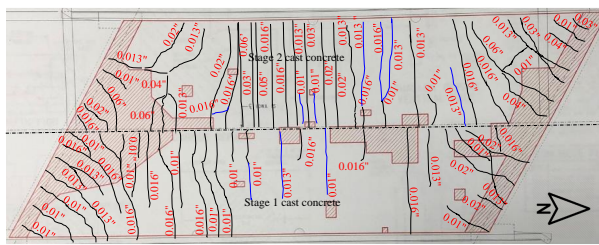
(c) Trip 3 (overlay age of 8.5 months)



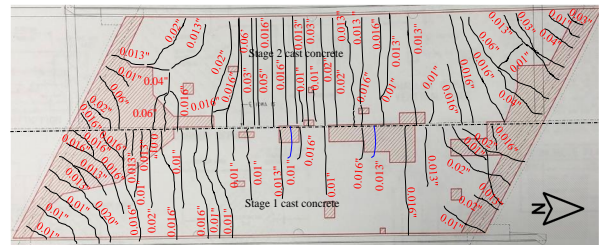
(d) Trip 4 (overlay age of 14 months)



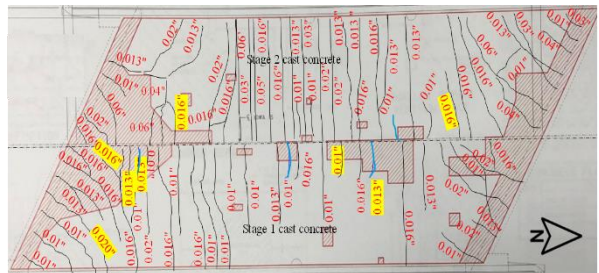
(e) Trip 5 (overlay age of 20 months)



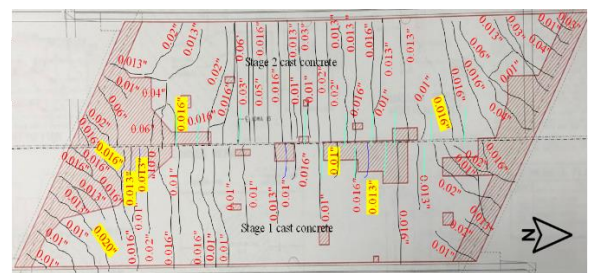
(f) Trip 6 (overlay age of 26 months)



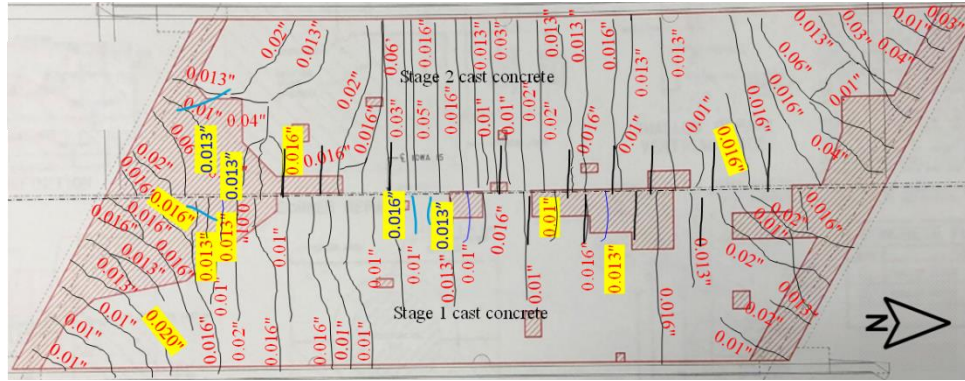
(g) Trip 7 (overlay age of 32 months)



(h) Trip 8 (overlay age of 38 months)



(i) Trip 9 (overlay age of 44 months)



(j) Trip 10 (overlay age of 50 months)

**Figure 5.10. Crack width development in the LMC-VE overlay over time**

Figure 5.11 compares the deck surface and Figure 5.12 shows the deteriorations observed at different ages throughout the project.



### Fall (November) Field Trips



(a) Trip 2 (overlay age of 2 months)

### Spring (May) Field Trips



(b) Trip 3 (overlay age of 8.5 months)



(c) Trip 4 (overlay age of 14 months)



(d) Trip 5 (overlay age of 20 months)



(e) Trip 6 (overlay age of 26 months)



(f) Trip 7 (overlay age of 32 months)



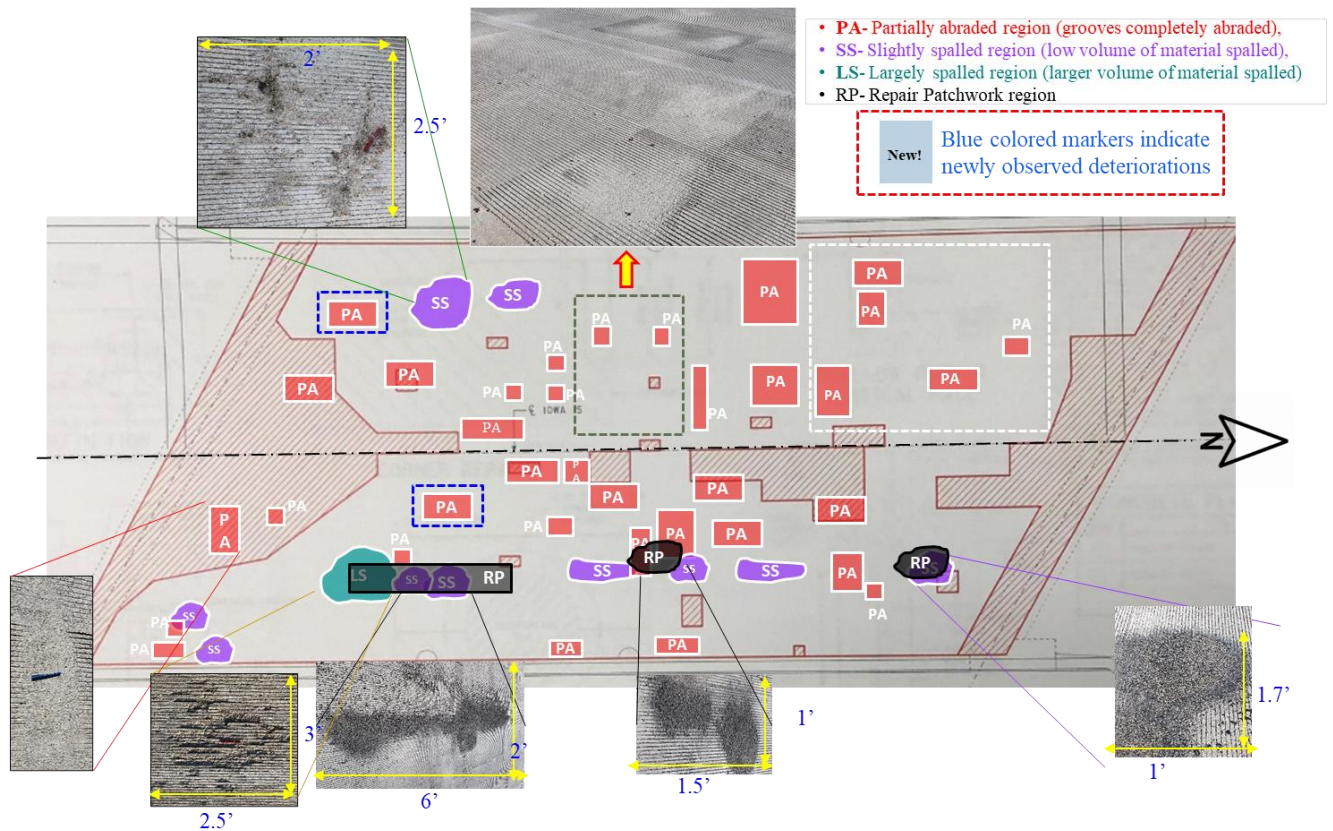
(g) Trip 8 (overlay age of 38 months)



(h) Trip 9 (overlay age of 44 months)

**Figure 5.11. Comparison of overlay deck surface at different ages (up to 44 months)**





**Figure 5.12. Deteriorations observed at an overlay age of 50 months (during Trip 10)**

The crack survey sketches in Figure 5.9 and Figure 5.10 indicate the occurrence of mostly transverse cracks, cracks that are perpendicular to the bridge abutments, and diagonal cracking at corner areas. However, there is no evidence of longitudinal cracking. The observed cracking pattern on the overlay surface could possibly be a result of a combination of factors, such as early-age shrinkage, thermal-based reflective cracks from the substrate, and structural factors (such as early loading and bridge skew angle). Generally, it is difficult to conclusively point to a single factor that causes the cracks observed in any structure such as a concrete deck or an overlay surface, as highlighted by Phares and Harrington (2016). Previous literature has reported that LMC-VE is susceptible to early-age shrinkage cracking as a result of high autogenous and thermal shrinkage (Yun et al. 2007). Although the laboratory investigation showed that the shrinkage behavior of LMC-VE was similar to that of conventional pavement concrete (Figure 4.22), the early opening of the overlay to traffic might have increased the likelihood of shrinkage cracks because the concrete continues to shrink after exposure to traffic loads. When such volumetric changes occur in an LMC-VE overlay that is placed on substrate concrete, the substrate concrete could act as a restraint, resulting in cracking of the overlay (Yun and Choi 2014). Such cracks could be visible even in a short period of time (a few weeks). Diagonal cracking observed only at the corners could be a result of the bridge skew angle because such cracking is most commonly observed in bridges with skew, as reported in Fu et al. (2007).

For skewed bridges with integral abutments and steel H-piles, Iowa bridge design practice approaches the orientation of the steel H-piles differently for bridges based upon the degree of

bridge skew. For bridges with a skew of 30 degrees or less, the steel H-piles are oriented with the weak axis parallel to the centerline of the abutment. For bridges with a skew greater than 30 degrees, the H-piles are oriented with the strong axis perpendicular to the abutment centerline. Considering this, when deck cracking perpendicular to the abutments is observed, it could be questioned whether the cracking is because of the steel H-pile orientation. Even if the original steel H-pile orientation was correct, the question would then be whether the steel H-piles had been installed correctly. If the steel H-piles were not correctly oriented for integral abutment designs, their orientation may resist the thermal expansion/contraction of the bridge, resulting in cracks perpendicular to the centerline of the abutments.

The cracking observed in the overlay could also be reflective cracking from the original deck surface. Bridge decks that are to be rehabilitated with a bridge deck overlay may have existing deck cracking (typically transverse deck cracking). At the point in a bridge deck's life cycle when a deck overlay is needed, the bridge deck has achieved its ultimate strength and maximum shrinkage. When a new deck overlay is placed and well bonded to the existing deck substrate (as was done for the LMC-VE overlay in the present case), any movement in the overlay will be restrained by the existing bridge deck substrate. If there are cracks in the existing bridge deck substrate, they will tend to propagate through the new bridge deck overlay during bridge expansion/contraction due to the bond between the new deck overlay and the existing bridge substrate. However, bridge inspection documentation prior to installation of the LMC-VE overlay showed minimal cracking, though a fair amount of deck patching and delamination was noted. Therefore, it is inferred that some cracks in the LMC-VE overlay might be reflective cracks, but most cracks observed in the LMC-VE overlay are likely not. Table 5.2 lists other possible reasons for the identified cracks on the LMC-VE overlay's surface.

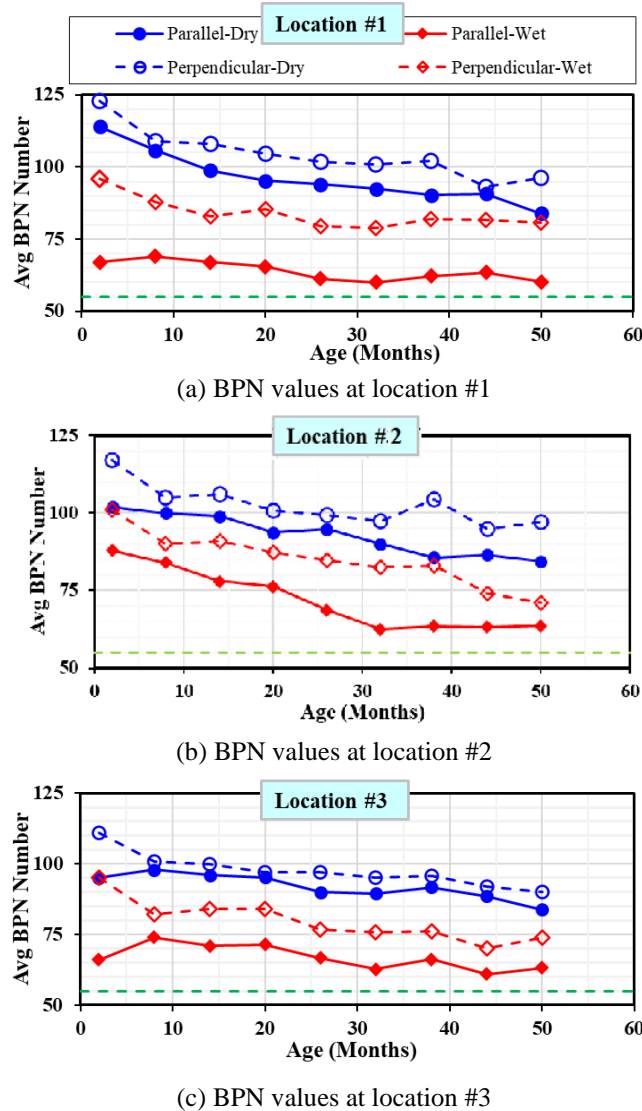
**Table 5.2. Summary of possible reasons for identified cracks on the overlay surface**

Type of Observed Cracking	Possible Causes
Transverse cracks	Early-age thermal and drying shrinkage of concrete
Cracks perpendicular to abutments	Bridge skew angle
Corner cracks	Bridge skew angle
Cracks perpendicular to grooves	Bridge skew angle

### 5.2.2 Friction Index

The friction properties of the overlay were measured using a British Pendulum Tester to obtain BPN values. BPN values were measured at the same three locations on the bridge deck during each field visit. At each location, measurements were made parallel and perpendicular to the grooves in the overlay surface when the surface was dry and wet. Figure 5.13 indicates the BPN values at different ages. Each data point in the figure represents an average of four BPN readings. Since grooves had not yet been made at an early age of 4 days, the measurements taken during the first field visit were made at each test location in only one direction on a wet overlay surface. Once grooves were made on the overlay surface (after 4 days and before 60 days), the BPN values increased at all test locations in general, as predicted (the only exception being parallel-wet measurements at location #3).





**Figure 5.13. BPN values at different overlay ages**

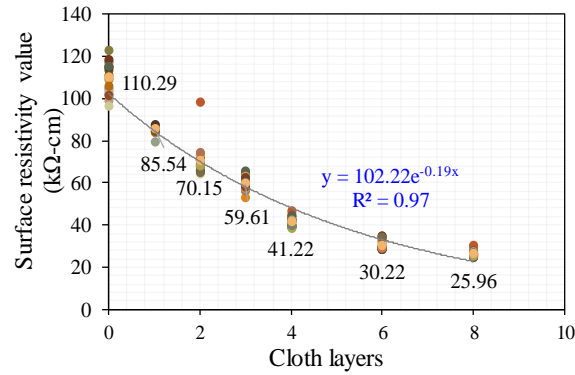
The figure shows that at each test location in a particular direction (parallel or perpendicular to the grooves), the BPN measurements made on a water-sprayed surface (i.e., wet surface) were lower than the corresponding measurements made on a dry surface, as expected. Additionally, in a particular moisture state (wet or dry), the measurements made perpendicular to the grooves were higher than the corresponding measurements made parallel to the grooves, also as expected. Overall, though a slight reduction in the average BPN values is evident at each test location from 4 days to 50 months, all BPN values at 50 months are still greater than 55, which is typically the minimum specified BPN value for safe traffic usage.

### 5.2.3 Surface Resistivity

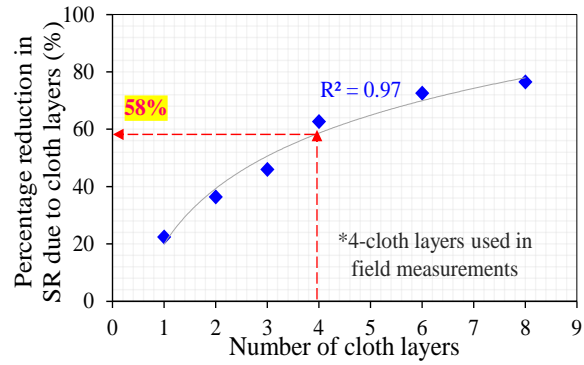
Surface resistivity in the field was measured on the moist (water-sprayed) overlay surface using a four-point Wenner probe, as mentioned previously. This procedure was used from Trip 1 through

Trip 3. During Trip 2 and Trip 4, however, using the same testing procedure resulted in unstable SR readings (highly fluctuating). Thus, during Trip 4 an attempt was made to use a saturated/wet cloth in between the instrument probes and the wet overlay surface, as shown in Figure 5.4b, to obtain stable SR readings. To obtain better contact between the probes and the overlay surface, a cloth thickness of four layers was used during the field SR measurements. It was observed that the use of the wet cloth provided not only stable SR measurements but also field measurements that were repeatable.

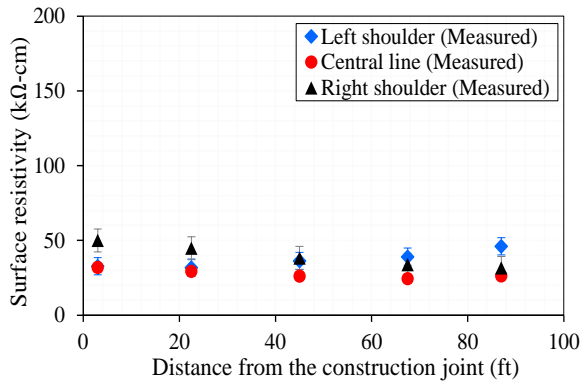
Since a wet cloth, being a saturated medium, could have a certain conductivity and associated resistivity, changes in the SR readings due to the use of the wet cloth had to be analyzed. To determine the effects of the wet cloth, numerous SR measurements were made on water-soaked standard cylinder specimens (the same cylinders used for laboratory SR measurements) using different cloth thicknesses (0 to 8 layers of wet cloth) in the laboratory. The SR measurements obtained using different numbers of cloth layers are shown in Figure 5.14a. The figure shows that measurements made following the conventional procedure (without using cloth) resulted in an SR value of 110.29 k $\Omega$ -cm at a specimen age of 440 days, whereas measurements made using any number of cloth layers resulted in SR values less than 110.29 k $\Omega$ -cm. With an increasing number of cloth layers (i.e., from 2 layers to 8 layers), the SR values decreased exponentially, and the curve started to flatten after 6 layers. This indicated that at higher numbers of cloth layers (i.e., 6 or 8 layers and higher), the Wenner probe started to indicate SR values corresponding only to those of the wet cloth. The percentage reduction in SR due to the use of different numbers of cloth layers is shown in Figure 5.14b. It can be observed that use of four cloth layers resulted in a 58% reduction in SR values compared to the SR values measured without cloth (i.e., 0 layers). Consequently, this correction for a 58% reduction in SR values was applied to the field SR values measured at 50 months using 4 cloth layers. Figure 5.14c shows the measured field SR values at 50 months, and Figure 5.14d shows the corresponding field SR values after applying the correction.



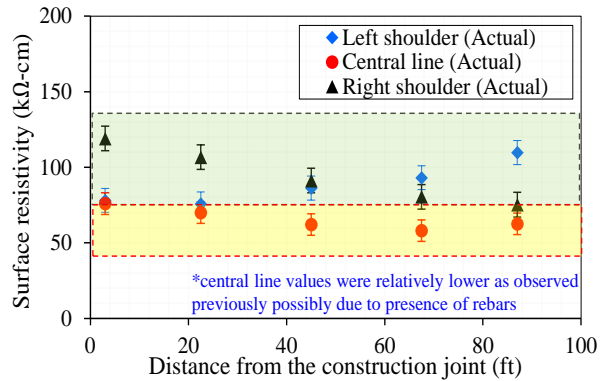
(a) Changes in SR due to different numbers of cloth layers



(b) Percentage reduction in SR due to different numbers of cloth layers



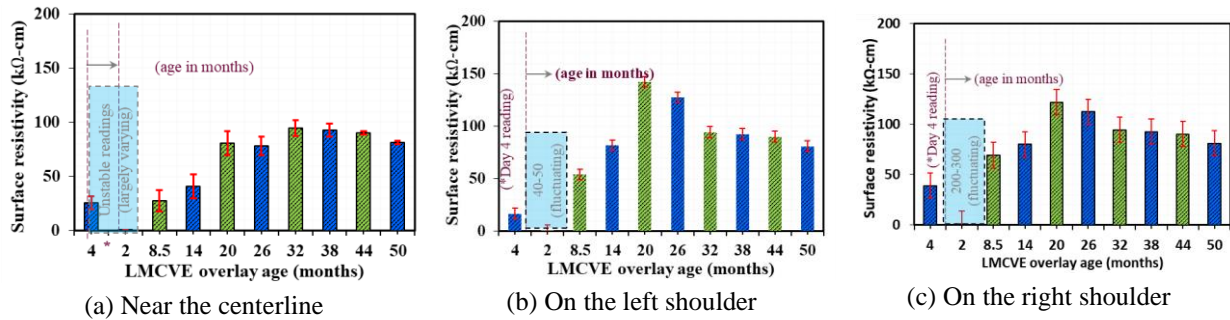
(c) Field SR values at 50 months (measured data)



(d) Field SR values at 50 months (corrected data)

**Figure 5.14. Correction to SR for using cloth layers in field measurements**

Figure 5.15a–c shows the development of SR with an increase in the age of the LMC-VE overlay at three measured locations, i.e., near the longitudinal construction joint, on the left shoulder, and on the right shoulder, respectively. Overall, it can be observed that at all three locations, the SR values increased as the overlay age increased, as expected. At an overlay age of 4 days, the SR values at the three locations were all different and were in the range of 16.75 to 39 kΩ-cm. At the age of 2 months (60 days), it can be observed that at two out of the three measured locations (i.e., on the left and right shoulders), the SR values fluctuated to a greater extent, as indicated in Figure 5.15b and Figure 5.15c. Though stable readings could be obtained near the centerline, the variation in SR values measured at this location was larger, as indicated by the error bar. The variation could possibly be due to improper contact of the electrodes with the overlay surface. The season (fall or spring) could also have had a significant effect on the SR values because SR fluctuations were specifically observed during the late fall (November) field trips and were not observed during the spring field trips.

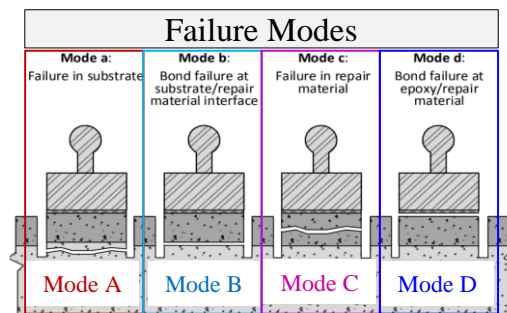


**Figure 5.15. Measured SR values at different locations on the deck surface**

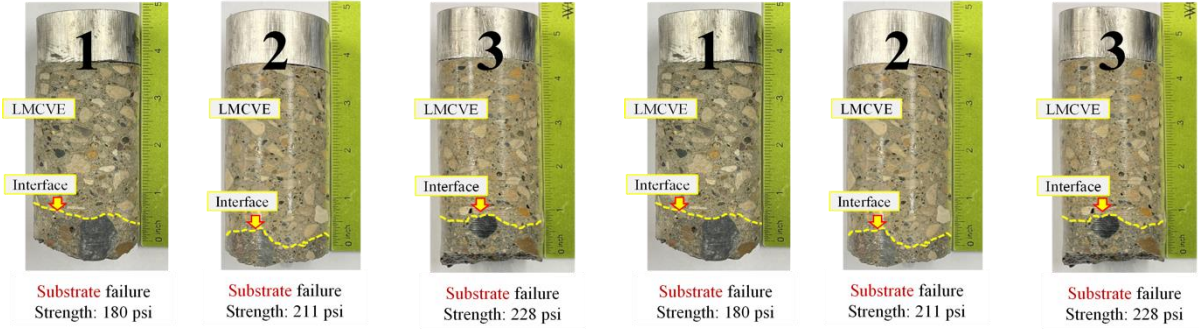
Later-age SR measurements at 8.5 months, 26 months, and 32 months indicated consistently higher SR values on both the right and left shoulders compared to those near the centerline. The lower SR values near the centerline could possibly be due to the presence of deck reinforcement bars underneath the measurement location. However, this was not clearly observed at 4 days because the SR values on the left shoulder were marginally lower than those near the centerline. When SR measurements made in same season are compared separately (to avoid complexity due to seasonal variations), a consistently increasing trend is evident in the SR values until an overlay age of 26 months. The SR values decreased slightly at all three locations at 50 months, indicating a slight reduction in the permeability resistance of the overlay material.

#### 5.2.4 Pull-Off Strength

Figure 5.16 shows typical failure modes according to ASTM C1583. A summary of all of the field pull-off strength test results along with the failure modes (observed from the images of the failed cores) are given in Figure 5.17a–j and Table 5.3. Three tests were conducted during each field trip, and hence a total of 30 pull-off tests were conducted in 10 trips.

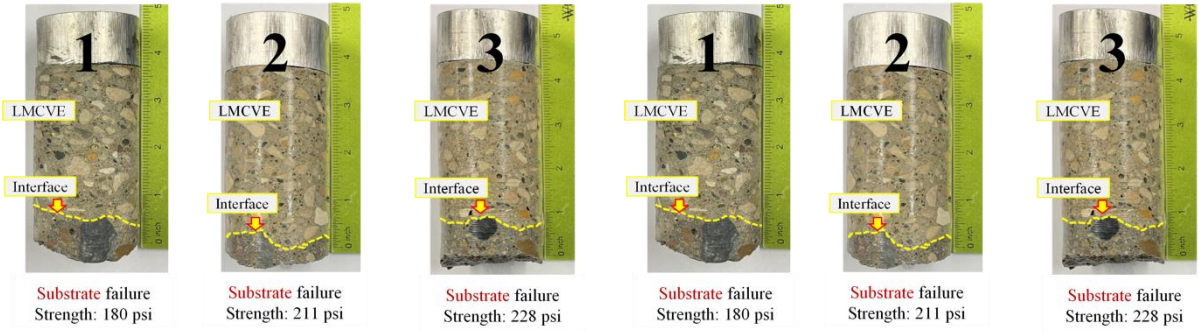


**Figure 5.16. Typical ASTM C1583 failure modes observed in pull-off tests**



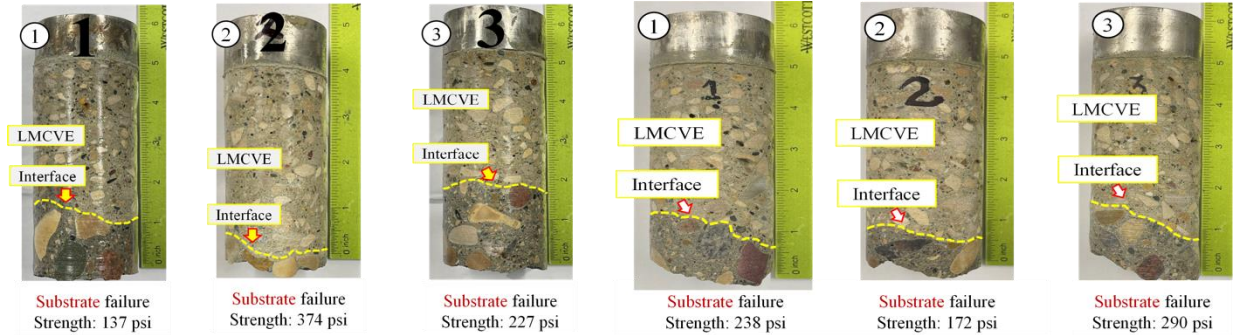
(a) Trip 10 (overlay age of 50 months)

(b) Trip 9 (overlay age of 44 months)



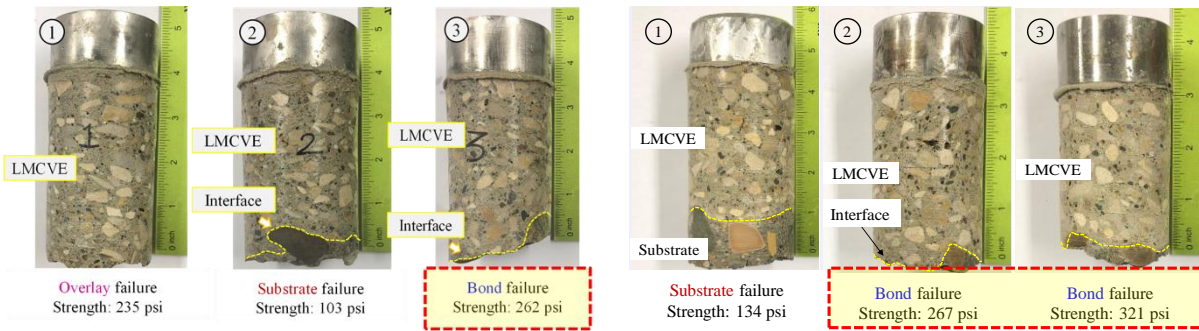
(c) Trip 8 (overlay age of 38 months)

(d) Trip 7 (overlay age of 32 months)



(e) Trip 6 (overlay age of 26 months)

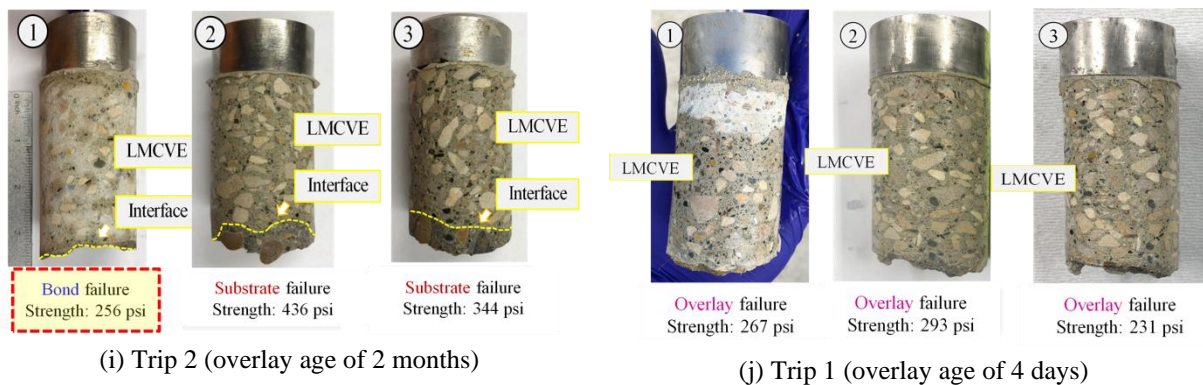
(f) Trip 5 (overlay age of 20 months)



(g) Trip 4 (overlay age of 14 months)

(h) Trip 3 (overlay age of 8.5 months)





**Figure 5.17. Comparison of pull-off test failure modes at different overlay ages (with bond failures highlighted in red dashed lines)**

**Table 5.3. Summary of field pull-off strength test results**

Test Date (Age)	Failure Mode and Individual Strength Values (psi)		
	Failure in Substrate	Failure at Interface	Failure in Overlay
Nov 06, 2023 (50 months)	189, 284, 259	-	-
May 23, 2023 (44 months)	218, 280, 205	-	-
Oct 28, 2022 (38 months)	299, 223, 232	-	-
May 19, 2022 (32 months)	180, 211, 228	-	-
Nov 08, 2021 (26 months)	137, 227, 374	-	-
May 12, 2021 (20 months)	172, 238, 290	-	-
Nov 02, 2020 (14 months)	103	262	235
May 20, 2020 (8.5 months)	134	267, 321	-
Nov 04, 2019 (2 months)	344, 435	256	-
Sept 10, 2019* (4 days)	-	-	231, 267, 293

\* All field tests at 4 days failed in the overlay because the coring done prior to the pull-off testing was only 3 in. deep, and hence the interface was not even encountered in the testing zone.

The following observations were made based on the field test results:

1. Cores that failed at the bond/interface at all ages indicated an LMC-VE-substrate bond strength greater than 250 psi (with the lowest strength being 256 psi). Thus, the LMC-VE-substrate bond strength could be classified as “very good” and adequate based on previous studies (Sprinkel 2000, Dahlberg and Phares 2016).
2. Overall, core specimens failed in the overlay LMC-VE at a very early age (4 days). As the age of the overlay increased (from 2 to 14 months), the failures of some core specimens appeared at the LMC-VE overlay and substrate interface, indicating that the interface was the weakest region as LMC-VE gained strength.
3. After 14 months, not only did the LMC-VE become stronger, the LMC-VE-substrate bond gained more strength. However, the strength of the substrate stabilized, and therefore most core specimens failed in the substrate.
4. There was greater variation in the substrate strength values, which ranged from 103 to 436 psi. The actual reason for the lower strength values (e.g., 103 psi) is unknown at this time. A possible reason could be damage to the substrate concrete caused by the milling operation



prior to overlay placement (Sprinkel 2000). The low substrate strength values might also indicate the differing quality of the substrate concrete in different locations.

It should be noted that, as seen in Table 5.3, there is a general trend that the core specimens failed in LMC-VE at a very early age (4 days). As the overlay age increased (from 2 to 14 months), most core failures occurred at the LMC-VE overlay and substrate interface. After 14 months, all core specimens tested failed at the substrate, indicating the growth of the bond strength between the LMC-VE overlay and substrate.

### **5.3 Chapter Summary**

The following is a summary of observations made from the field trips conducted from 4 days to 50 months:

- A number of cracks ranging in width from 0.01 to 0.16 in. were observed on the overlay surface. The cracks grew larger and more numerous over time. However, the appearance of newer cracks considerably decreased after approximately 20 months. In a few small areas, some spalling and abrasion were also observed on the deck surface. The cracking could possibly be due to a combination of various factors, such as early-age shrinkage, thermal-based reflective cracks from the substrate, and structural factors (such as loading and bridge skew angle).
- A very slight reduction in the average BPN values was observed over time. However, even the BPN values measured during the final field visit were still observed to be greater than 55, a BPN value that is deemed necessary for ensuring traffic safety.
- A general tendency for the SR values to increase with an increase in the overlay age was observed when the fall and spring field SR measurements were considered separately, up to an overlay age of 26 months. The measurements obtained after 26 months showed a slight decrease in the average SR values, possibly indicating a marginal deterioration in the permeability resistance of the overlay material.
- The field pull-off test results showed a general trend indicating that the LMC-VE-substrate bond failure mode changed with time. At a very early age (4 days), the failure occurred in the overlay LMC-VE. As the overlay age increased (from 2 to 14 months), most core failures occurred at the LMC-VE overlay and substrate interface. After that time (from 14 to 50 months), all core specimens tested failed at the substrate, indicating the growth of the bond strength between the LMC-VE overlay and substrate.
- Although exhibiting large variation, the strengths of most specimens at failure were greater than 250 psi, indicating that the LMC-VE-substrate bond strengths were higher than 250 psi, which could be classified as “very good” and adequate.
- At later ages (over 2.5 years), regions of surface degradation, such as spalling and abrasion, were noticed. These areas grew with time, and toward the end of the project (50 months) small areas of abrasion had spread around the deck.

## 6. LIFE-CYCLE COST ANALYSIS

LCCA is an economic analysis technique used to evaluate and compare various investment options based on their long-term economic efficiency (ACPA 2012). This technique has been widely applied for pavement design and preservation/rehabilitation (Wang and Wang 2019, Zhang et al. 2008, Babashamsi et al. 2016). In line with this, LCCA was employed in this study to analyze and compare the life-cycle cost of an LMC-VE overlay with those of various overlay alternatives. The analysis and results are presented in this chapter.

### 6.1 LCCA Approach

There are different approaches to performing an LCCA. This study adopted the approach recommended by the American Concrete Paving Association (ACPA) for conducting an LCCA of overlay alternatives. The steps are shown in Figure 6.1 and explained in more detail below:

1. **Select analysis period.** The analysis period is the number of years over which the alternatives are compared. For overlays, an analysis period of 30 years is generally selected.
2. **Select discount rate.** The discount rate accounts for fluctuations in both the investment interest rate and the rate of inflation. Based on input from the project's technical advisory committee (TAC) and the data available from the United States Office of Management and Budget, a discount rate of 3% was used in this study.
3. **Estimate initial agency costs.** Initial agency costs can be estimated by including the cost of subgrade preparation, material, equipment, and labor. In this study, pavement overlay alternatives were analyzed, and for simplicity the cost of construction (per square yard of overlay) was estimated as the initial agency cost. More details on the estimated cost for each overlay type evaluated in this study can be found in Table 6.3.
4. **Estimate user costs.** User costs are the costs that are incurred by users of the roadway over the analysis period. The costs associated with work zone, detours, vehicle operations, accidents, and delays due to capacity issues come under the purview of user costs.
5. **Estimate future agency costs.** Future agency costs are estimated by considering the cost and timing of maintenance and operation and preservation/rehabilitation.
6. **Estimate residual value.** The salvage value, if any, is estimated as the residual value. As per suggestions from the TAC, overlays were considered to have no residual value in this study.
7. **Compare alternatives.** The alternatives are compared based on a standard measure of economic value, such as net present value (NPV).

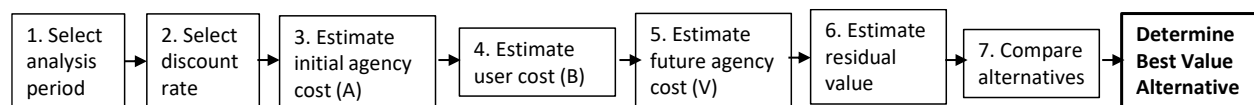


Figure 6.1. Steps involved in an LCCA of overlay alternatives

As described above, the alternatives in an LCCA are compared based on a standard economic indicator. The NPV and the equivalent uniform annual cost (EUAC) are the two commonly used indicators for this purpose. NPV is calculated as given in equation (1) to discount the future

agency cost to the present. EUAC provides an equivalent series of annual cash flows of uniform value over every year of the analysis period. The formula for EUAC is given in equation (2).

$$NPV = \text{Initial cons. cost} + \sum_{k=1}^N \text{Future cost}_k \left[ \frac{1}{(1+i)^{n_k}} \right] - \text{Salvage value} \left[ \frac{1}{(1+i)^{n_e}} \right] \quad (1)$$

$$EUAC = NPV \left[ \frac{1(1+i)^n}{(1+i)^n - 1} \right] \quad (2)$$

where  $N$  = number of future costs incurred over the analysis period,  $i$  = discount rate,  $n_k$  = number of years from initial construction to the  $k^{th}$  expenditure, and  $n_e$  = analysis period.

## 6.2 Overlay Alternatives

In this study, five pavement overlay alternatives belonging to two broad categories (polymer concrete and normal and high-performance concrete) were considered for the LCCA. The details of the alternatives are presented in Table 6.1. LMC-VE, LMC, PPC, PCC, and HPC overlays were evaluated. Low-slump PCC and HPC are the most commonly used overlays in Iowa, while the others have been used in only a limited number of projects. The LMC-VE overlay evaluated in this study was the first of its kind in Iowa, and hence minimal field data were available. Therefore, wherever necessary, the data from the literature have been used for the analysis.

**Table 6.1. Pavement overlay alternatives analyzed in this study**

Category	Overlay Alternatives	Details of a Typical Mixture
Polymer Concrete	LMC-VE	Made of special rapid-set cement; gains structural strength in 1.5 hours
	LMC	Made of conventional Type I/II cement; takes 72 hours to gain structural strength
	PPC	Contains polyester resin binder; gains structural strength in 4 hours (similar to LMC-VE)
Normal and High-Performance Concrete	Low-Slump PCC	Iowa DOT Class O concrete mix; requires a minimum of 3 days of wet curing (burlap with sprinkling) before opening to traffic
	HPC	Iowa DOT Class HPC-O concrete mix; requires a minimum of 3 days of wet curing before opening to traffic

## 6.3 Analysis and Results

The LCCA of the overlay alternatives in this study was performed using the RealCost 2.5 computer program developed by the FHWA. The program required common project-level inputs to be entered for all five alternatives. As shown in Table 6.2, the common inputs included analysis period, discount rate, and traffic-related data. Along with the fixed values, some inputs contained a distribution of values for deterministic analysis. For example, the discount rate was

assumed to be normally distributed with a mean and standard deviation of 3% and 1.5%, respectively. The corresponding input is denoted as LCCANORMAL(3, 1.5) in Table 6.2.

**Table 6.2. Common project-level inputs for the LCCA**

Type	Input	Value
Analysis Options	Analysis Period (Years)	40
	Beginning of Analysis Period	2019
	Discount Rate (%)	3.0 LCCANORMAL(3,1.5)
Traffic Data	Annual Average Daily Traffic Construction Year (total for both directions)	900
	Cars as Percentage of AADT (%)	81.0
	Single Unit Trucks as Percentage of AADT (%)	6.0
	Combination Trucks as Percentage of AADT (%)	13.0
	Annual Growth Rate of Traffic (%)	2.0 LCCANORMAL(2,1)
	Speed Limit Under Normal Operating Conditions (mph)	55
	No of Lanes in Each Direction During Normal Conditions	1
	Free Flow Capacity (vphpl)	2,000 LCCANORMAL(2000,500)
	Rural or Urban Hourly Traffic Distribution	Rural
	Queue Dissipation Capacity (vphpl)	1,000 LCCANORMAL(1000,200)
	Maximum AADT (total for both directions)	1,100

Table 6.3 presents the inputs used for different overlay alternatives. The service life, initial construction cost, maintenance activities and associated costs, and traffic control cost corresponding to each alternative are shown. The data were gathered from the Iowa DOT and the literature. As advised by the TAC, each of the three polymer overlay alternatives was assumed to last through its designed service life without requiring any epoxy injection and repair, whereas the PCC and HPC overlay alternatives were assumed to require epoxy injection and partial-depth repair at 20 and 25 years of service life. The traffic control cost was obtained from Sprinkel (1999). All project-level and alternative-level data entered into RealCost are also presented in Appendix C.

With the user-entered inputs, RealCost performs the following two types of analysis:

1. **Deterministic analysis.** Considering a single defined value for each activity, the undiscounted sum, NPV, and EUAC are calculated, furnishing a single value for each of these economic parameters.
2. **Probabilistic analysis.** The inputs are associated with some inherent variability that is not accounted for in deterministic analysis. Considering the variability of each input, probabilistic analysis is performed to generate a probability distribution for the calculated life-cycle cost.

**Table 6.3. LCCA inputs used for overlay alternatives**

Alternative	Overlay	Service Life (Years)	Initial Construction Cost		Planned Maintenance/Repair Activity	Maintenance/Repair Cost (\$/yd <sup>2</sup> )	Traffic Control Cost* (\$/yd <sup>2</sup> )
			\$/yd <sup>2</sup>	Details			
1	LMC-VE	30	303	Cost is from project bid in November 2018. It includes milling 0.25" off the top of the existing deck followed by 1.75" hydrodemolition removal. Cost does not include Class A and Class B deck repairs, traffic control, longitudinal grooving, or mobilization.	Overlay assumed to last through its designed service life without requiring any epoxy injection and repair	0	8
2	LMC	30	284	Obtained from Sprinkel (1999)		0	30
3	PPC	40	291	Cost is average of two projects bid in December 2018. Cost includes milling off existing 1.75" overlay and shot-blasting of the existing deck surface. Cost does not include Class A and Class B deck repairs, traffic control, longitudinal grooving, or mobilization.		0	8
4	Low-slump PCC	30	94	Average cost obtained from bid awarded contract unit price history from September 2019 to August 2020. Cost includes milling 0.25" off the top of the existing deck. Cost does not include removal of any existing overlays, Class A and Class B deck repairs, traffic control, longitudinal grooving or mobilization.	Epoxy injection and partial-depth repair required at 20 and 25 years of service life	42	40
5	HPC	30	100			42	40

\* Obtained from Sprinkel 1999



The results of the abovementioned analysis are presented and discussed in the sections below.

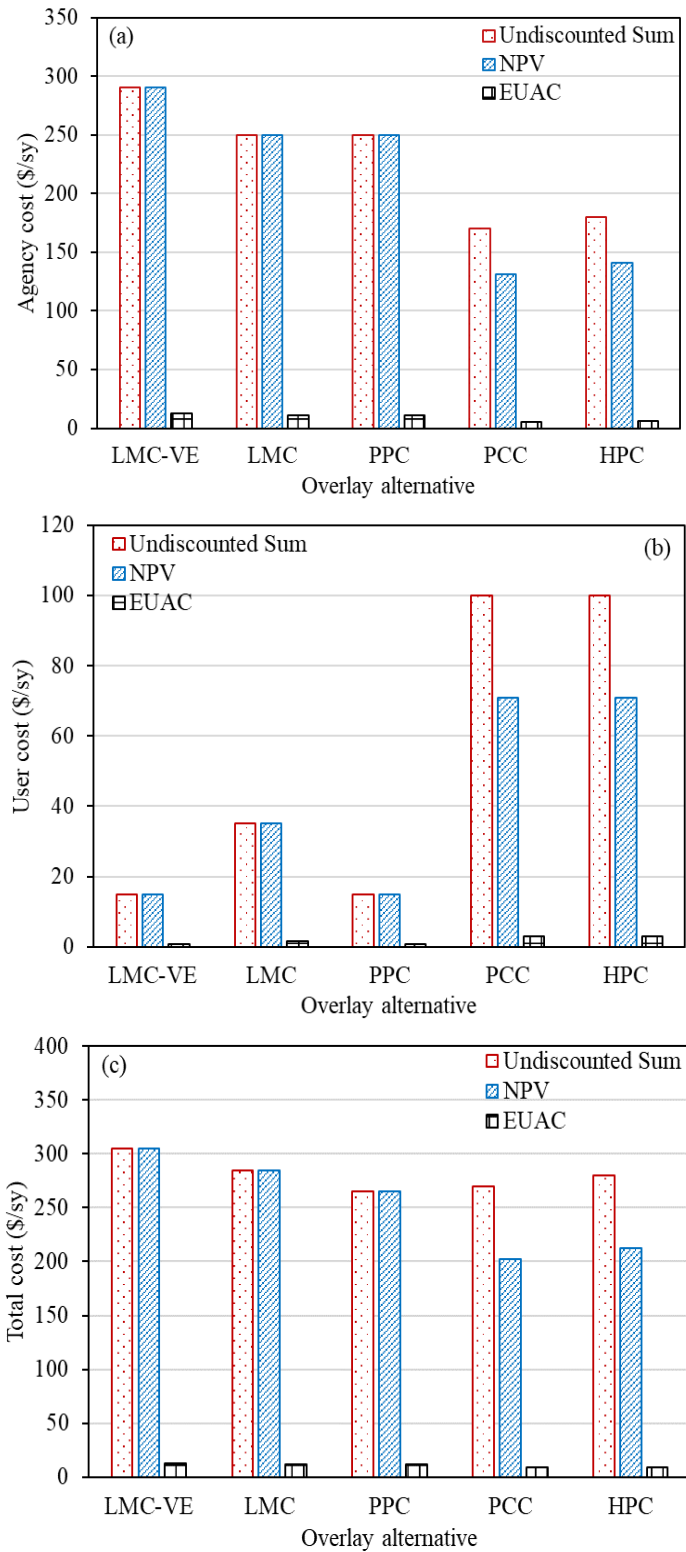
### *6.3.1 Deterministic Analysis*

The results of the deterministic analysis are shown in Figure 6.2. The undiscounted sum, NPV, and EUAC corresponding to the agency, user, and total cost of the five overlays are presented.

As mentioned above, no maintenance activity was considered for the polymer overlays, while two such activities were considered in the case of the PCC and HPC overlays. However, the agency costs (Figure 6.2a) of the polymer overlays were considerably higher (NPV = \$250–\$290/yd<sup>2</sup>) than those of the PCC and HPC overlays (NPV = \$170–\$180/yd<sup>2</sup>), mainly attributable to their high initial construction cost. The analysis revealed that the highest agency cost among all of the alternatives would be incurred by the LMC-VE overlay (NPV = \$290/yd<sup>2</sup>).

Contrary to the observations for the agency cost, the user costs (Figure 6.2b) of the PCC and HPC overlays (NPV = \$100/yd<sup>2</sup>) were higher than those of the polymer overlays (NPV = \$15–\$35/yd<sup>2</sup>). The relatively longer time for opening to traffic in the case of the PCC and HPC overlays increases the traffic control cost, thereby increasing the user cost. LMC-VE and PPC overlays were found to incur the lowest user cost (NPV = \$15/yd<sup>2</sup>). These two overlay types gain structural strength in 1.5 to 4 hours, due to which the pavement can be opened to traffic in a short time, reducing the traffic control and user costs.

Adding the agency and user costs, the total cost can be obtained, as shown in Figure 6.2(c). The wide gap observed in the agency and user costs of the polymer and PCC/HPC overlays was significantly narrowed vis-à-vis the total cost. However, the LMC-VE overlay still exhibited the highest total cost (NPV = \$305/yd<sup>2</sup>) among all of the alternatives, mainly due to its very high initial construction cost. Compared to the total cost NPV of the LMC-VE overlay, the NPVs of the LMC and PPC overlays were \$20/yd<sup>2</sup> and \$40/yd<sup>2</sup> less, respectively. The EUAC, in the case of all overlays, followed the same trend as the NPV.



**Figure 6.2. Costs of alternatives obtained from the deterministic analysis: (a) agency costs (b) user costs, and (c) total costs**

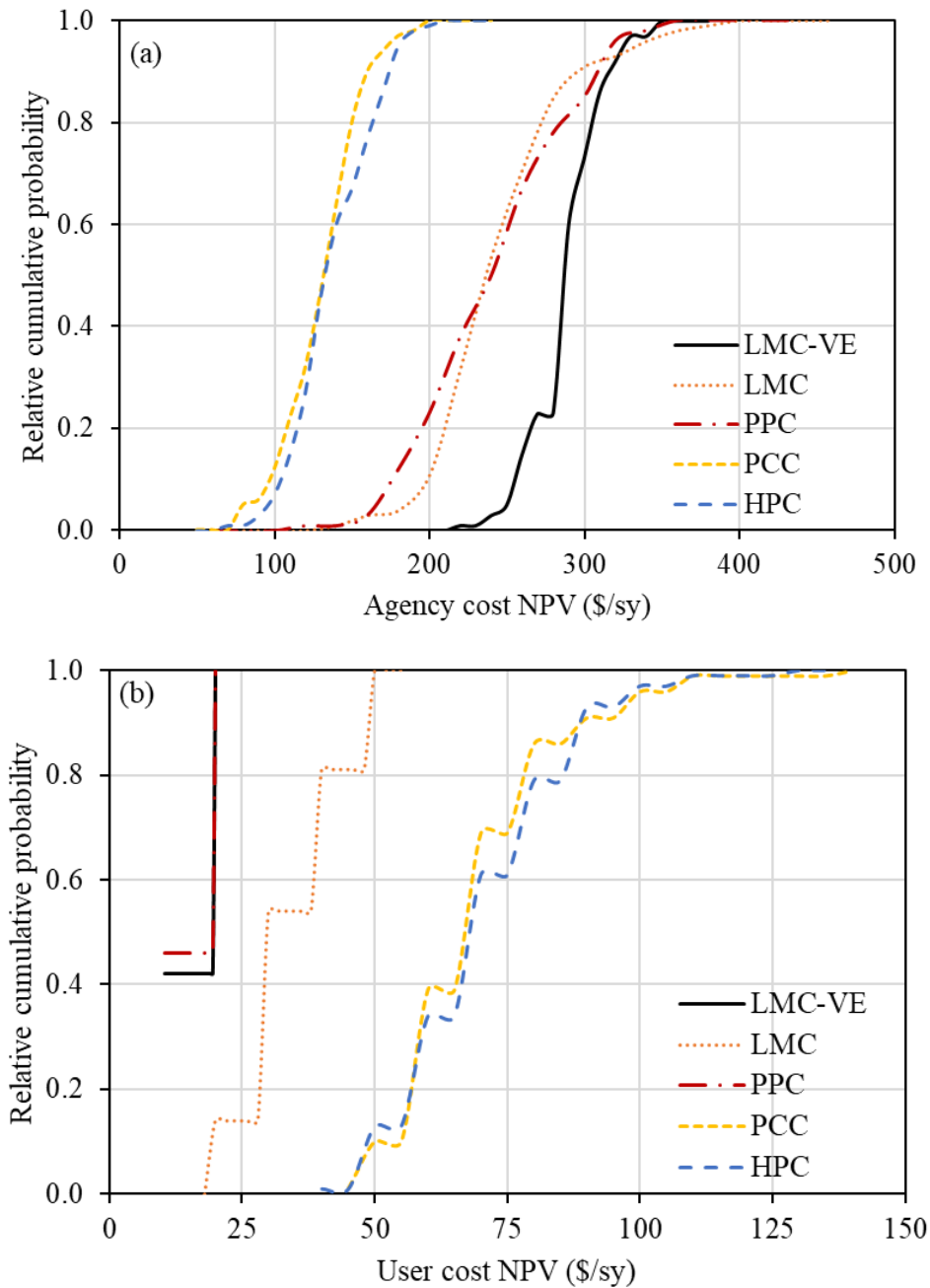
### 6.3.2 Probabilistic Analysis

The probabilistic analysis was conducted using the RealCost software's default values for the sampling scheme, number of iterations, and tail analysis percentiles. Table 6.4 shows the results of the probabilistic analysis of the agency and user costs. As the table shows, the mean NPVs obtained from the analysis are relatively close to the values obtained from the deterministic analysis. Although the mean agency cost NPV of the PPC overlay is the lowest among the polymer alternatives, it has the largest standard deviation (\$50). The LMC-VE overlay still shows the highest mean NPV; however, the standard deviation in this case is lower.

**Table 6.4. Results of the probabilistic analysis**

NPV	Overlay Alternative									
	LMC-VE		LMC		PPC		PCC		HPC	
	Agency Cost	User Cost	Agency Cost	User Cost	Agency Cost	User Cost	Agency Cost	User Cost	Agency Cost	User Cost
Mean	\$290	\$20	\$250	\$40	\$240	\$20	\$140	\$70	\$140	\$70
Std. Deviation	\$20	\$10	\$40	\$10	\$50	\$10	\$30	\$20	\$30	\$20
Minimum	\$220	\$10	\$140	\$20	\$120	\$10	\$80	\$40	\$70	\$40
Maximum	\$340	\$20	\$400	\$50	\$350	\$20	\$200	\$140	\$210	\$130

Figure 6.3 shows the relative cumulative probability distributions (ascending format) of the agency and user costs for the various alternatives. The distributions could be termed the risk profiles of the alternatives. The variability of the alternatives can also be assessed from their respective cumulative distributions. The variability is inversely proportional to the slope of the cumulative curve, i.e., the steeper the slope, the less variability, and vice-versa (Walls III and Smith 1998). Observing the agency cost distribution of the LMC-VE overlay (Figure 6.3a), there is a 60% probability that the NPV will be less than \$290/yard<sup>2</sup>. At the same probability level, the agency cost of the other four alternatives is expected to be less than that of the LMC-VE overlay, while the trend is the opposite for the user cost (Figure 6.3b). The results of the probabilistic analysis agree with those obtained from the deterministic analysis. Probabilistic analysis is advantageous because it provides a risk assessment profile of the alternatives.



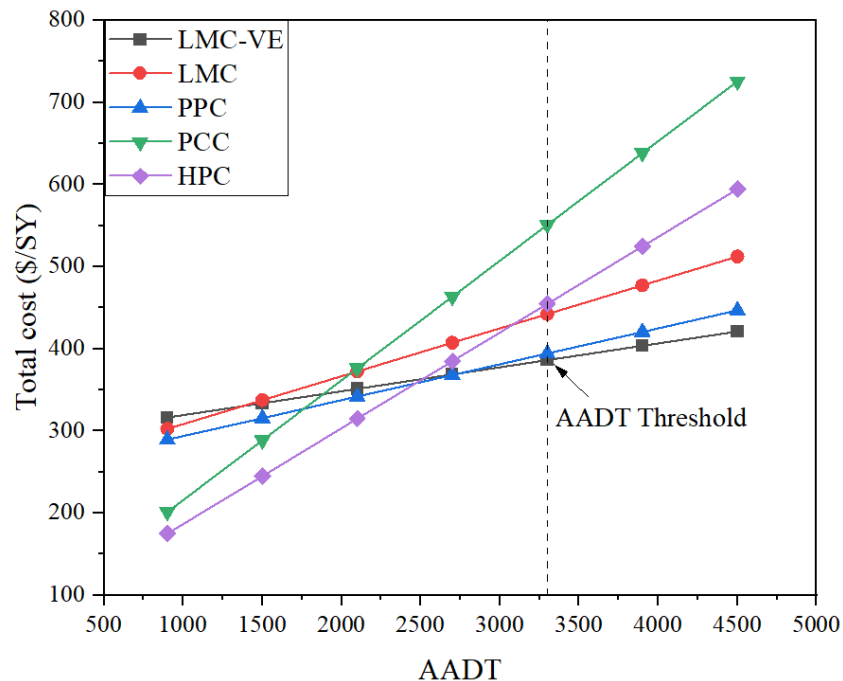
**Figure 6.3. Costs of alternatives obtained from the probabilistic analysis: (a) agency costs and (b) user costs**

### 6.3.3 Annual Average Daily Traffic Threshold

For the analysis run at an annual average daily traffic (AADT) of 900, representing rural roads, the LCCA results revealed that the highest total cost would be incurred in the case of the LMC-VE overlay. At the suggestion of the TAC, a further analysis was performed to determine an AADT threshold. The threshold was defined as the AADT value above which the total cost NPV

of the LMC-VE overlay would be the lowest compared to the other alternatives. For this analysis, only the AADT was changed (keeping other inputs unchanged), and the user cost values calculated by the RealCost software were considered. The agency cost remained the same as that presented in Section 6.3.1.

Figure 6.4 presents a plot of AADT versus total cost for the five overlay alternatives. A general trend of an increase in total cost with an increase in AADT is observed. The PCC and HPC overlays show a steeper increase in total cost than the polymer overlays. Above an AADT of 3,300, the cost of the LMC-VE overlay becomes less than that of the other four overlays, and hence this can be considered as the AADT threshold. Above this threshold, the cost further decreases as AADT increases.



**Figure 6.4. Determining AADT threshold for LMC-VE overlay**

## 6.4 Chapter Summary

The objective of this chapter was to evaluate the life-cycle cost of the first LMC-VE overlay constructed in Iowa. A deterministic and probabilistic LCCA was performed using the RealCost computer program with data from the Iowa DOT and the literature and the use of reasonable assumptions. The agency and user costs of the LMC-VE overlay were investigated along with those of four other overlay alternatives. The conclusions from this analysis are as follows:

- Polymer concrete overlays (LMC-VE, LMC, and PPC) require less maintenance during their service life; however, the agency cost of these overlays is considerably higher than that of the PCC and HPC overlays. Also, the agency cost of polymer overlays is heavily influenced by their initial construction cost.



- A relatively faster time for opening to traffic in the case of polymer overlays (e.g., 3 to 4 hours for LMC-VE) reduces the traffic control cost, thereby reducing the user cost.
- The deterministic analysis revealed that the highest agency cost among the five overlay alternatives (LMC-VE, LMC, PPC, low-slump PCC, and HPC) would be incurred in the case of the LMC-VE overlay, primarily due to its comparatively very high initial construction cost. On the other hand, the LMC-VE overlay is expected to incur the lowest user cost, mainly due to its faster time for opening to traffic. (Note that UHPC overlays were not included in this analysis.)
- The probabilistic analysis revealed that at the same probability level, the agency cost of the other four overlay alternatives is expected to be less than that of the LMC-VE overlay, while the trend is the opposite for the user cost. From the probabilistic analysis, too, it was inferred that the LMC-VE overlay has the highest mean NPV for the agency cost; however, the standard deviation in this case is lower.
- A rural road AADT threshold of 3,300 was determined for the LMC-VE overlay, which is the AADT above which the total cost of the LMC-VE overlay is expected to be less than that of the other four overlays.

Overall, it can be concluded from the LCCA that a very high initial construction cost adds significantly to the total life-cycle cost of the LMC-VE overlay, even though its user cost is very low. This suggests that the life-cycle cost of the LMC-VE overlay outweighs the associated potential benefits, such as faster time for opening to traffic. However, this statement is valid only for an AADT of 900 and the associated traffic distributions. As determined in this analysis, for cases where high AADT conditions exist (greater than 3,300), the LMC-VE overlay could be a better alternative.

## 7. CONCLUSIONS AND RECOMMENDATIONS

This study investigated the utilization of LMC-VE as a new overlay material for restoring a deteriorated bridge deck surface in the state of Iowa. The pre-construction, construction, and post-construction processes were thoroughly documented. An in-depth laboratory investigation of a wide range of LMC-VE material properties, including various mechanical and durability parameters, was conducted by casting numerous test specimens in the field during overlay construction. Additionally, the short-term (starting from four days) and long-term (up to five years) performance of the field overlay was monitored through frequent field visits, testing, and measurements. Lastly, a comprehensive LCCA was performed to evaluate the total economic value/cost of the construction and maintenance of the LMC-VE overlay in comparison to four other overlay types to assess the cost-effectiveness of different overlay alternatives and identify potential life-cycle cost savings through LCCA. The results of this research are expected to serve as a benchmark and assist in decision-making related to the selection of overlay alternatives for future bridge deck applications in Iowa.

### 7.1 Major Findings and Conclusions

A summary of the major findings from this study is presented below.

#### *7.1.1 Laboratory Performance of Field-Cast Specimens*

##### 7.1.1.1 Heat of Hydration

- The LMC-VE paste displayed rapid heat generation during a period spanning 5 to 10 hours after mixing. During this period, the heat of hydration of the paste increased from about 25 J/g to 180 J/g, an increase about twice that of a conventional pavement cement paste. Such rapid heat generation could be responsible for potential thermal cracking of the LMC-VE overlay.

##### 7.1.1.2 Mechanical Properties

- The LMC-VE developed a satisfactory compressive strength of 2,827 psi at 3 hours, which appears favorable for accelerating overlay construction on a bridge deck surface and quickly opening the bridge to vehicular traffic. The compressive strength increased to 5,952 psi at 28 days and 7,816 psi at 400 days (a factor of three).
- The corresponding early-age flexural strength of 685 psi recorded for the LMC-VE beams at 3 days increased to 865 psi at 28 days (a 26% increase and 14.5% of the 28-day compressive strength).
- The 28-day pull-off strength testing of LMC-VE-overlaid beams (over an HPC substrate) indicated an LMC-VE-substrate bond strength of over 283 psi (greater than 250 psi, the minimum specified pull-off strength value for thin epoxy overlays), typically indicating a “very good” bond.

#### 7.1.1.3 Chloride Intrusion Resistance

- The average SR values in laboratory-measured specimens were 24.9 k $\Omega$ -cm at 3 days and 70.3 k $\Omega$ -cm at 14 days. Since these specimens were moist cured only for the first 3 days and air cured thereafter, the measurements made on air-cured specimens at 28 days were unstable, likely due to the lack of efficient contact between the electrodes of the Wenner probe and the surfaces of the specimens. Hence, thereafter the cylindrical specimens were soaked in water for two days before SR measurements were taken (after a specimen age of 28 days).
- Accordingly, the SR measurements on specimens soaked in water for two days were 61.4 k $\Omega$ -cm at 170 days and 69 k $\Omega$ -cm at 340 days, indicating enhanced impermeability due to the synergistic effect of pore refinement as a result of continued hydration and the simultaneous development of a complex latex network within the bulk of the system.
- The chloride content determined from the 90-day salt ponding tests indicated average acid-soluble chloride contents of 0.36% and 0.13% in the top and bottom 1/2 in. layers, respectively. Accordingly, the results indicate that an LMC-VE overlay has a chloride penetration resistance better than that of an LSDC overlay but not as good as that of an epoxy overlay.

#### 7.1.1.4 Moisture Transport

The moisture transport properties of LMC-VE were evaluated using a standard water sorptivity test. The test was performed on specimens sliced from the field-cast, laboratory-cured LMC-VE cylinders and on relatively smaller test specimens sliced from the field cores obtained at different ages for pull-off testing. Two smaller specimens sliced from cores of the existing Class D concrete substrate of the field bridge were also tested for comparison.

- The initial sorptivity of the field-cast LMC-VE specimens (which were laboratory cured in water for 3 days and then air cured for an additional 25 days before testing) was similar to that of the substrate concrete studied. During the testing time, the water absorption of the substrate concrete became stable while the water absorption of the LMC-VE specimens continued to increase. As a result, the secondary sorptivity value of the LMC-VE specimens was much higher than that of substrate concrete, which could be responsible for the moisture-induced deterioration, like freeze-thaw damage.

#### 7.1.1.5 Other Durability Properties

The other durability properties evaluated included shrinkage (both drying and autogenous) and freeze-thaw resistance. The shrinkage tests utilized standard beam specimens, whereas the freeze-thaw tests were conducted using two specimen types: LMC-VE-only specimens and LMC-VE-overlaid beams (LMC-VE overlaid over an HPC substrate to simulate the field overlay).

- After 400 days, the LMC-VE beam specimens indicated autogenous and drying shrinkage values of 115 and 440 microstrain, respectively, which are well within those typically experienced by normal-strength PCC.
- The LMC-VE-only beams indicated relatively poor freeze-thaw resistance, contrary to what was expected based on the information from the existing literature on the freeze-thaw performance of this material. The LMC-VE-only specimens experienced significant mass loss and a decrease in the relative dynamic modulus to lower than 60% (below the lower relative dynamic modulus limit of 60% specified in ASTM C666) at 72 freeze-thaw cycles. The specimens experienced an increased rate of deterioration thereafter and hence lost their prismatic shape. The inability to further measure the relative dynamic modulus due to the latter led to the termination of testing after 112 freeze-thaw cycles. As mentioned earlier, the undesired freeze-thaw performance of the LMC-VE-only specimens might be associated with the high secondary sorptivity of the LMC-VE.
- The LMC-VE-overlaid beams, in contrast, showed relatively better freeze-thaw resistance than the LMC-VE-only beams. With no considerable mass loss, the relative dynamic modulus of these specimens was more than 85% up to 144 freeze-thaw cycles. However, after 144 cycles the LMC-VE-substrate interface failed and the LMC-VE overlay debonded from the substrate, resulting in the termination of the freeze-thaw test after 144 freeze-thaw cycles.
- It should be noted that the failure of the LMC-VE-substrate interface under freeze-thaw cycles was possibly due to the inadequate preparation of the substrate concrete's surface in the laboratory, resulting in insufficient microtexture/roughness of the exposed coarse aggregates. Since the field overlay placement consisted of efficient surface preparation techniques, including a combination of surface milling, hydrodemolition, and sand-blasting, the field test results are expected to be more realistic, and the field overlay is expected to perform better. (This is supported by the field LMC-VE-substrate bond strength results presented in the next section, which revealed insignificant change in the overlay-substrate adhesion properties in the field even after 5 years in service).

### *7.1.2 Short- and Long-Term Performance of In-Service/Field Overlay*

#### *7.1.2.1 Cracking and Deterioration*

- The LMC-VE overlay tended to develop cracks over time. Most cracks are thin/hairline ( $\leq 0.016$  in. in width at an age of 50 months), transverse or diagonal cracks perpendicular to the bridge abutments.
- The frequency of cracking slowed after three years, with very few newer cracks identified in subsequent field trips.
- The LMC-VE overlay cracking could possibly have developed due to a combination of various factors. A few of these factors might be the rapid, high heat generation of cement hydration at a very early age (5 to 10 hours after casting), the material's susceptibility to shrinkage under early traffic loading, the effect of bridge skew angle, reflective cracking from the substrate, and high vehicular loading at an early age, most of which have been reported in the existing literature on LMC-VE.

- The in-service overlay indicated signs of slight deterioration in terms of material spalling and abrasion/erosion of the grooves intentionally placed to aid in friction at a few areas on the overlay surface.

#### 7.1.2.2 Friction Index

- A very slight reduction in the average BPN values was observed over time. Nonetheless, the BPN values measured during the final field visit were still observed to be greater than 55, a BPN value that is deemed necessary for ensuring traffic safety.

#### 7.1.2.3 Surface Resistivity

- The positive results are consistent with the SR measurements of the laboratory specimens, both of which indicate a potential reduction in material permeability over time.
- When the fall and spring SR measurements were considered separately (to avoid complications associated with the effect of temperature fluctuations on the measurements), the measurements separately indicated a general trend of an increase in SR with an increase in the overlay age (up to 26 months), indicating improved microstructure and associated pore network disconnection. However, a slight reduction in the average SR values was observed from Trip 7 (32 months) through Trip 10 (50 months), which possibly indicates a slight deterioration in the permeability resistance of the overlay material (possibly due to the combination of spalling and cracking).

#### 7.1.2.2 Sorptivity

Sorptivity tests were performed in the PCC Research Laboratory on field specimens cored at various ages. The following observations were made:

- Both the initial sorptivity and secondary sorptivity values of the field LMC-VE specimens decreased with as the age of the LMC-VE overlay increased from 2 months to 8.5 months, indicating pore refinement and pore network disconnection within the bulk of the concrete over time.
- The average initial sorptivity of the field-cored LMC-VE specimens was comparable to or slightly lower than that of the HPC specimens sliced from the concrete of an existing deck, whereas the secondary sorptivity of the LMC-VE specimens was slightly higher than that of the HPC specimens until the age of the LMC-VE overlay reached 8.5 months. After 8.5 months, the secondary sorptivity values of the field-cored LMC-VE specimens started approaching those of the HPC specimens.

#### 7.1.2.3 LMC-VE – Substrate Bond Strength

- A total of 30 pull-off tests were conducted on field cored specimens at ages ranging from 4 days to 50 months. The field pull-off test results showed a general trend indicating that the



LMC-VE-substrate bond failure mode changed with time. At a very early age (4 days), the failure occurred in the overlay LMC-VE. As the overlay age increased (from 2 to 14 months), most core failures occurred at the LMC-VE overlay and substrate interface. After that time (from 14 to 50 months), all core specimens tested failed at the substrate, indicating the growth of the bond strength between the LMC-VE overlay and substrate.

- Although exhibiting large variation, the strengths of most specimens at failure were greater than 250 psi, indicating that without the consideration of cracking, the LMC-VE-substrate bond strengths were higher than 250 psi, which could be classified as “very good” and adequate.

### *7.1.3 Life-Cycle Cost Analysis*

- The three polymer concrete overlays considered (i.e., LMC-VE, LMC, and PPC) require less maintenance during their service life; however, the agency cost of these overlays is considerably higher than that of the low-slump PCC and HPC overlays. Also, the agency cost of polymer overlays is heavily influenced by their initial construction cost.
- A relatively faster time for opening to traffic in the case of polymer overlays (e.g., 3 to 4 hours for LMC-VE) reduces the traffic control cost, thereby greatly reducing the user cost.
- The deterministic analysis revealed that the highest agency cost among the five overlay alternatives (LMC-VE, LMC, PPC, low-slump PCC, and HPC) would be incurred in the case of the LMC-VE overlay, primarily due to its comparatively very high initial construction cost. On the other hand, the LMC-VE overlay is expected to incur the lowest user cost due to its faster time for opening to traffic. (Note that UHPC overlays were not included in this analysis.)
- The probabilistic analysis revealed that at the same probability level, the agency cost of the other four overlay alternatives is expected to be less than that of the LMC-VE overlay, while the trend is the opposite for the user cost. From the probabilistic analysis, too, it was inferred that the LMC-VE overlay has the highest mean NPV for the agency cost; however, the standard deviation in this case is lower.
- A rural road AADT threshold of 3,300 was determined for the LMC-VE overlay, which is the AADT above which the total cost of the LMC-VE overlay is expected to be less than that of the other four overlays.

Overall, it can be concluded from the LCCA that a very high initial construction cost adds significantly to the total life-cycle cost of the LMC-VE overlay, even though its user cost is very low. This suggests that the life-cycle cost of the LMC-VE overlay outweighs the associated potential benefits, such as faster time for opening to traffic. However, this statement is valid only for an AADT of 900 and the associated traffic distributions. As determined in this analysis, for cases where high AADT conditions exist (greater than 3,300), the LMC-VE overlay could be a better alternative. In addition, unexpected premature cracking of the LMC-VE overlay, as observed during the field investigation, was not considered in the analysis.

## 7.2 Recommendations

Based on the present study, the recommendations listed in the following sections can be made for further study, LMC-VE construction, and QA/QC practice.

### *7.2.1 Issues Related to Heat of Cement Hydration*

As shown in Figure 4.3, rapid heat generation occurred during hours 5 through 10 of cement hydration, and the high temperature of the LMC-VE overlay was also noticed by the investigators during the SR measurement of the field overlay 3 hours after casting. However, the field overlay concrete temperature was not monitored in this study. Such early and rapid heat generation resulting from the rapid hydration of CSA cement could be responsible for the thermal cracking of LMC-VE.

It is recommended that the temperature of the LMC-VE overlay be monitored in future LMC-VE overlay practice. Concrete cooling measures, such as the use of pre-cooling aggregates or chilled mixing water, may be taken to further reduce concrete placement temperature.

LMC-VE mix proportions, such as the latex and citric acid contents, may be adjusted to reduce rapid heat generation within the short period of early-age cement hydration, thus minimizing the early-age cracking due to rapid heat generation from cement hydration. Supplementary cementitious materials may also be used to reduce not only the heat of hydration but also the secondary sorptivity of the concrete, thus reducing cracking and deterioration.

### *7.2.1 Issues Related to Shrinkage Properties*

Although the laboratory investigation showed that the shrinkage behavior of the laboratory-cured LMC-VE was similar to that of conventional pavement concrete (Figure 4.22), the field LMC-VE overlay showed a number of fine/hairline transverse cracks, which was possibly related to the shrinkage of the LMC-VE. The following measures can be considered to minimize shrinkage cracking:

- The early opening of the field overlay to traffic might have increased the likelihood of shrinkage cracks because the concrete continues to shrink after exposure to traffic loads. Therefore, one possible measure for addressing this issue is to further improve LMC-VE curing. Because LMC-VE exhibits rapid strength gain and high shrinkage at a very early age, extending the curing time and properly removing the burlap to avoid sudden temperature and moisture changes may help reduce some shrinkage-related cracking.
- Techniques for shrinkage reduction, such as the use of shrinkage-reducing agents and/or lightweight fine aggregates (LWAs) as internal curing agents, could also be considered.
- Since the extent of shrinkage varies with the latex dosage, further study is needed to consider different latex dosages (low to medium) in combination with the use of internal curing agents, as recommended above.

- Since shrinkage is significantly influenced by the high initial heat of cement hydration (due to the use of rapid-set cement), heat should be measured at the site of material placement (e.g., using an i-button sensor or a thermocouple). This could be supplemented with laboratory-based isothermal/semi-adiabatic calorimetry tests.
- Future applications of LMC-VE need to consider all of the above to ensure that the constructed overlay is free from shrinkage cracking. A small dosage of fibers ( $\leq 2\%$  by volume) may also be used to control crack propagation.

### *7.2.2 Correlating LMC-VE Microstructure to Durability*

The laboratory investigation showed that the secondary sorptivity of the laboratory-cured LMC-VE specimens (at 28 days) was much higher than that of the conventional HPC used for overlays, and the freeze-thaw resistance of LMC-VE-only specimens was low. Small areas of spalling were observed at a few locations on the field LMCVE overlay. All of those could be attributed to improper pore structure in the LMC-VE, possibly due to chemical reactions among the cement, latex, and citric acid components in the overlay and the deicer chemicals applied to the deck surface. Future research should be conducted to investigate these physico-chemical phenomena through detailed microstructural investigation. Through a better understanding of the interactions of the material components, LMC-VE mix proportions can be optimized for a better performance.

### *7.2.3 Potential Cost Savings through LMC-VE Applications*

- In the comprehensive LCCA, the construction cost of the LMC-VE overlay was recognized as being higher than that of the other overlay alternatives considered. However, the LCCA revealed a potential for cost savings with LMC-VE when the AADT is greater than 3,300. This result establishes an AADT threshold above which the total life-cycle cost of the LMC-VE overlay (encompassing the construction and maintenance costs throughout its service life) is expected to be less than that of the other four overlay alternatives.
- Therefore, the use of LMC-VE as an overlay material is not preferable for low AADT values (i.e., less than 3,300).

## REFERENCES

- ACI Committee 548. 2009. *ACI 548.3R-09, Report on Polymer-Modified Concrete*. American Concrete Institute, Farmington Hills, MI.
- ACPA. 2012. *Life-Cycle Cost Analysis: A Tool for Better Pavement Investment and Engineering Decisions*. American Concrete Pavement Association, Skokie, IL.
- Alderete, N. M., Y.A. Villagran Zaccardi, and N. De Belie. 2020. Mechanism of long-term capillary water uptake in cementitious materials. *Cement and Concrete Composites*, Vol. 106. <https://doi.org/10.1016/j.cemconcomp.2019.103448>.
- Babashamsi, P., N. Izzi, M. Yusoff, H. Ceylan, N. Ghani, M. Nor, H. S. Jenatabadi, and S. Jenatabadi. 2016. Evaluation of pavement life-cycle cost analysis: Review and analysis. *International Journal of Pavement Research Technology*, Vol. 9, pp. 241–254. <https://doi.org/10.1016/j.ijprt.2016.08.004>.
- Bentz, D. P., M. A. Ehlen, C. F. Ferraris, and E. J. Garboczi. 2001. Sorptivity-based service life predictions for concrete pavements. *Proceedings of the 7th International Conference on Concrete Pavements, Orlando, FL*, pp. 181–193.
- Bordeleau, D., M. Pigeon, and N. Banthia. 1993. Comparative Study of Latex-Modified Concretes and Normal Concretes Subjected to Freezing and Thawing in the Presence of a Deicer Salt Solution, *ACI Materials Journal*, Vol. 89, No. 6, pp. 547–553.
- Bukhari, S. J., and M. Khanzadeh. 2023. Assessing the freeze-thaw performance of CSA systems. Spring 2023 ACI Convention, April 2–6, San Francisco, CA. [https://www.concrete.org/portals/0/files/pdf/webinars/ws\\_S23\\_Bukhari.pdf](https://www.concrete.org/portals/0/files/pdf/webinars/ws_S23_Bukhari.pdf).
- Choi, P., and K. Yun. 2014. Experimental analysis of latex-solid content effect on early-age and autogenous shrinkage of very-early strength latex-modified concrete. *Construction and Building Materials*, Vol. 65, pp. 396–404. <https://doi.org/10.1016/j.conbuildmat.2014.05.007>.
- Clear, K. C., and B. H. Chollar. 1978. *Styrene-Butadiene Latex Modifiers For Bridge Deck Overlay Concrete*. Federal Highway Administration, Washington, DC.
- Dahlberg, J., and B. Phares. 2016. *Polymer Concrete Overlay Evaluation*. InTrans Project 13-463. Institute for Transportation and Federal Highway Administration, Ames, IA.
- El-Dieb, A. S., and R. D. Hooton. 1995. Water-permeability measurement of high performance concrete using a high-pressure triaxial cell. *Cement and Concrete Research*, Vol. 25, pp. 1199–1208.
- Fu, G., J. Feng, J. Dimaria, and Y. Zhuang. 2007. *Bridge deck corner cracking on skewed structures*. CE-2007-05. Wayne State University, Detroit, MI.
- Hall, C. 1989. Water sorptivity of mortars and concretes: a review. *Magazine of Concrete Research*, Vol. 41, pp. 51–61.
- Hall, C., and M. H. Raymond Yau. 1987. Water movement in porous building materials–IX. The water absorption and sorptivity of concretes. *Building and Environment*, Vol. 22, pp. 77–82. [https://doi.org/10.1016/0360-1323\(87\)90044-8](https://doi.org/10.1016/0360-1323(87)90044-8).
- Hall, C., and T. K. M. Tse. 1986. Water movement in porous building materials–VII. The sorptivity of mortars. *Building and Environment*, Vol. 21, No. 2, pp. 113–118. [https://doi.org/10.1016/0360-1323\(86\)90017-X](https://doi.org/10.1016/0360-1323(86)90017-X).

- Henkensiefken, R., J. Castro, D. Bentz, T. Nantung, and J. Weiss. 2009. Water absorption in internally cured mortar made with water-filled lightweight aggregate. *Cement and Concrete Research*, Vol. 39, pp. 883–892.  
<https://doi.org/10.1016/j.cemconres.2009.06.009>.
- Khan, M. I., and C. J. Lynsdale. 2002. Strength, permeability, and carbonation of high-performance concrete. *Cement and Concrete Research*, Vol. 32, pp. 123–131.
- Kuhlmann, L. A., and N. C. Foor. 1984. Chloride Permeability Versus Air Content of Latex-Modified Concrete. *Cement, Concrete, and Aggregates*, Vol. 6, No. 1, pp. 11–16.
- Lee, B. J., and Y. Y. Kim. 2018. Durability of Latex-Modified Concrete Mixed with a Shrinkage Reducing Agent for Bridge Deck Pavement. *International Journal of Concrete Structures and Materials*, Vol. 12. <https://doi.org/10.1186/s40069-018-0261-8>.
- Lin, L., R. Wang, and Q. Lu. 2018. Influence of polymer latex on the setting time, mechanical properties, and durability of calcium sulfoaluminate cement mortar. *Construction and Building Materials*, Vol. 169, pp. 911–922.
- Liu, H., S. Wang, Y. Huang, B. Melugiri-Shankaramurthy, S. Zhang, and X. Cheng. 2020. Effect of SCMs on the freeze-thaw performance of iron-rich phosphoaluminate cement. *Construction and Building Materials*, Vol. 230, 117012.  
<https://doi.org/10.1016/j.conbuildmat.2019.117012>.
- Martens, P. 2015. Latex-Modified Concrete for Bridge Deck Overlays. Ohio Transportation Engineering Conference, Columbus, OH, October 27–28, 2015.
- Melugiri-Shankaramurthy, B., B. S. Dhanya, and M. Santhanam. 2016. Study of Influence of Moisture Content, Portlandite Content and Pore Solution Conductivity on Surface Resistivity of Concrete. 14th fib Symposium, Cape Town, South Africa.
- Melugiri-Shankaramurthy, B., Y. Sargam, K. Wang. 2018. Experimental Data on the Influence of Factors on Concrete Surface Resistivity. 3rd R. N. Raikar Memorial International Conference on Science and Technology of Concrete, December 14–15, Mumbai, India.
- Melugiri-Shankaramurthy, B., K. Wang, and F. Hasiuk. 2021. Influence of carbonate coarse aggregate properties on surface resistivity of high-performance concrete, *Construction and Building Materials*, Vol. 312, 125402.  
<https://doi.org/10.1016/j.conbuildmat.2021.125402>.
- Milla, J., T. Cavalline, T. Rupnow, B. Melugiri-Shankaramurthy, G. Lomboy, and K. Wang. 2021. Methods of Test for Concrete Permeability: A Critical Review. *Advances in Civil Engineering Materials*, Vol. 10, No. 1, pp. 172–209.  
<https://doi.org/10.1520/ACEM20200067>.
- Neithalath, N. 2007. Analysis of Moisture Transport in Mortars and Concrete Using Sorption-Diffusion Approach. *ACI Materials Journal*, Vol. 103, No. 3, pp. 209–217.
- Ohama, Y. 1973. *Study on Properties and Mix Proportioning of Polymer-Modified Mortars for Buildings*. Report of the Building Research Institute, No. 65. Building Research Institute, Tokyo, Japan.
- Ohama, Y. 1995. *Handbook of Polymer-Modified Concrete And Mortars: Properties and Process Technology*. Noyes Publications, Park Ridge, NJ.
- Phares, B., and D. Harrington. 2016. *Causes of Early Cracking in Concrete Bridge Decks*. MAP Brief. National Concrete Pavement Technology Center, Ames, IA.

- Ramezaniapour, A. A., A. Pilvar, M. Mahdikhani, and F. Moodi. 2011. Practical Evaluation of Relationship between Concrete Resistivity, Water Penetration, Rapid Chloride Penetration and Compressive Strength, *Construction and Building Materials*, Vol. 25, pp. 2472–2479. <https://doi.org/10.1016/j.conbuildmat.2010.11.069>.
- Rupnow, T. D. 2013. Quality Control Tools to Identify Source Variability of Class C Fly Ash and Its Impact on Freshly Mixed Cement-Fly Ash Paste. 2013 World Coal Ash Conference, Lexington, KY.
- Sargam, Y., M. Faytarouni, K. Riding, K. Wang, C. Jahren, and J. Shen. 2019a. Predicting Thermal Performance of a Mass Concrete Foundation: A Field Monitoring Case Study. *Case Studies in Construction Materials*, Vol. 11. <https://doi.org/10.1016/j.cscm.2019.e00289>.
- Sargam, Y., B. Melugiri-Shankaramurthy, and K. Wang. 2019b. Characterization of RCAs and Their Concrete Using Simple Test Methods. *Journal of Sustainable Cement-Based Materials*, Vol. 9. No. 2, pp. 1–17. <https://doi.org/10.1080/21650373.2019.1692093>.
- Sen Li, S., S. de Wang, H. Liu, B. Melugiri-Shankaramurthy, S. Xin Zhang, and X. Cheng. 2020. Variation in the sulfate attack resistance of iron rich-phosphoaluminate cement with mineral admixtures subjected to a Na<sub>2</sub>SO<sub>4</sub> solution. *Construction and Building Materials*, Vol. 230, 116817. <https://doi.org/10.1016/j.conbuildmat.2019.116817>.
- Shaker, F. A., A. S. EL-Dieb, and M. M. Reda Taha. 1997. Durability of Styrene-Butadiene Latex-Modified Concrete. *Cement and Concrete Research*, Vol. 27, pp. 711–720.
- Sprinkel, M. M. 1998. *Technical Assistance Report: Very-Early-Strength Latex-Modified Concrete Overlay*. Virginia Transportation Research Council, Charlottesville, VA.
- Sprinkel, M. M. 1999. Very-Early-Strength Latex-Modified Concrete Overlay. *Transportation Research Record*, Vol. 1668, pp. 18–23.
- Sprinkel, M. M. 2000. *Evaluation of Latex-Modified and Silica Fume Concrete Overlays Placed on Six Bridges in Virginia*. VTRC 01-R3. Virginia Transportation Research Council, Charlottesville, VA.
- Sprinkel, M. M. 2005. *Latex-Modified Concrete Overlay Containing Type K Cement*. VTRC 05-R26. Virginia Transportation Research Council, Charlottesville, VA.
- Steele, B., E.M. Liberati, and P. Martens. 2019. Latex Modified Concrete - Very Early Strength. Purdue Road School, West Lafayette, IN. <https://docs.lib.purdue.edu/roadschool/2019/presentations/104/>.
- Tan, Y., K. Freeseaman, and K. Wang. 2020. *Long-Term Performance of Overlays: Thin Epoxy Overlay versus Traditional Rigid Overlay*. InTrans Project 17-627. Bridge Engineering Center, Ames, IA.
- Tartar, J., M. Head, S. Larfi, and A. Okeola. 2022. *Bonding of Overlays to Ultra High Performance Concrete*. DCT 285. Delaware Center for Transportation, Newark, DE.
- Theodore II, H., C. Goff, D. Wells, and S. Palle. 2015. *Technical Assistance Report: Hydrodemolition and Use of a Rapid Early Strength Latex-Modified Concrete Overlay*. University of Kentucky, Kentucky Transportation Center, Lexington, KY.
- Tibbetts, C. M., J. M. Paris, C. C. Ferraro, K. A. Riding, and T. G. Townsend. 2020. Relating Water Permeability to Electrical Resistivity and Chloride Penetrability of Concrete Containing Different Supplementary Cementitious Materials. *Cement and Concrete Composites*, Vol. 107, 103491. <https://doi.org/10.1016/j.cemconcomp.2019.103491>.



- Walls III, J., and M. Smith. 1998. *Life-Cycle Cost Analysis in Pavement Design*. Interim Technical Bulletin. FHWA-SA-98-079. Federal Highway Administration, Washington, DC.
- Wang, H., and Z. Wang. 2019. Deterministic and probabilistic life-cycle cost analysis of pavement overlays with different pre-overlay conditions. *Road Materials and Pavement Design*, Vol. 20, pp. 58–73. <https://doi.org/10.1080/14680629.2017.1374996>.
- Wang, K., B. Melugiri-Shankaramurthy, and F. Hasiuk. 2020a. *Role of Coarse Aggregate Porosity on Chloride Intrusion in HPC Bridge Decks*. TR-728. Institute for Transportation, Ames, IA.
- Wang, K., Y. Sargam, K. Riding, M. Faytarouni, C. Jahren, and J. Shen. 2020b. *Evaluate, Modify, and Adapt the ConcreteWorks Software for Iowa's Use*. TR-712. Institute for Transportation, Ames, IA.
- Wenzlick, J. D. 2006. *Evaluation of Very High Early Strength Latex-Modified Concrete Overlays, Organizational Results Research Report*. OR06.004. Missouri Department of Transportation, Jefferson City, MO.
- Yun, K., and P. Choi. 2014. Causes and Controls of Cracking at Bridge Deck Overlay with Very-Early Strength Latex-Modified Concrete. *Construction and Building Materials*, Vol. 56, pp. 53–62. <https://doi.org/10.1016/j.conbuildmat.2014.01.055>.
- Yun, K., D. Kim, and S. Choi. 2004. Durability of Very-Early-Strength Latex-Modified Concrete Against Freeze-Thaw and Chemicals. *Transportation Research Record*, Vol. 1893, pp. 1–10.
- Yun, K., P. Choi, S. Choi, and K. Kim. 2007. Thermal and Autogenous Shrinkages of Very Early Strength Latex-Modified Concrete. *Transportation Research Record*, Vol. 2020, pp. 30–39. <https://doi.org/10.3141/2020-04>.
- Zhang, H., G. A. Keoleian, and M. D. Lepech. 2008. An integrated life-cycle assessment and life-cycle analysis model for pavement overlay systems. *Life-Cycle Civil Engineering*. CRC Press, Boca Raton, FL. pp. 907–912. <https://doi.org/10.1201/9780203885307.ch141>.
- Zhutovsky, S., and R. Douglas Hooton. 2019. Role of sample conditioning in water absorption tests. *Construction and Building Materials*, Vol. 215, pp. 918–924. <https://doi.org/10.1016/j.conbuildmat.2019.04.249>.

## APPENDIX A

Additional material (i.e., cement and latex) related information is given below.



**MILL CERTIFICATE  
RAPID SET CEMENT**  
November 06, 2018

Reported To: CTS Cement Manufacturing  
Corporation

Project: Bulk Cement Stock.

PLANT	Juarez, Plant 1
RAPID SET CEMENT, BULK	10731 tons (9735 mt)
IDENTIFICATION, lot number	J62
SPECIFIC GRAVITY	2.98
TIME OF SETTING, Minutes (ASTM C191 MODIFIED)	
INITIAL	17
FINAL	21
COMPRESSIVE STRENGTH – PSI (MPa)	
3 HOURS	6709 (46.3)
24 HOURS	8090 (55.8)

Tested in accordance with ASTM C109 as modified by CTS 101-17.

This cement was sampled from Juarez Plant 1 and test results shown herein are representative of the Rapid Set® cement identified with the above lot number.

Seller, having no control over the use of Rapid Set® cement, will not guarantee finished work in which it is used.

**CTS CEMENT MANUFACTURING COMPANY**

  
Authorized Representative

See California all-purpose  
acknowledgement certificate  
Attachment.

Controlled Copy – Do Not Duplicate

CTS 8-032 Rev. NC 09/13/18

CTS CEMENT MANUFACTURING CORP. | AN EMPLOYEE-OWNED COMPANY  
12442 KNOTT ST., GARDEN GROVE, CA 92841 | 800.929.3030 | CTSCEMENT.COM

**Rapid Set**

# SAFETY DATA SHEET

## 1. Identification

**Product identifier** Rapid Set Cement

**Other means of identification**

**Product code** 101002000, 101010050, 101010088, 101012000, 101013000

**Recommended use** Industrial use.

**Recommended restrictions** None known.

**Manufacturer/Importer/Supplier/Distributor information**

**Company name** CTS Cement Manufacturing Corporation

**Address** 12442 Knott Street Garden  
Grove, CA 92841  
United States  
1-800-929-3030  
[info@ctscement.com](mailto:info@ctscement.com)

**Telephone**

**E-mail**

**Contact person** Safety Officer

**Emergency telephone number** 1-800-929-3030 (8 AM - 5 PM)

## 2. Hazard(s) identification

### Physical hazards

### Health Hazards

Not classified.

Skin corrosion/irritation

Category 2

Serious eye damage/eye irritation

Category 1

Carcinogenicity

Category 1A

Specific Target Organ Toxicity, Single Exposure

Category 3 respiratory tract irritation

Specific Target Organ Toxicity, Repeated Exposure

Category 2 (Lungs)

### OSHA defined hazards

### Label elements

Not classified.



### Signal word

Danger

### Hazard statement

Causes skin irritation. Causes serious eye damage.

### Precautionary statement

#### Prevention

Wash thoroughly after handling. Wear protective gloves/protective clothing/eye protection/face protection.

#### Response

If in eyes: Rinse cautiously with water for several minutes. Remove contact lenses, if present and easy to do. Continue rinsing. Immediately call a poison center/doctor. If on skin: Wash with plenty of water. If skin irritation occurs: Get medical advice/attention. Take off contaminated clothing and wash before reuse.

#### Storage

Store in dry location. Store away from incompatible materials.

#### Disposal

Dispose of waste and residues in accordance with local authority requirements.

### Hazard(s) not otherwise classified (HNOC)

None known.

## 3. Composition/information on ingredients

### Mixtures

#### Chemical name

Chemical name	CAS number	%
Calcium Sulfoaluminate Cement	960375-09-1	90-100
Silica (Quartz) Crystalline	14808-60-7	<0.1

### Composition comments


All concentrations are in percent by weight unless ingredient is a gas. Gas concentrations are in percent by volume.

Rapid Set Cement

Version #: 02 Revision date: - Issue date: 27-January-2018

SDS US

1 / 7

		MODIFIED CONCRETE SUPPLIERS <span style="float: right;">L-1</span> LLC <span style="float: right;">5419</span> 6455 GRAND AVE. FORT SMITH AR 72904			
		Ship From: MIDLAND United States			
<b>Certificate of Analysis</b>		<b>Customer Information</b>			
Product Name Modifier A/NA Delivery No. 854521624 / 000010 Order Number 145330667 Shipment No. 44512877		Customer Name MODIFIED CONCRETE SUPPLIERS Customer PO number 4009  Container ID 549  Specification Number 000000012803			
Batch Number Seal Number Quantity Manufacturing Plant Manufacturer Address		US01J82009 1308726/1308727 46000.000 LB MFG MDL BINDERS MIDLAND 3892 S Saginaw Rd 1303 BLDG MIDLAND Michigan 48667-0001			
<b>Test</b>	<b>Unit</b>	<b>Lower Limit</b>	<b>Upper Limit</b>	<b>Value</b>	<b>Method</b>
Solids	%	47.0	49.0	49.0	DOWM 100008
pH		9.0	11.0	10.0	DOWM 100429
200 Mesh Residue per 900mL	g	-	0.500	0.001	DOWM 101784
Brookfield Viscosity #1 spindle @ 10rpm	cP	5	40	31	DOWM 100317
Particle Size	nm	175	205	185	DOWM 102392
Surface Tension	mN/m	22.0	31.0	28.0	DOWM 100362
Freeze Thaw Stability	g	-	0.10	0.00	DOWM 101785
Shipping Temperature	°C	10.0	30.0	25.0	LTM 100003
Butadiene Content	%	30.0	40.0	34.8	LTM 100001
Density	lb/gal	8.40	8.60	8.55	DOWM 100364
For inquiries please contact Customer Service or local sales ™ Trademark of Trinseo S.A. or its affiliates					

### CERTIFICATION OF COMPLIANCE - PART A

Date Shipped 08/04/19

Mail to:

MODIFIED CONCRETE SUPPLIERS, LLC  
6455 GRAND AVE.  
FORT SMITH, AR 72904

Shipped to:

MODIFIED CONCRETE SUPPLIERS, LLC  
6455 GRAND AVE.  
FORT SMITH, AR 72904

Customer Order No, 4009

Trinseo Invoice No. 44512877

Shipped From Midland, MI

Manufactured At Midland, MI

Material MOD A NA

Manufactured Date 8-4-2019

Quantity Shipped 5,600 gal

Lot Number USØ1J82ØØ9

This is to certify that on the date of shipment, as shown above, the material covered on above Trinseo Invoice Number and supplied under the subject purchase order(s) meets requirements of both the Trinseo Sales Specification and those of Report No. FHWA 78-35 "Styrene-Butadiene Latex Modifiers for Bridge Deck Overlay Concrete."

Signed and Subscribed before me on this  
4th Day of August 2019

TRINSEO, LLC

By



*Tyrone D. Seeburger*

### CONTRACTOR'S CERTIFICATION - PART B (WHEN REQUIRED)

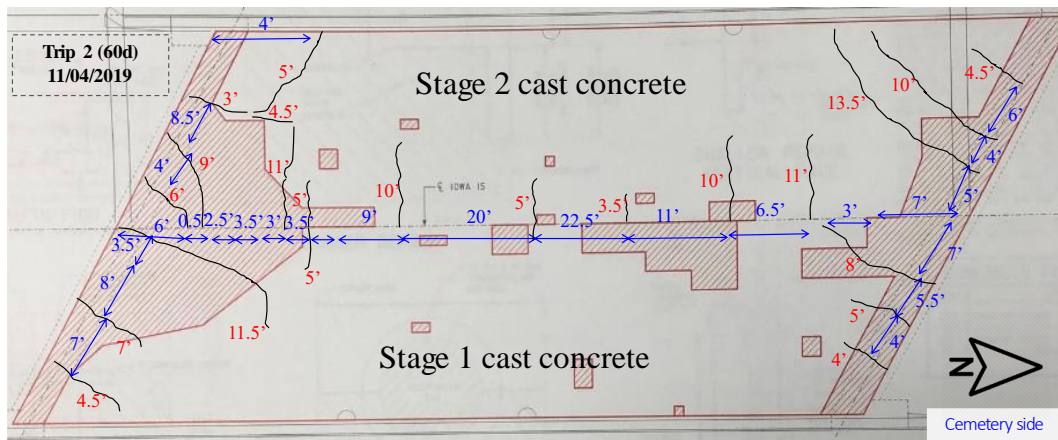
Quantity \_\_\_\_\_

Project Number \_\_\_\_\_

Job Number \_\_\_\_\_

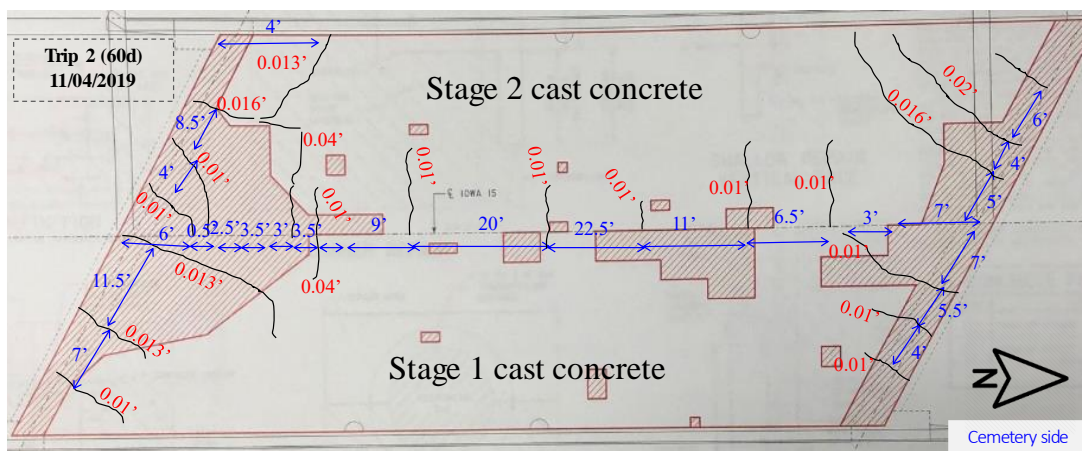
Structure Number \_\_\_\_\_

The following are detailed crack survey results obtained from the individual field trips starting at an overlay age of two months.



- Black: Cracks identified at 60d
- Red: Crack lengths at 60d
- Blue: Distances to cracks

(a) Crack survey results showing their locations and lengths at an age of 2 months

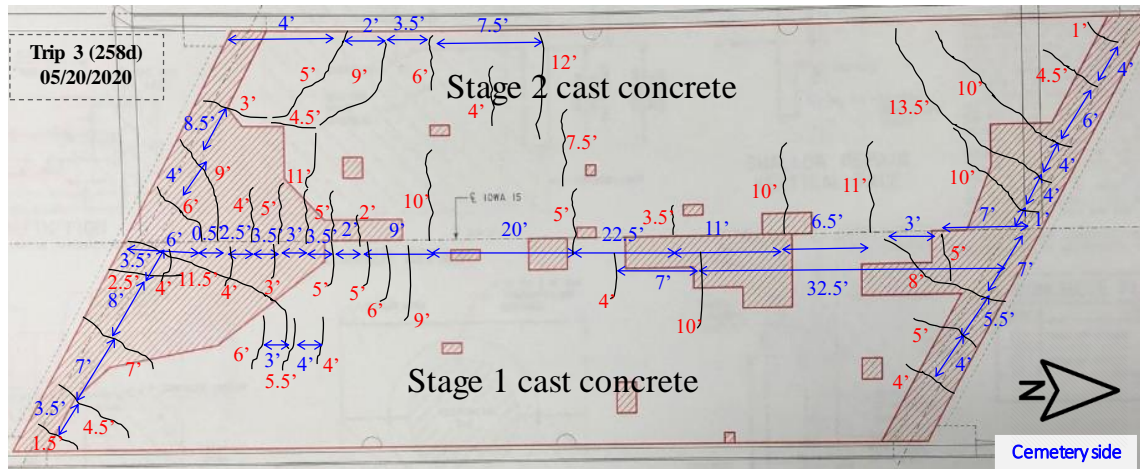


- Black: Cracks identified at 60d
- Red: Crack widths at 60d
- Blue: Distances to cracks

(b) Crack survey results showing their locations and widths at an age of 2 months

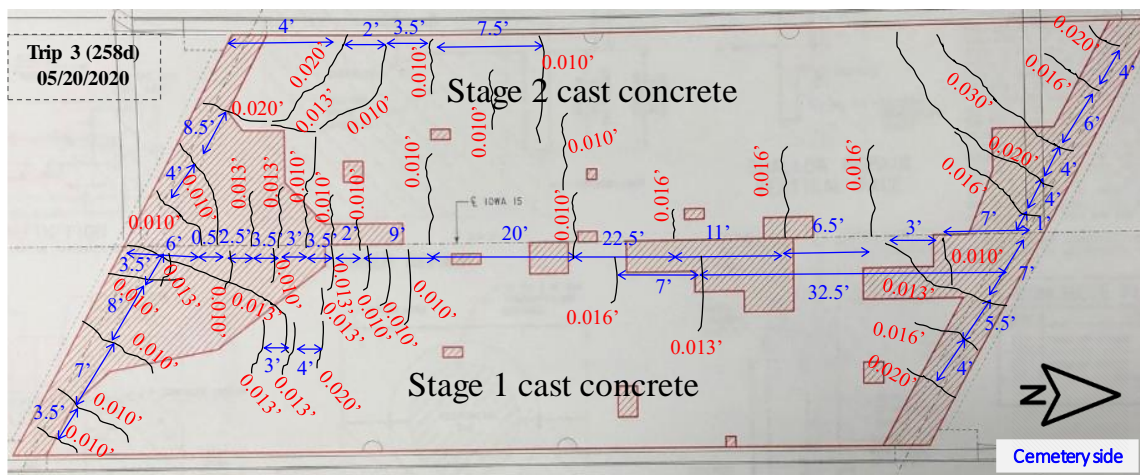
**Figure B.1. Crack survey results from Trip 2 (overlay age of 2 months)**





- Black: Cracks identified during Trip-3
- Red: Trip-3 crack lengths
- Blue: Distances to cracks

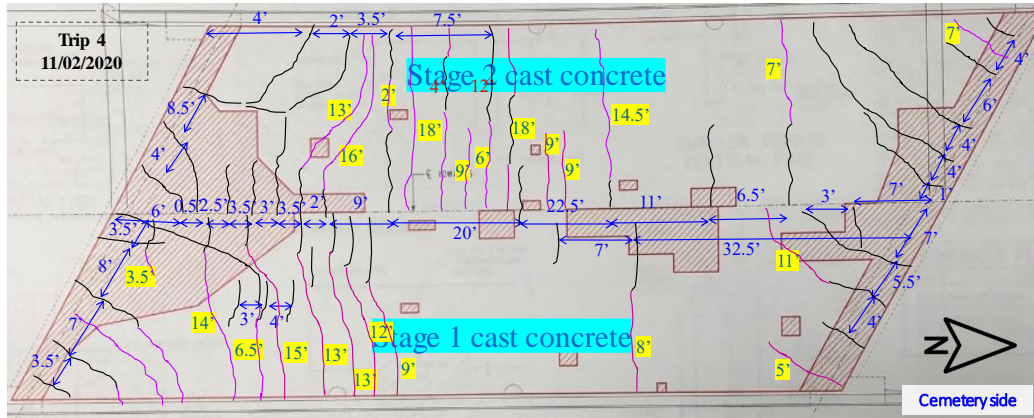
(a) Crack survey results showing their locations and lengths at an age of 8.5 months



- Black: Cracks identified during Trip-3
- Red: Trip-3 crack widths
- Blue: Distances to cracks

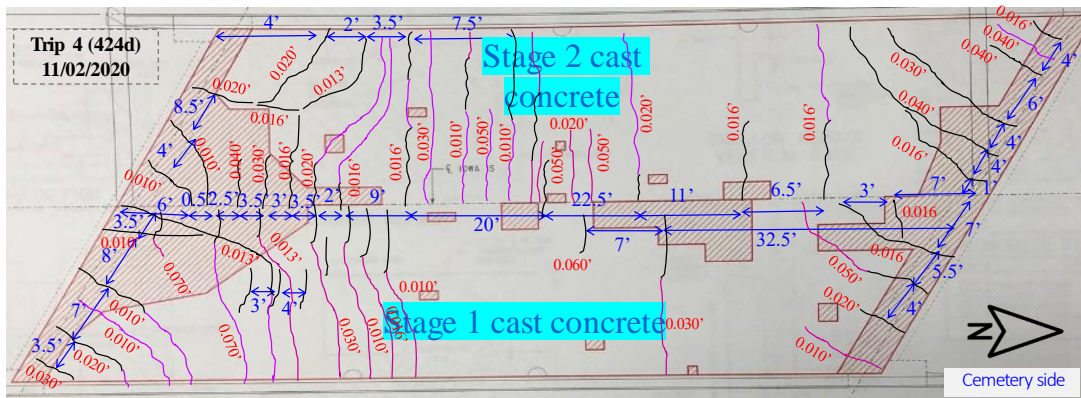
(b) Crack survey results showing their locations and widths at an age of 8.5 months

**Figure B.2. Crack survey results from Trip 3 (overlay age of 8.5 months)**



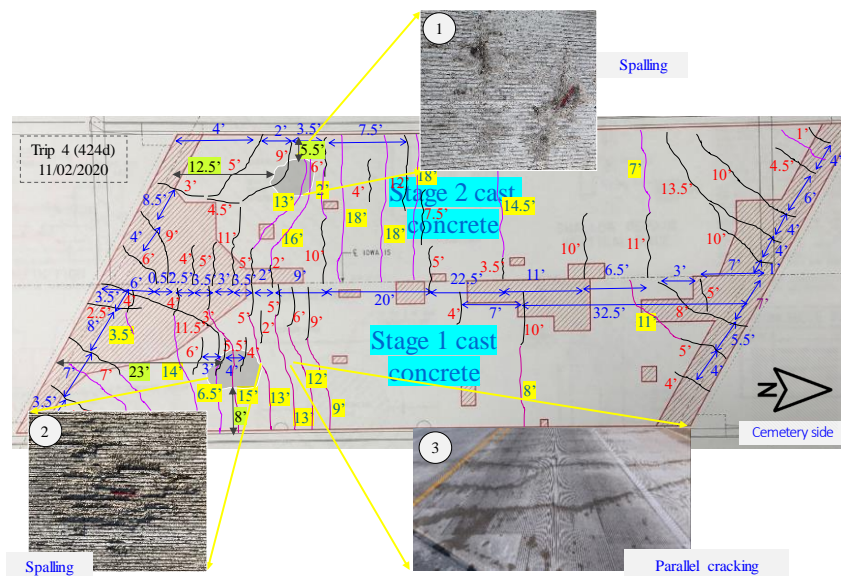
Black: Earlier cracks from Trip-3; Pink: Newer or extended cracks; Dark teal-Newer or extended crack lengths, Blue: Distances to cracks

(a) Crack survey results showing their locations and lengths at an age of 14 months



Black: Earlier cracks from Trip-3; Pink: Newer or extended cracks; Red: Latest crack widths from Trip-4, Blue: Distances to cracks

(b) Crack survey results showing their locations and widths at an age of 14 months



(c) Spalling damage observed at an age of 14 months

**Figure B.3. Cracking and other deteriorations observed during Trip 4 (overlay age of 14 months)**



## APPENDIX C

The following are all project-level and alternative-level data that were entered into RealCost.

**Table C1. RealCost input data**

<b>1. Economic Variables</b>	
Value of Time for Passenger Cars (\$/hour)	\$10.00 LCCANORMAL(10,2)
Value of Time for Single Unit Trucks (\$/hour)	\$18.00 LCCANORMAL(18,2)
Value of Time for Combination Trucks (\$/hour)	\$22.00 LCCANORMAL(22,2.5)

<b>2. Analysis Options</b>	
Include User Costs in Analysis	Yes
Include User Cost Remaining Life Value	Yes
Use Differential User Costs	Yes
User Cost Computation Method	Specified
Include Agency Cost Remaining Life Value	Yes
Traffic Direction	Both
Analysis Period (Years)	40
Beginning of Analysis Period	2019
Discount Rate (%)	3.0 LCCANORMAL(3,1.5)
Number of Alternatives	5

<b>3. Project Details</b>	
State Route	IA 15
Project Name	LMC-VE Overlay
Region	IA
County	Emmett
Analyzed By	
Mileposts	
Begin	
End	
Length of Project (miles)	
Comments	

<b>4. Traffic Data</b>	
AADT Construction Year (total for both directions)	900
Cars as Percentage of AADT (%)	81.0
Single Unit Trucks as Percentage of AADT (%)	6.0
Combination Trucks as Percentage of AADT (%)	13.0
Annual Growth Rate of Traffic (%)	2.0 LCCANORMAL(2,1)
Speed Limit Under Normal Operating Conditions (mph)	55
No of Lanes in Each Direction During Normal Conditions	1
Free Flow Capacity (vphpl)	2,000 LCCANORMAL(2000,500)
Rural or Urban Hourly Traffic Distribution	Rural
Queue Dissipation Capacity (vphpl)	1,000 LCCANORMAL(1000,200)
Maximum AADT (total for both directions)	1,100
Maximum Queue Length (miles)	2

<b>Alternative 1</b>	<b>LMC-VE</b>
<b>Number of Activities</b>	<b>1</b>

Activity 1	Initial	
Agency Construction Cost (\$1,000)	\$0.29 LCCANORMAL(0.29,0.02)	
User Work Zone Costs (\$1,000)	\$0.01 LCCAUNIFORM(0.01,0.02)	
Work Zone Duration (days)	2 LCCAUNIFORM(1,3)	
No of Lanes Open in Each Direction During Work Zone	1	
Activity Service Life (years)	30.0	
Activity Structural Life (years)	30.0	
Maintenance Frequency (years)	0	
Agency Maintenance Cost (\$1,000)	0	
Work Zone Length (miles)	0.25	
Work Zone Speed Limit (mph)	25	
Work Zone Capacity (vphpl)	500 LCCAUNIFORM(400,600)	
Traffic Hourly Distribution	Week End 2	
Time of Day of Lane Closures (use whole numbers based on a 24-hour clock)		
Inbound	Start	End
First period of lane closure	0	24
Second period of lane closure	0	0
Third period of lane closure	0	0
Outbound	Start	End
First period of lane closure	0	24
Second period of lane closure	0	0
Third period of lane closure	0	0



<b>Alternative 2</b>	<b>LMC</b>
<b>Number of Activities</b>	<b>1</b>

Activity 1	Initial	
Agency Construction Cost (\$1,000)	\$0.25 LCCANORMAL(0.25,0.05)	
User Work Zone Costs (\$1,000)	\$0.04 LCCAUNIFORM(0.02,0.05)	
Work Zone Duration (days)	5 LCCAUNIFORM(3,7)	
No of Lanes Open in Each Direction During Work Zone	1	
Activity Service Life (years)	30.0	
Activity Structural Life (years)	30.0	
Maintenance Frequency (years)	0	
Agency Maintenance Cost (\$1,000)	0	
Work Zone Length (miles)	0.25	
Work Zone Speed Limit (mph)	25	
Work Zone Capacity (vphpl)	500 LCCAUNIFORM(400,600)	
Traffic Hourly Distribution	Week End 2	
Time of Day of Lane Closures (use whole numbers based on a 24-hour clock)		
Inbound	Start	End
First period of lane closure	0	24
Second period of lane closure	0	0
Third period of lane closure	0	0
Outbound	Start	End
First period of lane closure	0	24
Second period of lane closure	0	0
Third period of lane closure	0	0

<b>Alternative 3</b>	PPC
<b>Number of Activities</b>	1

Activity 1	Initial	
Agency Construction Cost (\$1,000)	\$0.25 LCCANORMAL(0.25,0.05)	
User Work Zone Costs (\$1,000)	\$0.01 LCCAUNIFORM(0.01,0.02)	
Work Zone Duration (days)	2 LCCAUNIFORM(1,3)	
No of Lanes Open in Each Direction During Work Zone	1	
Activity Service Life (years)	40.0	
Activity Structural Life (years)	40.0	
Maintenance Frequency (years)	0	
Agency Maintenance Cost (\$1,000)	0	
Work Zone Length (miles)	0.25	
Work Zone Speed Limit (mph)	25	
Work Zone Capacity (vphpl)	500 LCCAUNIFORM(400,600)	
Traffic Hourly Distribution	Week End 2	
Time of Day of Lane Closures (use whole numbers based on a 24-hour clock)		
Inbound	Start	End
First period of lane closure	0	24
Second period of lane closure	0	0
Third period of lane closure	0	0
Outbound	Start	End
First period of lane closure	0	24
Second period of lane closure	0	0
Third period of lane closure	0	0

<b>Alternative 4</b>	<b>PCC</b>
<b>Number of Activities</b>	<b>3</b>

Activity 1	Initial	
Agency Construction Cost (\$1,000)	\$0.09 LCCANORMAL(0.09,0.02)	
User Work Zone Costs (\$1,000)	\$0.04 LCCAUNIFORM(0.03,0.05)	
Work Zone Duration (days)	8 LCCAUNIFORM(6,10)	
No of Lanes Open in Each Direction During Work Zone	1	
Activity Service Life (years)	20.0	
Activity Structural Life (years)	20.0	
Maintenance Frequency (years)	0	
Agency Maintenance Cost (\$1,000)	0	
Work Zone Length (miles)	0.25	
Work Zone Speed Limit (mph)	25	
Work Zone Capacity (vphpl)	500 LCCAUNIFORM(400,600)	
Traffic Hourly Distribution	Week End 2	
Time of Day of Lane Closures (use whole numbers based on a 24-hour clock)		
Inbound	Start	End
First period of lane closure	0	24
Second period of lane closure	0	0
Third period of lane closure	0	0
Outbound	Start	End
First period of lane closure	0	24
Second period of lane closure	0	0
Third period of lane closure	0	0

Activity 2	Maintenance 1	
Agency Construction Cost (\$1,000)	\$0.04 LCCANORMAL(0.04,0.005)	
User Work Zone Costs (\$1,000)	\$0.03 LCCAUNIFORM(0.01,0.05)	
Work Zone Duration (days)	2 LCCAUNIFORM(1,3)	
No of Lanes Open in Each Direction During Work Zone	1	
Activity Service Life (years)	5.0	
Activity Structural Life (years)	5.0	
Maintenance Frequency (years)	20	
Agency Maintenance Cost (\$1,000)	0	
Work Zone Length (miles)	0.25	
Work Zone Speed Limit (mph)	25	
Work Zone Capacity (vphpl)	500 LCCAUNIFORM(400,600)	
Traffic Hourly Distribution	Week End 2	
Time of Day of Lane Closures (use whole numbers based on a 24-hour clock)		
Inbound	Start	End
First period of lane closure	0	24
Second period of lane closure	0	0
Third period of lane closure	0	0
Outbound	Start	End
First period of lane closure	0	24
Second period of lane closure	0	0
Third period of lane closure	0	0

Activity 3	Maintenance 2	
Agency Construction Cost (\$1,000)	\$0.04 LCCANORMAL(0.04,0.005)	
User Work Zone Costs (\$1,000)	\$0.03 LCCAUNIFORM(0.01,0.05)	
Work Zone Duration (days)	2 LCCAUNIFORM(1,3)	
No of Lanes Open in Each Direction During Work Zone	1	
Activity Service Life (years)	5.0	
Activity Structural Life (years)	5.0	
Maintenance Frequency (years)	25	
Agency Maintenance Cost (\$1,000)	0	
Work Zone Length (miles)	0.25	
Work Zone Speed Limit (mph)	25	
Work Zone Capacity (vphpl)	500 LCCAUNIFORM(400,600)	
Traffic Hourly Distribution	Week End 2	
Time of Day of Lane Closures (use whole numbers based on a 24-hour clock)		
Inbound	Start	End
First period of lane closure	0	24
Second period of lane closure	0	0
Third period of lane closure	0	0
Outbound	Start	End
First period of lane closure	0	24
Second period of lane closure	0	0
Third period of lane closure	0	0

<b>Alternative 5</b>	<b>HPC</b>
<b>Number of Activities</b>	<b>3</b>

Activity 1	Initial	
Agency Construction Cost (\$1,000)	\$0.10 LCCANORMAL(0.1,0.02)	
User Work Zone Costs (\$1,000)	\$0.04 LCCAUNIFORM(0.03,0.05)	
Work Zone Duration (days)	7 LCCAUNIFORM(6,8)	
No of Lanes Open in Each Direction During Work Zone	1	
Activity Service Life (years)	20.0	
Activity Structural Life (years)	20.0	
Maintenance Frequency (years)	0	
Agency Maintenance Cost (\$1,000)	0	
Work Zone Length (miles)	0.25	
Work Zone Speed Limit (mph)	25	
Work Zone Capacity (vphpl)	500 LCCAUNIFORM(400,600)	
Traffic Hourly Distribution	Week End 2	
Time of Day of Lane Closures (use whole numbers based on a 24-hour clock)		
Inbound	Start	End
First period of lane closure	0	24
Second period of lane closure	0	0
Third period of lane closure	0	0
Outbound	Start	End
First period of lane closure	0	24
Second period of lane closure	0	0
Third period of lane closure	0	0



Activity 2	Maintenance 1	
Agency Construction Cost (\$1,000)	\$0.04 LCCANORMAL(0.04,0.005)	
User Work Zone Costs (\$1,000)	\$0.03 LCCAUNIFORM(0.01,0.05)	
Work Zone Duration (days)	2 LCCAUNIFORM(1,3)	
No of Lanes Open in Each Direction During Work Zone	1	
Activity Service Life (years)	5.0	
Activity Structural Life (years)	5.0	
Maintenance Frequency (years)	20	
Agency Maintenance Cost (\$1,000)	0	
Work Zone Length (miles)	0.25	
Work Zone Speed Limit (mph)	25	
Work Zone Capacity (vphpl)	500 LCCAUNIFORM(400,600)	
Traffic Hourly Distribution	Week End 2	
Time of Day of Lane Closures (use whole numbers based on a 24-hour clock)		
Inbound	Start	End
First period of lane closure	0	24
Second period of lane closure	0	0
Third period of lane closure	0	0
Outbound	Start	End
First period of lane closure	0	24
Second period of lane closure	0	0
Third period of lane closure	0	0

Activity 3	Maintenance 2	
Agency Construction Cost (\$1,000)	\$0.04 LCCANORMAL(0.04,0.005)	
User Work Zone Costs (\$1,000)	\$0.03 LCCAUNIFORM(0.01,0.05)	
Work Zone Duration (days)	2 LCCAUNIFORM(1,3)	
No of Lanes Open in Each Direction During Work Zone	1	
Activity Service Life (years)	5.0	
Activity Structural Life (years)	5.0	
Maintenance Frequency (years)	25	
Agency Maintenance Cost (\$1,000)	0	
Work Zone Length (miles)	0.25	
Work Zone Speed Limit (mph)	25	
Work Zone Capacity (vphpl)	500 LCCAUNIFORM(400,600)	
Traffic Hourly Distribution	Week End 2	
Time of Day of Lane Closures (use whole numbers based on a 24-hour clock)		
Inbound	Start	End
First period of lane closure	0	24
Second period of lane closure	0	0
Third period of lane closure	0	0
Outbound	Start	End
First period of lane closure	0	24
Second period of lane closure	0	0
Third period of lane closure	0	0





**THE INSTITUTE FOR TRANSPORTATION IS THE FOCAL POINT FOR TRANSPORTATION  
AT IOWA STATE UNIVERSITY.**

**InTrans** centers and programs perform transportation research and provide technology transfer services for government agencies and private companies;

**InTrans** contributes to Iowa State University and the College of Engineering's educational programs for transportation students and provides K–12 outreach; and

**InTrans** conducts local, regional, and national transportation services and continuing education programs.



**IOWA STATE  
UNIVERSITY**

Visit [InTrans.iastate.edu](https://InTrans.iastate.edu) for color pdfs of this and other research reports.